Spring 2013

Effects of machining parameters on cutting forces,shear angle and friction in orthogonal turning of titanium alloys

Hilary Onyishi

Department:

EFFECTS OF MACHINING PARAMETERS ON CUTTING FORCES, SHEAR ANGLE AND FRICTION IN ORTHOGONAL TURNING OF TITANIUM ALLOYS

by

HILARY ANAYOCHUKWU ONYISHI

A THESIS

Presented to the Graduate Faculty of the

MISSOURI UNIVERSITY OF SCIENCE AND TECHNOLOGY

In Partial Fulfillment of the Requirements for the Degree

MASTER OF SCIENCE IN MECHANICAL ENGINEERING

2013

Approved by
Anthony C. Okafor, Advisor
K. Chandrashekhara
V.A. Samaranyake

PUBLICATION THESIS OPTION

This thesis has been prepared in the publication option format as two separate papers for publication. Paper 1, comprising pages 1 through 49, is to be submitted for publication in the *Journal of Materials Processing Technology*, under the title, "Investigations on the Effects of Machining Parameters on Cutting Forces, Shear Angle and Friction in Orthogonal Turning of Titanium Alloy Tube." Paper 2, comprising pages 53 through 106, is to be submitted for publication in the *Journal of Materials Processing Technology*, under the title, "Investigations on the Effects of Machining Parameters on Cutting Forces, Shear Angle and Friction in Orthogonal Turning of Titanium Alloy using Ribbed Solid Bar."

ABSTRACT

Paper 1 presents the results of the investigations on the effects of machining parameters on cutting forces, shear angle and friction in orthogonal turning of titanium alloy tube. Uncoated fine-grained cemented tungsten carbide (WC/Co) and Physical Vapour Deposition (PVD) TiAlN coated grade turning tool inserts, with 5^0 and 15^0 rake angles were used under low and high cutting speeds of 120 and 240m/min, at three different feedrates (0.05, 0.075 and 0.1 mm/rev). The experiments were conducted under flooded coolant to reflect what is practically obtainable in manufacturing industries. The experimental results show that cutting forces at two selected cutting speeds of 120 and 240 m/min and the three selected feedrates increased with increase in feedrates for both uncoated and coated cutting tools. Paper 2 presents the results of the effects of machining parameters on cutting forces, shear angle and friction in orthogonal turning of titanium alloy using ribbed solid bar. Uncoated WC/Co and PVD TiAlN coated grade turning tool inserts, with 5^0 and 16^0 rake angles were used under low and high cutting speeds of 120 and 240m/min, at three different feedrates (0.05, 0.075 and 0.1 mm/rev). The experiments were conducted under flooded coolant to reflect what is practically obtainable in manufacturing industries. The experimental results show that cutting forces at the two selected cutting speeds of 120 and 240 m/min and three selected feedrates increased with increase in feedrates for both the uncoated and coated cutting tools.

ACKNOWLEDGMENTS

Firstly, I would like to express my gratitude to the Almighty God for the gift of life, without which all this would not have been possible. Through His grace, I have been able to succeed where it surely would have been impossible.

Immense appreciation goes to my research advisor, Dr. Anthony Chukwujekwu Okafor, who has not only provided highly relevant technical and educational guidance but also played a mentoring role in ensuring that I have progressed in numerous aspects of my life. For his contribution to my educational and personal development, I will forever be indebted. I also want to thank Dr. K. Chandrashekhara and Dr. Sam for serving as committee members and examining the thesis.

I especially would like to thank Chidiebere Onyishi, my Mom, Lady Justina Onyishi, and everyone in my family. Without their love, encouragement, understanding and support, I would not have carried it through. Also, I would like to thank my friends, Emenike Chukwuma, Ozgur Kilicay, Abdulhakim Sultan, and Mr. Mitch Cottrell, for assisting me during the course of my research.

Finally, the financial assistance provided to me in the form of Graduate Research Assistantship by my advisor, Dr. Okafor, from his National Science Foundation (NSF) grant and the Graduate Teaching Assistantship from the Department of Mechanical and Aerospace Engineering are gratefully acknowledged.

TABLE OF CONTENTS

Page

PUBLICATION THESIS OPTION iii

ABSTRACT iv

ACKNOWLEDGMENTS v

LIST OF ILLUSTRATIONS x

LIST OF TABLES xiii

NOMENCLATURE xv

SECTION

1. INTRODUCTION 1

PAPER

I. INVESTIGATIONS ON THE EFFECTS OF MACHINING PARAMETERS ON CUTTING FORCES, SHEAR ANGLE AND FRICTION IN ORTHOGONAL TURNING OF TITANIUM ALLOY TUBE 4

ABSTRACT 4

1. INTRODUCTION 6

1.1. MECHANICS OF ORTHOGONAL CUTTING 11

2. EXPERIMENTAL SET-UP AND PROCEDURES 13

2.1. CALIBRATION OF THE FORCE MEASUREMENT SYSTEM 21

2.2. MULTIPLE REGRESSIONS TO ESTABLISH CALIBRATION MATRIX 30

2.3. OVERVIEW OF THE CUTTING FORCE MEASUREMENT SYSTEM 33

2.4. SIGNAL PROCESSING 35

3. RESULTS AND DISCUSSION 37

3.1. EFFECTS OF FEEDRATE ON CUTTING FORCES 37

3.2. EFFECTS OF CUTTING TOOL COATING ON CUTTING FORCES AND FRICTION 38

3.3. EFFECTS OF RAKE ANGLE ON CUTTING FORCES AND FRICTION COEFFICIENT 39

3.4. EFFECT OF RAKE ANGLE ON SHEAR FORCE 42

3.5. EFFECT OF CUTTING SPEED ON MAIN CUTTING FORCE 43

3.6. EFFECTS OF FEEDRATES ON COEFFICIENT OF FRICTION 44

3.7. EFFECTS OF FEEDRATES ON SHEAR ANGLE 44

4. CONCLUSION 46

ACKNOWLEDGEMENTS 48

REFERENCES 49

II. INVESTIGATIONS ON THE EFFECTS OF MACHINING PARAMETERS ON CUTTING FORCES, SHEAR ANGLES, AND FRICTIONS DURING ORTHOGONAL TURNING OF TITANIUM ALLOY USING SOLID RIBBED BAR…..**…….....**53

ABSTRACT 53

1. INTRODUCTION 55

1.1. MECHANICS OF ORTHOGONAL CUTTING 60

2. EXPERIMENTAL SET- UP AND PROCEDURE 62

2.1. CALIBRATION OF THE FORCE MEASUREMENT SYSTEM 70

2.2. MULTIPLE REGRESSION TO ESTABLISH THE CALIBRATION MATRIX 80

2.3. OVERVIEW OF THE CUTTING FORCE MEASUREMENT SYSTEM 83

2.4. SIGNAL PROCESSING 85

3. RESULTS AND DISCUSSION 87

3.1. EFFECTS OF FEEDRATE ON CUTTING FORCES 87

3.2. EFFECTS OF CUTTING TOOL COATING ON CUTTING FORCES AND FRICTION 88

3.3. EFFECTS OF RAKE ANGLE ON CUTTING FORCES AND FRICTION COEFFICIENT 89

3.4. EFFECT OF RAKE ANGLE ON SHEAR FORCE 92

3.5. EFFECT OF CUTTING SPEED ON MAIN CUTTING FORCE 92

3.6. EFFECT OF FEEDRATES ON COEFFICIENT OF FRICTION 94

3.7. EFFECT OF FEEDRATES ON SHEAR ANGLE 94

4. CONCLUSION 97

ACKNOWLEDGEMENTS ..... .99

REFERENCES 100

SECTION

2. CONCLUSION 104

VITA……………….. 106

LIST OF ILLUSTRATIONS

Page

Paper 1

Figure 1. Circular Force Diagram (Ernest & Merchant (1941, 1945)) for Orthogonal Cutting 11

Figure 2. Schematic Diagram of the Experimental Set-up and Data Acquisition System for Orthogonal Turning 13

Figure 3. Titanium Alloy Tube Workpiece Clamped in the Lathe Chuck to Simulate Orthogonal Turning 20

Figure 4. Chip Morphologies 20

Figure 5. Set-up for the Calibration of the Load Cell 21

Figure 6. Calibration Set-up 22

Figure 7. Feed Axis Calibration for Tool 1 25

Figure 8. Radial Axis Calibration for Tool 1 26

Figure 9. Tangential Axis Calibration for Tool 1 27

Figure 10. Load Cell Response to Applied Load (Feed Axis, Tool 1) 28

Figure 11. Load Cell Response to Applied Load (Radial Axis, Tool 1) 29

Figure 12. Load Cell Response to Applied Load (Tangential Axis, Tool 1) 30

Figure 13. Tool 1 Feed Axis Calibration 32

Figure 14. Unprocessed and Processed F_x/feed Signal 34

Figure 15. Unprocessed and Processed Fy/tangential Signal 34

Figure 16. Cutting Forces vs Feedrate in Orthogonal Turning 40

Figure 17. Average Shear Force vs Rake Angle 42

Figure 18. Average Cutting Force vs Cutting Speed 43

Figure 19. Coefficient of Friction vs Feedrate 44

Figure 20. Shear Angle vs Feedrates 45

Paper 2

Figure 1. Circular Force Diagram (Ernest & Merchant 1941, 1945) for Orthogonal Cutting 60

Figure 2. Schematic Diagram of the Experimental Set-up and Data Acquisition System for Orthogonal Turning 62

Figure 3. Titanium Alloy Workpiece with Ribs Clamped in the Lathe Chuck to Simulate Orthogonal Turning 69

Figure 4. Chip Morphologies 70

Figure 5. Set-up for the Calibration of the Load Cell 71

Figure 6. Calibration Set-up 71

Figure 7. Feed Axis Calibration for Tool 5 74

Figure 8. Radial Axis Calibration for Tool 5 76

Figure 9. Tangential Axis Calibration for Tool 5 77

Figure 10. Load Cell Response to Applied Load (Feed Axis, Tool 5) 78

Figure 11. Load Cell Response to Applied Load (Radial Axis, Tool 5) 79

Figure 12. Load Cell Response to Applied Load (Tangential Axis, Tool 5) 80

Figure 13. Tool 5 Feed Axis Calibration 82

Figure 14. Unprocessed and Processed F_x Signal 84

Figure 15. Unprocessed and Processed F_y Signal 84

Figure 16. Cutting Forces vs Feedrate in Orthogonal Turning of Ribbed Workpiece 90

Figure 17. Average Shear Force vs Rake Angles 92

Figure 18. Average Cutting Force vs Cutting Speed 93

Figure 19. Coefficient of Friction vs Feedrate 94

Figure 20. Factors Influencing Shear Angle 95

LIST OF TABLES

Page

Paper 1

Table 1. Physical Properties of Titanium Alloy Ti-6Al-4V 14

Table 2. Chemical Composition of Titanium Alloy Ti-6Al-4 14

Table 3. Machining Parameters, Measured and Calculated Cutting Forces and Friction Coefficients at V=120m/min Using Uncoated Tool Inserts 16

Table 4. Machining Parameters, Measured and Calculated Cutting Forces and Friction Coefficients at 240m/min Using Uncoated Tool Inserts 17

Table 5. Machining Parameters, Measured and Calculated Cutting Forces and Friction Coefficients at 120m/min Using Coated Tool Insert 18

Table 6. Machining Parameters, Measured and Calculated Cutting Forces and Friction Coefficients at 240m/min Using Coated Tool Insert 19

Table 7. Summary of Machining Parameters Used for the Orthogonal Cutting Tests 36

Paper 2

Table 1. Physical Properties of Titanium Alloy Ti-6Al-4V 63

Table 2. Chemical Composition of Titanium Alloy Ti-6Al-4 63

Table 3. Machining Parameters, Measured and Calculated Cutting Forces and Friction Coefficients at V=120m/min Using Uncoated Tool Inserts 65

Table 4. Machining Parameters, Measured and Calculated Cutting Forces and Friction Coefficients at 240m/min Using Uncoated Tool Inserts 66

Table 5. Machining Parameters, Measured and Calculated Cutting Forces and Friction Coefficients at 120m/min Using Coated Tool Insert 67

Table 6. Machining Parameters, Measured and Calculated Cutting Forces and Friction Coefficients at 240m/min Using Coated Tool Insert 68

Table 7. Summary of Machining Parameters 86

Table 8. Comparative Table of Thrust Force and Cutting Force for Titanium Tube and Ribbed Alloys..... 96

NOMENCLATURE

Symbol	Description
t_o	undeformed chip thickness
t_c	chip thickness
α	rake angle
ϕ	shear angle
τ_s	shear stress
N	normal force
F	friction force
μ	coefficient of friction
F_s	shear force
F_c	cutting force
F_t	thrust force
W	width of cut (tube or rib thickness in orthogonal turning)

1. INTRODUCTION

Significant advances made in the field of material science have led to a better understanding of the behavior of engineering materials during processing. This has enabled the continual development and introduction of new engineering materials with superior properties, such as titanium alloys. Titanium alloys are classified into three main groups; α-alloys, β-alloys, and α-β alloys. Ti-6Al-4V, which is α - β alloy is the most widely used titanium alloy grades in aircraft manufacturing industries. Numerous experimentations and modeling have been carried out on this particular grade of titanium alloy due to its unique properties. Titanium alloys in general exhibit a high strength-to-weight ratio, high resistance to corrosion, ability to retain strength at high temperatures, high melting point, and hence they are used at elevated temperatures up to 600^{o} C. They are more capable of retaining their mechanical properties, such as hardness at elevated temperatures, than steel and stainless steel alloys.

Titanium alloys are widely used in aerospace industries for the manufacturing of components that require lighter, stronger, tougher, stiffer, and more corrosion-resistant materials. Their unique and desirable low thermal conductivity characteristics that make them capable of retaining their properties at elevated temperatures, such as in jet engines, automobiles, the chemical, nuclear, and medical industries, also impair their machinability due to the extremely high temperature generated at the tool-chip interface. The heat generated in the cutting zone is not conducted away but remains present there and builds to extreme temperatures, thus causing the tool to wear rapidly and consequently leading to high cutting forces and friction. Cutting forces are the most essential determinants in machining processes. Excessive cutting forces cause the cutting

tool, workpiece, machine tool and machined part to suffer unacceptable large deformations and quality of machined parts, as well as tool breakage. Therefore, adequate knowledge of cutting forces and the effects of cutting parameters on those forces is highly important in the machining process. Details regarding cutting forces, shear angle and friction are required not only to design the machine tools and cutter, but also to determine the cutting parameters, especially for programming the numerical control machine tool for machining. The quest to lower cutting forces at tool-chip interface when cutting hard metals like titanium alloys has posed enormous challenges for many manufacturing industries.

Paper 1 presents the results of the investigations of the effects of machining parameters on cutting forces, shear angle and friction in orthogonal cutting of titanium alloy tube. The problem of measuring cutting forces on the Okuma CNC turret lathe used for this research was addressed by the design and installation of a Kistler 3-component force sensor on a suitable force path for the Okuma LB15 CNC Lathe. The cutting forces could not be measured directly during machining operations, therefore calibration of the force measurement system to establish the relationship between cutting tool-tip forces (feed, radial, and tangential) with the measured three orthogonal components of any force acting on the sensor in the X, Y, and Z orthogonal force sensor axis were performed for tool number 1 that is used for the orthogonal cutting experiments. Calibration was carried out using specially made fixtures. A hydraulic jack instrumented with Kistler 9212 single axis load cell was used to apply loading and unloading forces at the tool tip in the respective coordinate directions for the turret position indexed to the cutting tool position. For each loading and unloading cycles, the 3-component force sensor output was

acquired using a 4-channel Tektronix TDS 420A oscilloscope. A simple least square model fitting technique was applied to each respective loading/unloading data record using STATISTICA^{TM} software from StarSoft^{R} to generate the calibration equations. The forces at the tool tip were calculated using the equations developed during the calibration process.

Although there have been several studies on the orthogonal turning of Ti-6Al-4V alloys, most of them were conducted with round tube at low cutting speeds and under dry cutting conditions. Hence, paper 2 presents an experimental investigation on the effects of cutting parameters on cutting forces, shear angle, and friction in orthogonal turning of titanium alloys using solid ribbed bar. In this paper, the same processes used in paper 1 will be repeated, and the results will be analyzed. Also, the forces could not be measured directly during the machining operations, therefore calibration of the force measurement system to establish the relationship between cutting tool-tip forces (feed, radial, and tangential) with the measured X, Y, and Z force load cell outputs were performed for tool number 2. A simple least square model fitting technique was applied to each respective loading/unloading data record using STATISTICA^{TM} software from StarSoft^{R} to generate the calibration equations. The forces at the tool tip were calculated using the equations developed during the calibration process. The effect of feedrate, cutting speed, and rake angles were explained in details in paper 1 and 2.

PAPER

I. INVESTIGATIONS ON THE EFFECTS OF MACHINING PARAMETERS ON CUTTING FORCES, SHEAR ANGLE AND FRICTION IN ORTHOGONAL TURNING OF TITANIUM ALLOY TUBE

A. Chukwujekwu Okafor, Hilary Onyishi
Laboratory for Industrial Automation and Flexible Manufacturing
Department of Mechanical and Aerospace Engineering
Missouri University of Science and Technology
327 Toomey Hall, Rolla, MO-65409-005, USA
E-mail:okafor@mst.edu

ABSTRACT

Titanium alloys, due to their unique and excellent combination of low density, high strength-to-weight ratio, ability to retain strength at high temperatures, and exceptional resistance to corrosion, are attractive materials for aerospace industries. The quest for enhanced material removal and tool life has necessitated research into cutting forces during high-speed cutting of titanium alloys. This paper presents the result of experimental investigations on the effects of machining parameters on cutting forces, shear angle and friction in orthogonal turning of Ti-6Al-4V round tube. Uncoated fine-grained cemented tungsten carbide (WC/Co) and Physical Vapour Deposition (PVD) TiAlN coated grade turning tool inserts, with 5^0 and 15^0 rake angles were used under low

and high cutting speeds of 120 and 240m/min at three different feedrates (0.05, 0.075 and 0.1 mm/rev). The experiments were conducted under flooded emulsion coolant to reflect what is practically obtainable in manufacturing industries.

The experimental results show that the cutting force components, F_c, are significantly higher that the thrust force components, F_t, and that all cutting force components (F_c,F_t,and F) at two selected cutting speeds of 120 and 240 m/min and the three selected feedrates increased with increase in feedrate for both uncoated and coated cutting tools. However, for both uncoated and coated tools, an increase in the positive rake angle from 5^0 to 15^0 led to a decrease in cutting force. The 15^o tool rake angle results in an increase of the shear angle and friction coefficient, and thus lower shear force and friction force. In contrast, PVD coated tools gave the largest cutting forces.

Keywords: Orthogonal cutting of round tube, Cutting forces, Shear angle, Friction coefficient, Machining parameters, Titanium machining

1. INTRODUCTION

Significant advances made in the field of material science have led to a better understanding of the behaviors of engineering materials during processing**.** This has enabled the continual development and introduction of new engineering materials with superior properties, such as titanium alloys. Titanium alloys are classified into three main groups; α-alloys, β-alloys, and α-β alloys. Titanium alloys such as Ti-6Al-4V, which is a α - β alloy, is the most widely used titanium alloy grades in aerospace and defense manufacturing industries, as well as in automotive and biomedical industries; and belong to the group of difficult to cut metals. Titanium alloys in general exhibit a high strength-to-weight ratio, high toughness, excellent resistance to corrosion and wear, ability to retain their strength at high temperature, high melting point, bio-compatibility, and hence are used at elevated temperatures up to 600^{o} C. They are more capable of retaining their mechanical properties, such as hardness at elevated temperatures, than steel and stainless steel alloys.

Titanium alloys are widely used in aerospace industries for the manufacturing of components that require lighter, stronger, tougher, stiffer, and more corrosion-resistant materials. Their unique and desirable low thermal conductivity characteristics that make them capable of retaining their properties at elevated temperatures, such as in jet engines, automobiles, chemical, nuclear, and medical industries, also impair their machinability due to the extremely high temperature generated at the tool-chip interface. The heat generated in the cutting zone is not conducted away due to the low thermal conductivity

and diffusivity, but remains present there and builds-up to extreme temperatures, along with high chemical reactivity at elevated temperatures, thus causing the tool to wear rapidly and consequently leading to high cutting forces and friction.

Cutting forces are the most essential determinants in machining processes. These forces generated in machining have direct influence on heat generation; tool deflection, wear and failure; power requirements and the quality of the machined parts. Excessive cutting forces cause the cutting tool, workpiece, machine tool and machined part to suffer unacceptable large deformations, excessive cutting temperatures, unstable vibrations, tool breakage, and poor quality of machined parts. Therefore, adequate knowledge of cutting forces and the effects of cutting parameters on those forces is highly important in machining process. Details regarding cutting forces, shear angle and friction coefficients are required not only for designing machine tools and cutting tools, but also for the analysis of the cutting process to determining optimum machining parameters; and to provide machining data for the formulation of mechanistic, Finite Element (FE) and empirical cutting force models for machining simulation. The quest to lower cutting force at the cutting tool-chip interface when cutting hard metals like titanium alloys has posed enormous challenges for manufacturing industries.

Few studies have been conducted to determine the correlations between cutting forces and cutting parameters when cutting titanium alloys. An experimental investigation into high-speed turning of the titanium alloy Ti-6Al-4V (with coated and uncoated carbide turning inserts) was conducted by Srivastava et al. (2010); they found that cutting forces increased with increase in cutting speed and feedrate, except at the lowest feedrate, where lower forces were observed with uncoated inserts; in addition,

they reported that cutting forces decreased with an increase in rake angle from 0^o to 5^o. Fang and Wu (2009) conducted a comparative study of cutting forces in orthogonal high speed finish machining of Ti-6Al-4V and Inconel 718 tube workpiece materials, using coated carbide tools with no cutting fluids or coolant. They reported that for both Ti-6Al-4V and Inconel 718 workpiece materials, the cutting force, thrust force, and resultant force all decrease as cutting speed increases, while the force ratio (F_c/F_t) increases. They also reported that as the feedrate increases, the cutting force, the thrust force, the resultant force, as well as the force ratio all increases. However, cutting force and thrust force in machining Inconel 718 are higher than those in machining Titanium Ti-6Al-4V. Baldoukas et al. (2008) investigated the effects of depth of cut, tool rake angle and workpiece type on the main cutting force during an orthogonal turning process. They concluded that the influence of rake angle on the main cutting force depends on the type of workpiece material; also, they reported that the main cutting force increased linearly with increase in depth of cut. Similar observations were also made by Saglam et al. (2006), as they investigated the effects of rake angle and approach angle on the main cutting force and tool-tip temperature in orthogonal turning of AlSl 1040 steel. They discovered that approach angle and rake angle have considerable effect on cutting forces and temperature at the tool-chip interface. Their findings on the effect of tool rake angle corresponds with the finding by Baldoukas et al. that increasing positive rake angle decreases the cutting forces significantly. This occurs because a positive rake angle produces a higher shear angle, which helps to reduce cutting forces and thus produces a better surface finish because it assists the chip to flow away from the workpiece. Another notable effort was made by Gunay et al. (2004) when they investigated the effect of rake

angle on main cutting force. They reported that the main cutting force increased with increase of negative rake values and decreased with increase of positive rake values. This was attributed to a reduction in the tool-chip contact area and friction force. Marusich (2001) investigated the effects of friction and cutting speed on cutting force in simulation validation process, and suggested that a decrease in the cutting force must come from a reduction in the effective friction at the tool-chip interface. Additionally, Iqbal et al. (2007) investigated the effect of interface friction on tool-chip contact length in orthogonal cutting using the finite element method. Their results showed that reduced chip compression ratios lead to a lower tool-chip contact length. Their finite element analysis revealed that friction distribution schemes significantly affect the ability to predict contact length, while chip thickness seemed insensitive to friction schemes. Seker et al. (2004) investigated the effect of feedrate on cutting forces when machining with linear motion. They concluded that the main cutting force increased with an increase in the feedrate when the depth of cut and cutting speed were held constant. Considering cutting tools, Ezugwu et al. (2005), Zoya and Krishnamurthy (2000), and Ozel et al. (2010) independently reported that coated tools exhibited the largest cutting forces at high cutting speeds than uncoated tools, but less tool wear were observed, during dry machining of Ti-6Al-4V alloy.

Although several studies have investigated the effects of machining parameters on cutting forces in orthogonal cutting of low strength alloys, there is insufficient knowledge on the effects of cutting parameters (cutting speed, feedrate, tool rake angle and workpiece geometry) on orthogonal cutting of difficult-to-cut metals such as titanium. Most published orthogonal cutting tests were conducted using tubular workpiece, and

only a few using ribbed solid workpiece, and there is no comparative study of the two orthogonal cutting test approaches has been reported in the literature. Also most studies on the machinability of titanium alloys were based on dry cutting operations and low cutting speeds; thus, they do not reflect actual practices in manufacturing industries today. Therefore, the objective of the present study reported in this paper, is to investigate the effects of machining parameters (feedrate, cutting speed, rake angle, uncoated and coated tool inserts) on cutting forces (cutting force, $F_{c,}$ thrust force, F_t, friction force, F, and normal to friction force, N), shear angle, friction coefficient, and shear stress during high speed orthogonal turning of titanium Ti-6Al-4V alloy tube workpiece, under flooded coolant conditions, typical of the practice in manufacturing industry. The second objective of the research is to obtain orthogonal cutting data base, which will be transformed to oblique milling geometry, and used to determine specific cutting and edge force coefficients, for mechanistic modeling and simulation of cutting forces in high speed bull nose helical end-milling of titanium alloys. Uncoated fine-grained cemented tungsten carbide (WC/Co) and Physical Vapour Deposition (PVD) TiAlN coated grade turning tool inserts, with 5^0 and 15^0 rake angles were used under low and high cutting speeds of 120 and 240m/min at three different feedrates (0.05, 0.075 and 0.1 mm/rev).

In recent years, many predictive models have been developed successfully for practical machining operations. These approaches depend upon a detailed understanding of orthogonal and oblique cutting processes traditionally used in fundamental studies of cutting actions. Orthogonal cutting is the process by which a straight-edged tool moves with a constant speed perpendicularly to the cutting edge. It is a two-dimensional (2D) case of machining that can be approximated in the planing, shaping, and end turning of a

thin-walled tube, Ernst and Merchant (1941, 1945), Stephenson et al. (2006) or in the turning of a specially prepared ribbed (grooved) solid workpiece. Experimentally, it has been found that the shear angle and, hence, the cutting ratio, depend upon the workpiece, tool material and cutting conditions. Several attempts have been made to establish a theoretical law that predicts the shear angle. Ernst and Merchant (developed the first reasonable theory) Stephenson et al. (2006). They assumed that the shear angle would adopt a value that would minimize the work of cutting.

1.1. MECHANICS OF ORTHOGONAL CUTTING

The shear plane model of orthogonal cutting (Figure 1) was first proposed by Ernst and Merchant (1941, 1945), (Stephenson et al. (2006). They assumed that the chip is formed by shear along a single plane inclined at an angle, ϕ, the shear angle, with respect to the machined surface. This assumption is consistent with deformation patterns observed in many chip samples from quick-stop tests. The shear angle can be calculated from the cutting ratio, r, according to the geometric relationships shown in Figure 1.

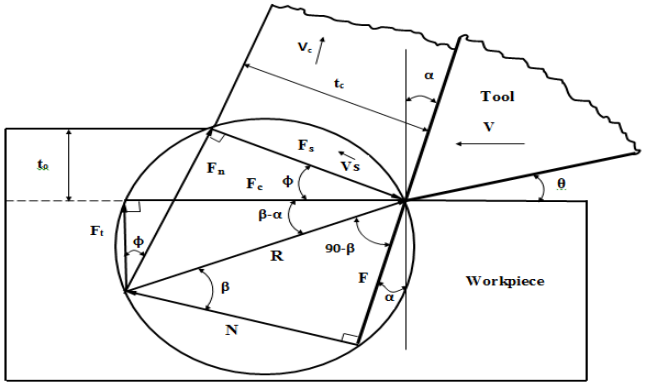

Figure 1. Circular Force Diagram (Ernest & Merchant (1941, 1945)) for Orthogonal Cutting

When the chip thickness ratio is known from Eq. 1, the shear angle, ϕ, can be estimated from Eq. 2.The shear force and shear stress, τ_s, can be calculated from Eq. 3 and Eq. 4. From the experimentally obtained cutting and trust forces, the normal force and friction force can be deduced as shown in Eq. 5 and Eq. 6. The coefficient of friction can be estimated from Eq. 7.

Cutting ratio: $r = \frac{t_o}{t_c} = \frac{\sin\phi}{\cos(\phi-\alpha)}$ (1)

Shear angle: $\phi = tan^{-1}\frac{r\cos\alpha}{1-r\sin\alpha}$ (2)

Shear force: $F_s = F_c\cos\phi - F_t\sin\phi$ (3)

Normal to shear force: $F_n = F_c\sin\phi + F_t\cos\phi$ (4)

Shear stress: $\tau_s = \frac{F_c\cos\phi\sin\phi - F_t\sin^2\phi}{Wt_0}$ (5)

Cutting force: $F_c = N\cos\alpha + F\sin\alpha$ (6)

Thrust force: $F_t = F\cos\alpha - N\sin\alpha$ (7)

Normal force $N = F_c\cos\alpha - F_t\sin\alpha$ (8)

Friction force: $F = F_c\sin\alpha + F_t\cos\alpha$ (9)

Coefficient of friction: $\mu = \frac{F}{N} = \frac{F_c\sin\alpha + F_t\cos\alpha}{F_c\cos\alpha - F_t\sin\alpha} = \frac{F_t + F_c\tan\alpha}{F_c - F_t\tan\alpha}$ (10)

2. EXPERIMENTAL SET-UP AND PROCEDURES

A schematic diagram of the experimental set-up and data acquisition system for the orthogonal cutting of a tubular workpiece is shown in Figure 2. All machining operations were carried out on an Okuma LB15 CNC turret lathe. The workpiece material used in this experiment was α-β titanium alloy Ti-6Al-4V; its physical property and chemical composition are listed in Tables 1 and 2, respectively. A Ti-6Al-4V tube with an outer diameter of 50.8 mm, length of 88.9 mm and constant wall thickness of 3.175 mm were machined from solid bars and used as the workpiece, as shown in Figure 2.

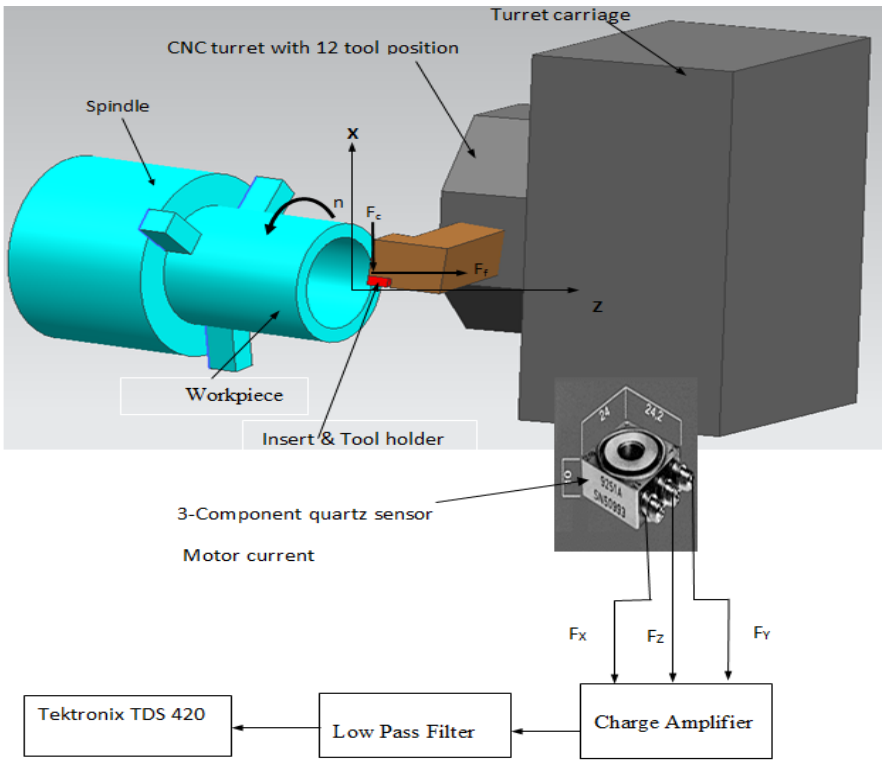

Figure 2. Schematic Diagram of the Experimental Set-up and Data Acquisition System for Orthogonal Turning

Table 1. Physical Properties of Titanium Alloy Ti-6Al-4V

Density $g.cm^{-3}$	Melting Point ^0C	Young's modulus (GPa)	Poisson ratio	Shear modulus (Gpa)	Electrical Resistivity $n.\Omega.m^{-1}$	Thermal Conductivity $(w.m^{-1}.k^{-1})$	Corrosion resistance
4.506	1668	116	0.32	44	420	21.9	<1

Table 2. Chemical Composition of Titanium Alloy Ti-6Al-4V

Titanium Ti-6Al-4V	Ti	Mo	V	Al	C0	Cr	Fe	Si	C
Elements (%)	88	6.3	3.0	2.0	0	0	0	0	0

The tubular workpiece was rotated at the selected cutting speed about its central axis, and the straight-edge cutting tool insert was fed directly into the workpiece parallel to the axial direction, thus continuously shortening the length of the tube by removing a chip from its end surface. Thus the condition of cutting by a single edge is satisfied, where the tube wall thickness becomes the chip width, w, and the uncut chip thickness, t_o, is equal to the feed per revolution of the tubular workpiece, f_r. A screw-on, high positive, uncoated tungsten carbide (WC/Co) inserts (CPGT3251HP K313) with a 5^0 rake angle, and inserts (CPGT3251LF K313) with 15^0 rake angle, as well as a PVD TiAlN coated carbide inserts (CPGT3251HP KC5010) with a 5^0 rake angle and inserts (CPGT3251LF

KC5010) with 15^0 rake angle, were used in the machining experiments. Each of the uncoated and coated carbide tools has two cutting edges with relief angle of 7^0.

The CNC program containing the G and M codes for machining one test run is given below:

```
G00 X2.1 Z0.1 S240 T010101 M41 M03
G00 X1.494
G01 Z-0.05 F0.1
G00 Z0.05
G00 X7 Z8 M05
```

For each experiment, axial machined length of L = Z = -1.27 mm (-0.05 in.) was made, with a new cutting edge at each selected feedrate to eliminate the effect of tool wear. Each condition was replicated once with the same cutting edge to reduce experimental error under all cutting conditions. Two cutting speeds (120 and 240 m/min) and three feedrates (0.05, 0.075, and 0.1 mm/rev) were investigated. At a cutting speed of 120m/min, uncoated carbide tools with 5^0, and 15^0 rake angles were used to cut the workpiece for the three selected feedrates; each cut was replicated once. To maintain consistency, the initial position (zero) was reset for every cut. At a high cutting speed of 240m/min, the same processes were performed for the same uncoated tools with 5^0 and 15^0 rake angles, respectively. The same procedures were carried out for coated carbide tools with 5^0 and 15^0 rake angles, respectively. In all the cuttings, a large amount of emulsion coolant was flooded at the cutting zone at low pressure to serve as a coolant and lubricant, and to reflect actual practices in manufacturing industries, unlike most experiments reported in the literature, which were conducted under dry conditions.

During these cutting tests, chips were collected and later their thicknesses were measured at three different cross-sectional points along its length. The average thickness per sample per test condition was obtained, recorded for all the cutting conditions and replications, and used for further calculations. Chip thickness was measured using a Neiko 01407A Stainless steel 6–inch digital caliper with extra-large LCD screen. Tables 3, 4, 5 and 6 show all the experimental plans and the measured and calculated parameters.

Table 3. Machining Parameters, Measured and Calculated Cutting Forces and Friction Coefficients at V=120m/min Using Uncoated Tool Inserts

Test No.	Rake Angle (^{0})	Feed rate (mm/rev) to = f [in/rev]	Chip thickness t_c (mm) [in]	Cutting ratio $r = t_o/t_c$	F_c (N)	$F_t = F_f$ (N)	ϕ (^{0})	Coeff. of friction μ	F_s (N)	Shear stress τ_s
1	5	0.05 [0.002]	0.003	0.67	1078	318	35.81	0.39	688.16	1.16E6
2	5	0.075 [0.003]	0.0043	0.71	1515	477	37.80	0.41	909.28	1.48E6
3	5	0.1 [0.004]	0.0058	0.70	1897	552	37.16	0.39	1178.28	1.42E6
4	15	0.05 [0.002]	0.0028	0.74	700	152	43.98	0.52	398.39	1.11E6
5	15	0.075 [0.003]	0.0038	0.81	979	267	48.13	0.58	454.60	904970
6	15	0.1 [0.004]	0.006	0.67	1643	586	39.81	0.69	886.92	1.13E6

Table 4. Machining Parameters, Measured and Calculated Cutting Forces and Friction Coefficients at 240m/min Using Uncoated Tool Inserts

Test No.	Rake Angle (^{0})	Feed rate (mm/rev) to = f [in/rev]	Chip thickness t_c (mm) [in]	Cutting ratio $r = t_o/t_c$	F_c (N)	$F_t = F_f$ (N)	ϕ (^{0})	Coeff. of friction μ	F_s (N)	Shear stress τ_s
1	5	0.05 [0.002]	0.0028	0.74	1091	235	38.91	0.31	701.34	1.76E6
2	5	0.075 [0.003]	0.0043	0.71	1749	424	37.60	0.34	1127.01	1.83E6
3	5	0.1 [0.004]	0.0053	0.77	2023	490	40.16	0.34	1229.18	1.59E6
4	15	0.05 [0.002]	0.003	0.67	1015	305	39.81	0.62	584.42	1.50E6
5	15	0.075 [0.003]	0.0035	0.86	1128	329	51.09	0.61	467.70	966311
6	15	0.1 [0.004]	0.0058	0.70	1521	470	41.60	0.63	825.36	1.09E6

Table 5. Machining Parameters, Measured and Calculated Cutting Forces and Friction Coefficients at 120m/min Using Coated Tool Insert

Test No	Rake Angle (^{0})	Feed rate (mm/rev) to = f [in/rev]	Chip thickness t_c (mm) [in]	Cutting ratio $r = t_o/t_c$	F_c (N)	$F_t = F_f$ (N)	ϕ (^{0})	Coeff. of friction μ	F_s (N)	Shear stress τ_s
1	5	0.05 [0.002]	0.0028	0.74	1324	293	38.91	0.32	846.22	2.13E6
2	5	0.075 [0.003]	0.004	0.77	1716	386	40.19	0.32	1061.77	1.83E6
3	5	0.1 [0.004]	0.0045	0.89	1969	551	45.06	0.38	1000.81	1.42E6
4	15	0.05 [0.002]	0.003	0.67	842	216	39.81	0.56	508.51	1.30E6
5	15	0.075 [0.003]	0.0045	0.67	1173	293	39.81	0.56	713.47	1.21E6
6	15	0.1 [0.004]	0.0053	0.77	1710	810	45.76	0.85	621.71	90000

Table 6. Machining Parameters, Measured and Calculated Cutting Forces and Friction Coefficients at 240m/min Using Coated Tool Insert

Test No	Rake Angle (^{0})	Feed rate (mm/rev) to = f [in/rev]	Chip thickness t_c (mm) [in]	Cutting ratio $r = t_o/t_c$	F_c (N)	$F_t = F_f$ (N)	φ (0)	Coeff. of friction μ	F_s (N)	Shear stress τ_s
1	5	0.05 [0.002]	0.0028	0.74	1729	435	38.91	0.35	1072.17	2.69E6
2	5	0.075 [0.003]	0.0038	0.81	1914	563	41.86	0.39	1049.81	1.87E6
3	5	0.1 [0.004]	0.0053	0.77	2603	702	40.19	0.37	149.53	1.98E6
4	15	0.05 [0.002]	0.003	0.67	1154	336	39.81	0.21	671.35	1.72E6
5	15	0.075 [0.003]	0.004	0.81	1582	373	39.81	0.54	899.55	1.64E6
6	15	0.1 [0.004]	0.005	0.81	1961	518	43.13	0.57	1077.01	1.47E6

Solid titanium alloy Ti-6Al-4V round bars of 50.0mm (2 inches) in diameter and 88.9 mm (3.5inches) in length were bought and pre-machined into hollow round bar (tubular) workpieces with 3.175 mm wall thickness to simulate orthogonal turning, as shown clamped in the CNC lathe chuck in Figure 3, to simulate orthogonal cutting.

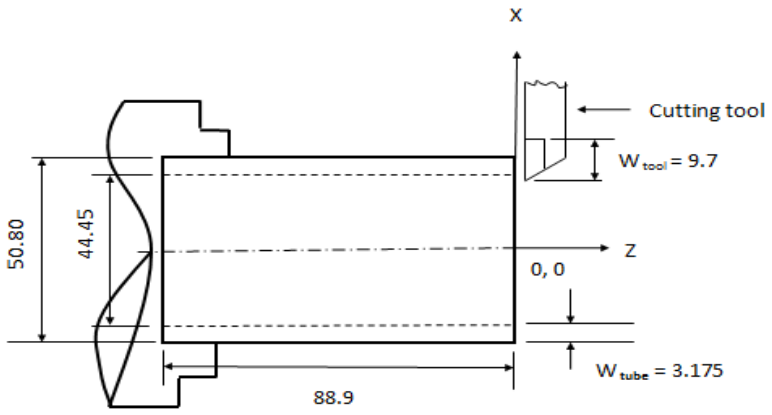

Figure 3. Titanium Alloy Tube Workpiece Clamped in the Lathe Chuck to Simulate Orthogonal Turning

According to the popular chip classification developed by ISO 3685 and issued in 1977, chip types usually have the following forms: straight ribbon, tubular, corkscrew (washer), and conical helical. Based on this definition, chips obtained in this study varied depending on the cutting conditions. In Figure 4, (a) shows a conical helical chip obtained under a low cutting speed of 752 rpm (120 m/mins) and a feedrate of 0.075mm/rev, (b) shows a spiral chip obtained under a high cutting speed of 1504 rpm (240 m/min)and a feedrate of 0.05mm/rev, and (c) shows the corkscrew (washer) chip obtained under a low cutting speed of 752 rpm (120 m/min) and a feedrate of 0.1 mm/rev.

(a)  (b)  (c) 

Figure 4. Chip Morphologies
(a) Conical helical chips, v = 120m/mins, feedrate = 0.075mm/rev, (b) Spiral chips, v = 240m/mins, feedrate = 0.05mm/rev, (c) Corkscrew (washer) chips, v = 120m/mins, feedrate = 0.1mm/rev

2.1. CALIBRATION OF THE FORCE MEASUREMENT SYSTEM

Before calibrating the force measurement system to establish the relationship between cutting tool-tip forces (feed, radial, and tangential) with the measured X, Y, and Z force load cell outputs, a 3-axis Kistler load cell (model number 9251A) was installed on the machined slot using a Kistler preloading wedge (model number 9463) by Okafor and Ukpong [1998]. Preloading the load cell at mounting with the specified 25 KN load limit was necessary to allow shear transmission through friction. Once installed, the load cell becomes a permanent fixture of the machine tool structure and requires no maintenance. Calibrating the measuring system is not only necessary for establishing the tool's point-load cell output force relationship; it is also a vital step for checking the behavior of the transducer to the applied forces. Figure 5 offers a picture of the experimental set-up of the calibrations, while Figures 6a, 6b and 6c show the schematic diagrams of the calibration set-up for the feed, radial and tangential axis, respectively. Calibration was carried out using a steel clamp plate specially fabricated in-house. Each axis has a different fixture for loading and unloading. A Kistler 9212 single-axis load cell was mounted on top of a pro-lift hydraulic jack, which in turn was mounted on the respective steel clamp plate fixture and used to apply loading and unloading forces at the tool tip in the respective coordinate directions for tools (1) used for the orthogonal cutting experiment.

Figure 5. Set-up for the Calibration of the Load Cell

(a)

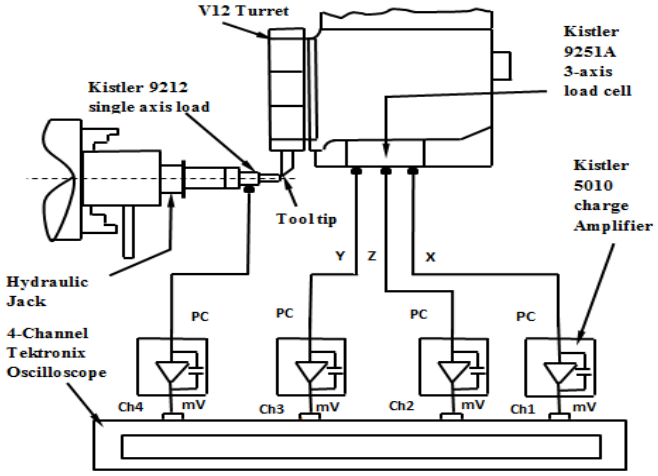

(b)

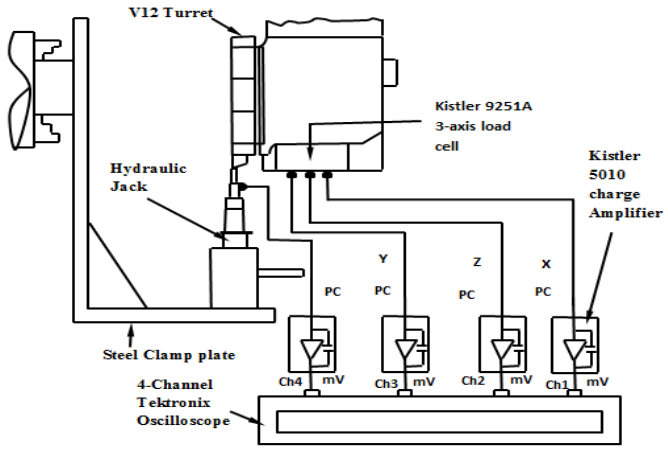

(c)

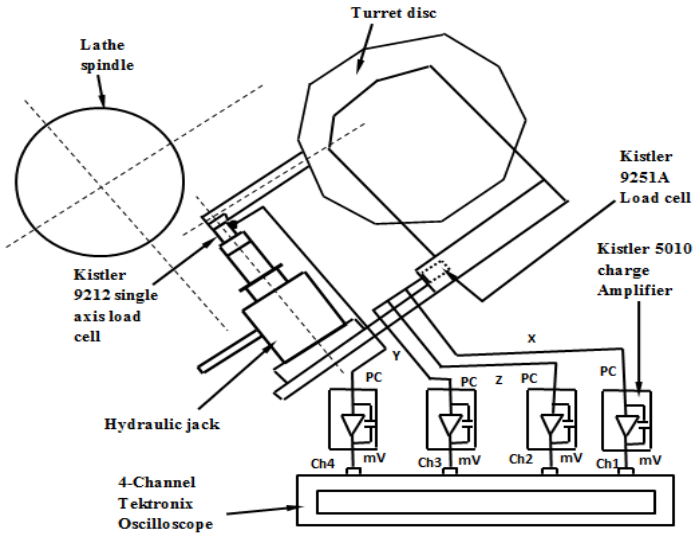

Figure 6. Calibration Set-up: (a) Feed axis, (b) Radial axis (c) Tangential axis

Calibration was performed for different turret positions because the position of the tool in the X, Y, and Z coordinates obviously affects the point of force application on the structure. For the loading and unloading cycles, the single axis transducer, Kistler 9212 output and 3-axis Kistler 9251A load cell output were passed through a Kistler 5010 dual-mode amplifier and were acquired using a 4-channel Tektronix TDS 420A oscilloscope. The sensitivity of the single-axis Kistler 9212 transducer was set to 11.24 pC/N (50pC/N); the sensitivities of the 3-axis Kistler 9251A load cell were set to 8 pC/N in the X and Y axis components and to 4 pC/N in the Z axis component of the Kistler 5010 dual-mode amplifier. The X, Y and Z output components of the charge amplifier were connected to Channels 1, 2, and 3 of the Tektronix oscilloscope, respectively, while the transducer output was connected to Channel 4 of the Tektronix oscilloscope, as was shown in Figure 5. The vertical scales of Channels 1 and 2 were set to 200mV/division each in the Tektronix TDS 420A oscilloscope at the scale of 1000 mechanical units (MU) per volt in the charge amplifier, Channel 3 was set to 500mV/division at 2000 mechanical units (MU/Volt), and Channel 4, which is connected to the transducer, was set to 1Volt/division in the Tektronix TDS 420A oscilloscope at the scale of 4000 mechanical units (MU/Volt) in the charge amplifier. A sampling rate of 50Hz, 1000 data points and a trigger level of 20mV were used during the calibration process. Each axis was calibrated by applying an unspecified unilateral load on the handle of the pro-lift hydraulic jack (model number B-002 NC) until it reached maximum loading. The unloading was observed when the continuous unilateral load on the pro-lift hydraulic jack caused no further significant increment. At this point, the wave signals were acquired using the 4-channel Tektronix oscilloscope. The same procedure was repeated for all the axes of Tool

1. The calibration load limit used does not prevent higher values of force from being used on the lathe, but does allow better accuracy to be obtained in the normal working range for tool status monitoring.

Figures 7, 8, and 9 show the applied load versus time and the transducer force response for the feed, radial and tangential tool-tip coordinates, respectively, for Tool 1. The data were processed using a moving average period of 20 for each signal captured.

Particularly interesting was the unusual behavior of the load cell during the tangential and radial axes loading and unloading of the turret-tool tip. For higher load limits, the turret housing behaved as if it were to be lifted off the bolted base, so the transducer attempted to mimic the profile. Linearity was kept in check by applying lower load limits for both axes. Figures 10, 11, and 12. show the load cell force response and applied force relationships for the 3-coordinate directions using Tool 1. The data were processed using a polynomial of 5 degrees. The loading and unloading follows similar trends in nearly all cases, thus indicating a desirable linear transducer response.

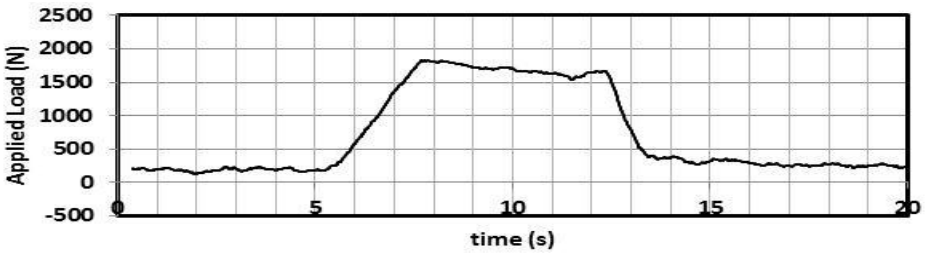

(a)

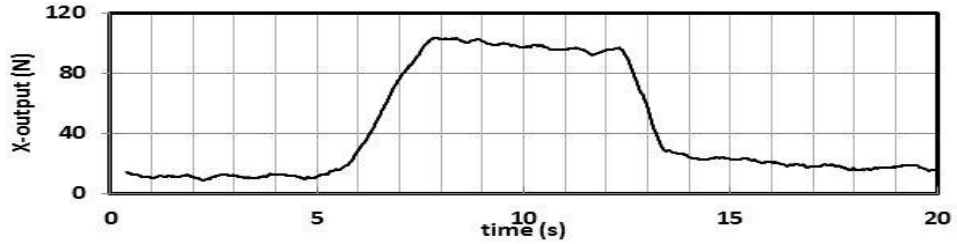

(b)

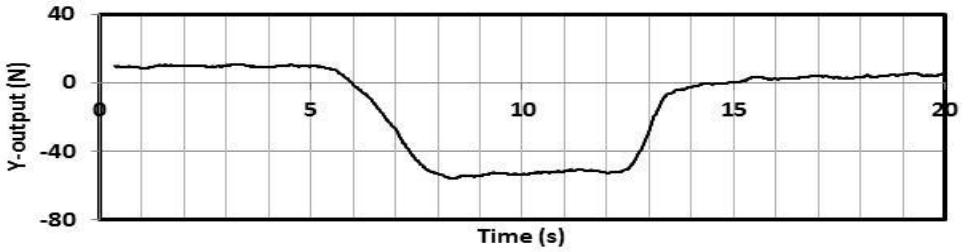

(c)

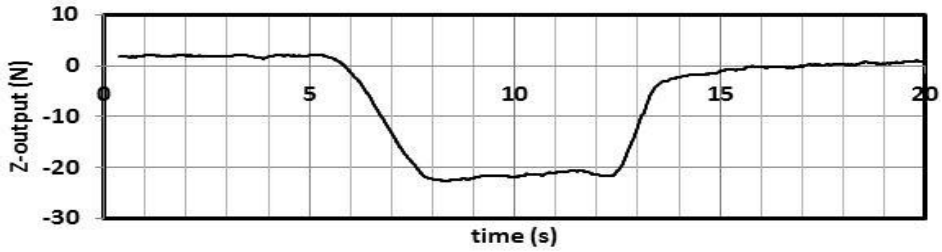

(d)

Figure 7. Feed Axis Calibration for Tool 1: (a) Load Cell Input, (b) X-output, (c) Y-output, (d) Z-output

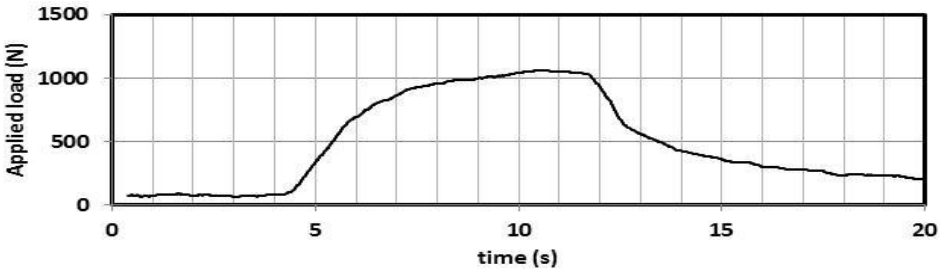

(a)

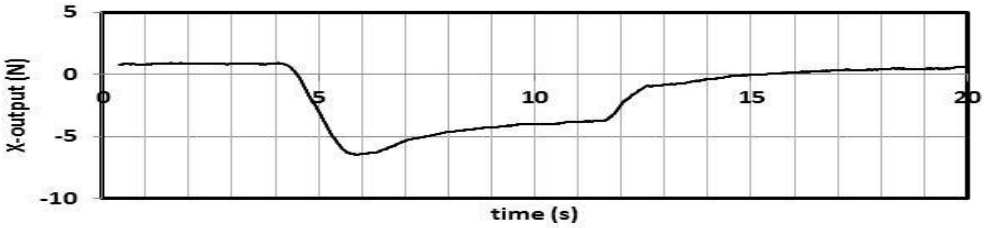

(b)

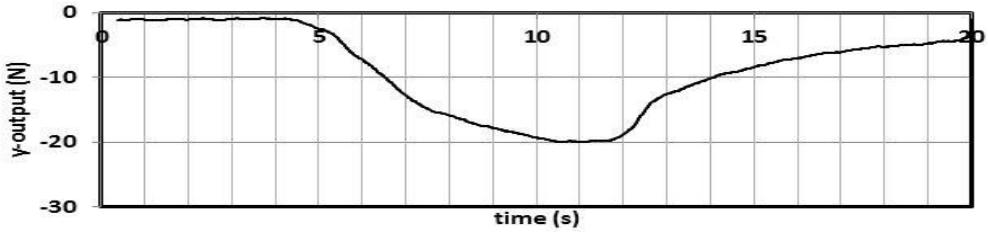

(c)

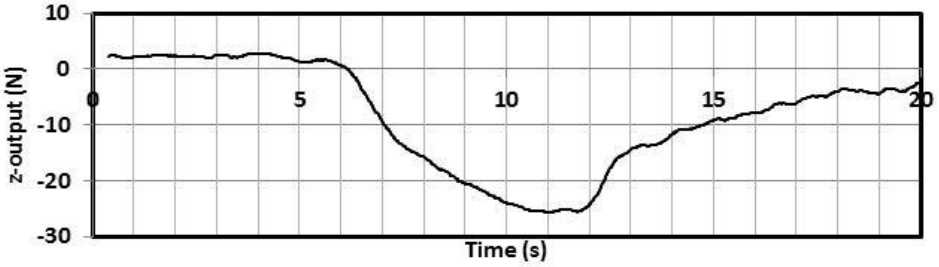

(d)

Figure 8. Radial Axis Calibration for Tool 1: (a) Load Cell Input, (b) X-output, (c) Y-output, (d) Z-output

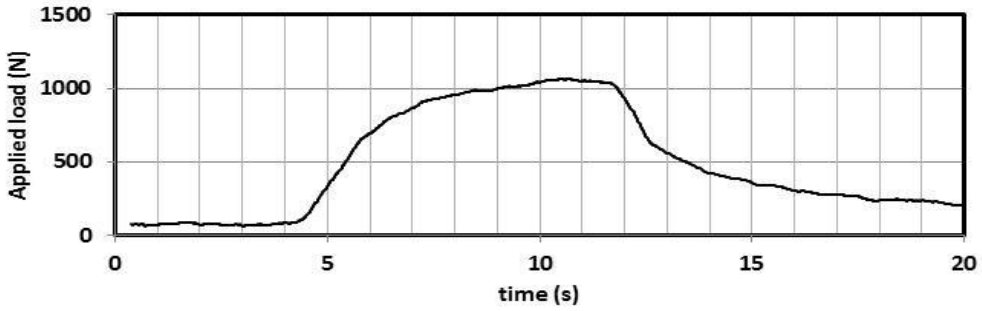

(a)

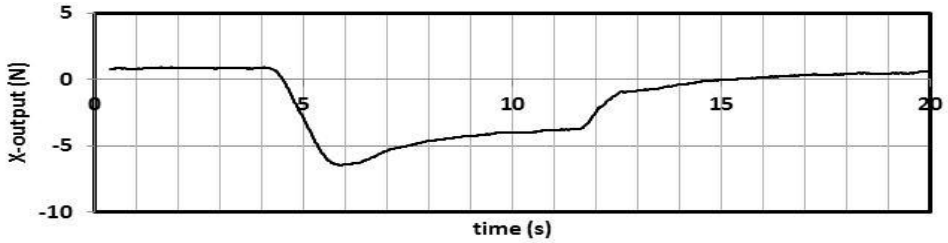

(b)

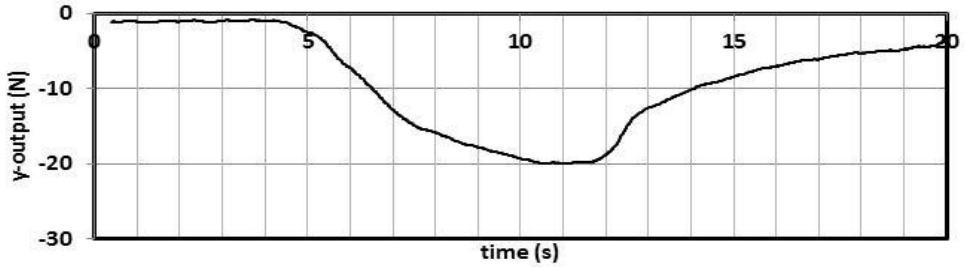

(c)

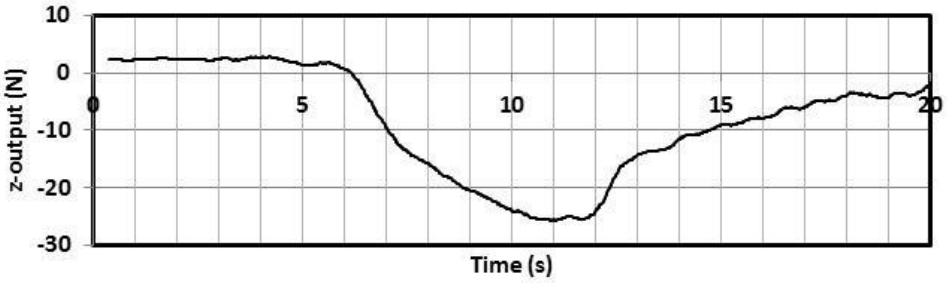

(d)

Figure 9. Tangential Axis Calibration for Tool 1: (a) Load Cell Input, (b) X- output, (c) Y-output and (d) Z-output

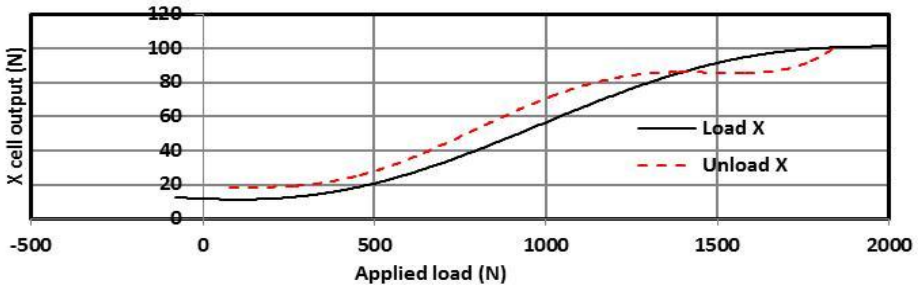

(a)

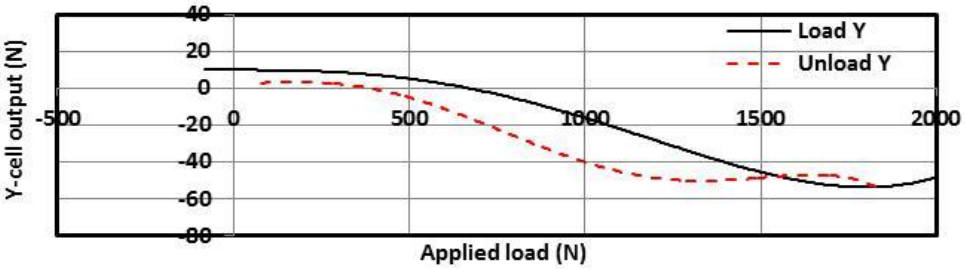

(b)

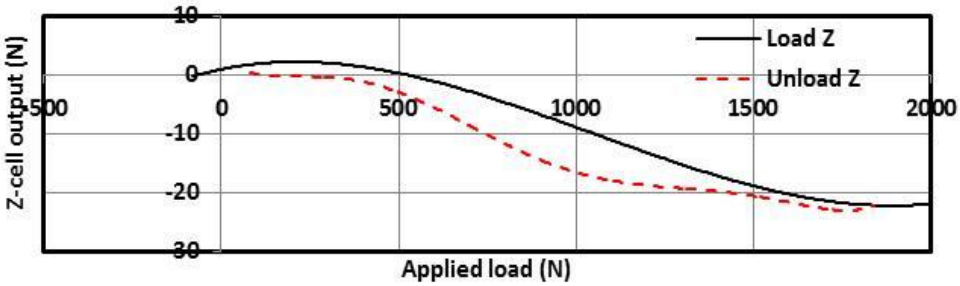

(c)

Figure 10. Load Cell Response to Applied Load (Feed Axis, Tool 1): (a) X-axis Cell Output, (b) Y-axis Cell Output, (c) Z-axis Cell Output

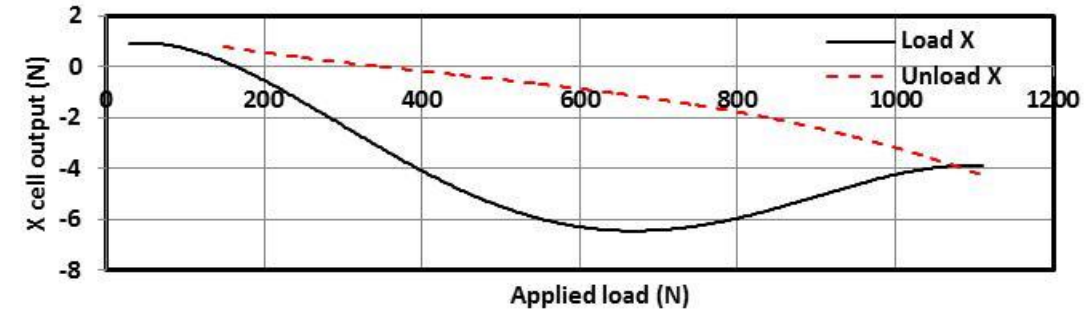

(a)

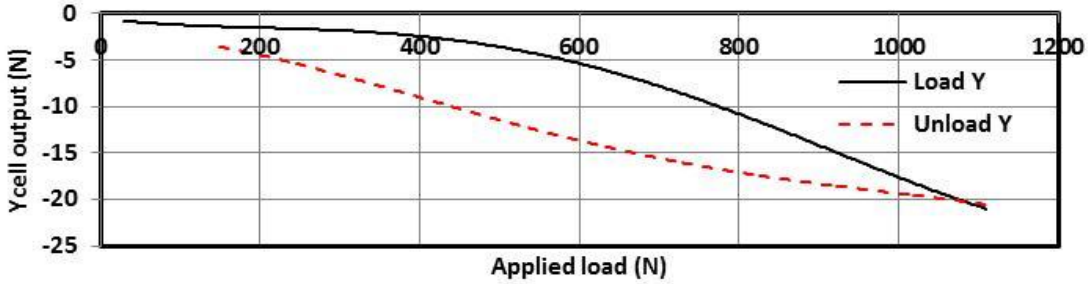

(b)

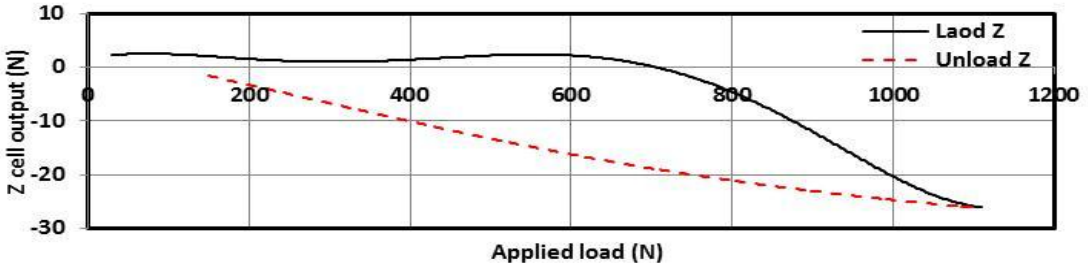

(c)

Figure 11. Load Cell Response to Applied Load (Radial Axis, Tool 1): (a) X-axis Cell Output, (b) Y-axis Cell Output, (c) Z-axis Cell Output

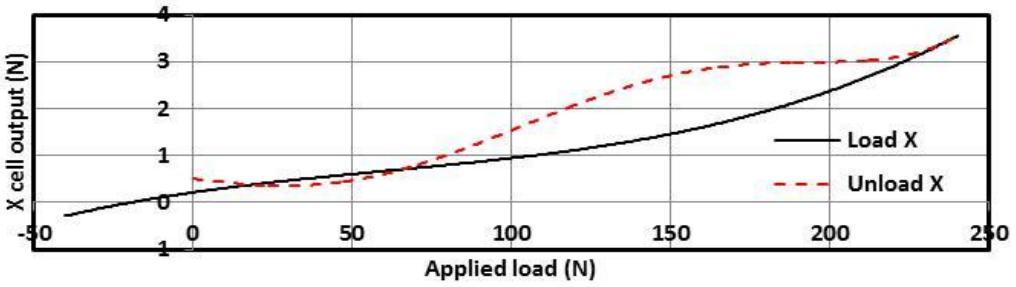

(a)

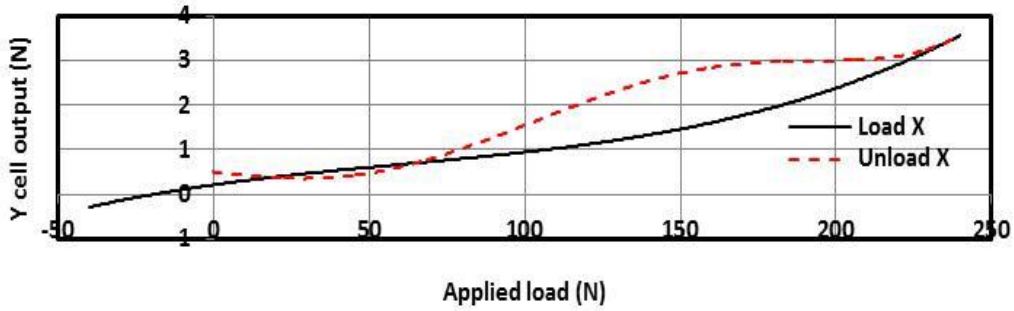

(b)

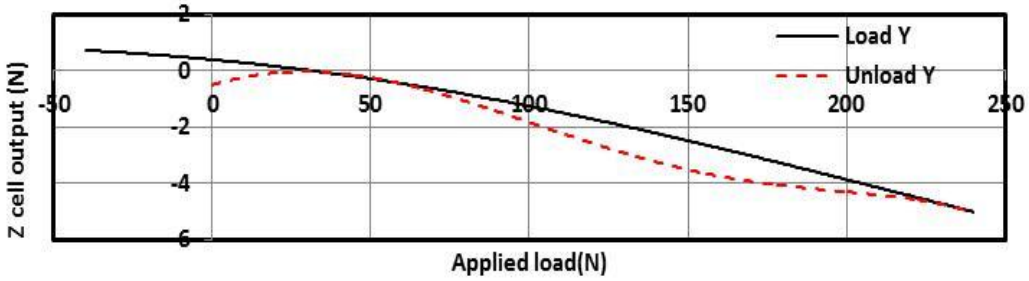

(c)

Figure 12. Load Cell Response to Applied Load (Tangential Axis, Tool 1): (a) X-axis Cell Output, (b) Y-axis Cell Output, (c) Z-axis Cell Output

2.2. MULTIPLE REGRESSIONS TO ESTABLISH CALIBRATION MATRIX

The following linear relationships are assumed to exist between the cutting forces at the tool tip (feed, radial and tangential) and the corresponding transducer (X, Y, and Z) measured force outputs.

$$F_f = A_f f_x + B_f f_y + C_f f_z \quad (11)$$

$$F_r = A_r f_x + B_{rfy} + C_{rfz} \quad (12)$$

$$F_t = A_t f_x + B_t f_y + C_t f_z \quad (13)$$

Where F_f, F_r, and F_t are the feed, radial and tangential cutting forces at the tool tip, respectively. For the orthogonal cutting of the titanium tube, the feed force F_f = the thrust force (F_t), and the tangential force F_t = the cutting force, F_c ; f_x, f_y, and f_z are the measured load cell output forces in the X, Y and Z load cell coordinates, respectively, and A_f, B_f, And C_t are the parameters to be estimated.

A simple least square model fitting technique was applied to each respective loading/unloading data record using STATISTICA^{TM} software from StarSoft^{R}. The calibration equations for Tool 1 become:

$$F_t = F_f = 71 + 12f_x - 0.3f_y - 20f_z \quad \ldots. R^2 = 0.9621 \quad (14)$$

$$F_r = 77.4 - 59f_x - 36f_y - 1f_z \quad \ldots. R^2 = 0.9889 \quad (15)$$

$$F_c = F_t = 56 - 14f_x - 32f_y - 4f_z \quad \ldots. R^2 = 0.9461 \quad (16)$$

The normal probability plot and residual plot for the regression are given in Figures 13a and b, which again confirms the adequacy of the regression models.

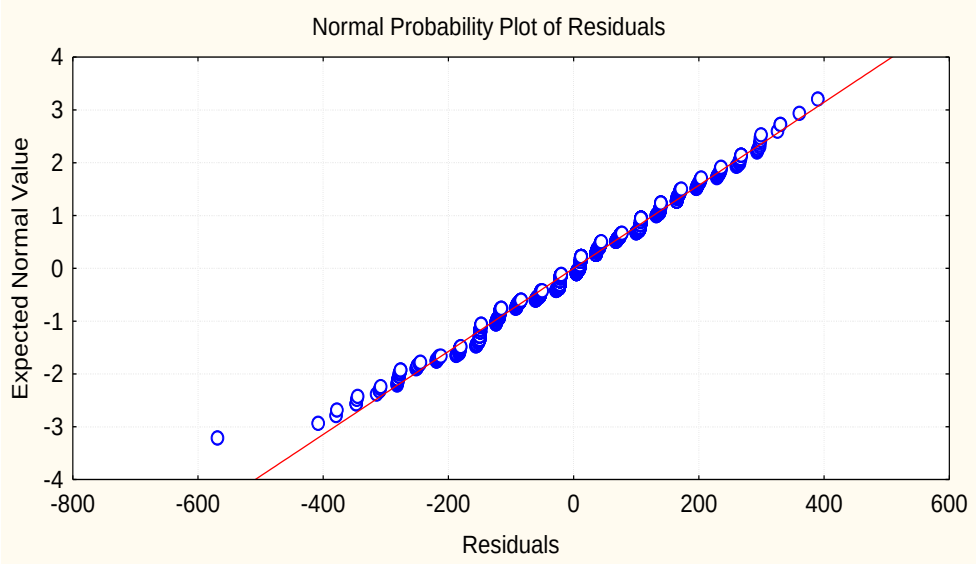

(a) Normal probability plot

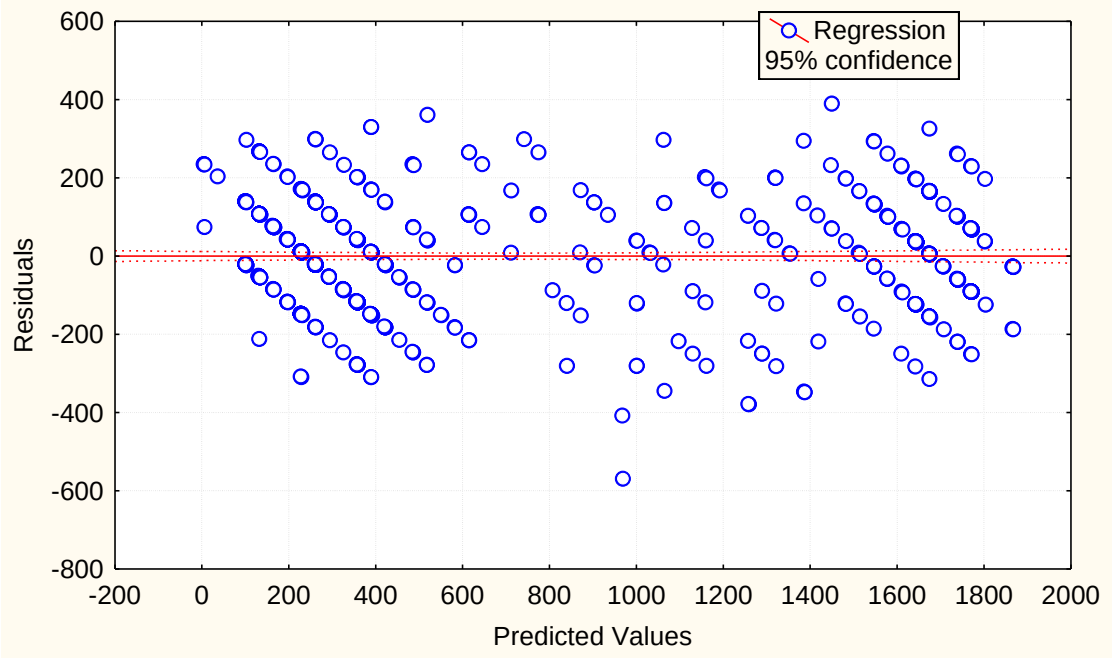

(b) Residual plot

Figure 13. Tool 1 Feed Axis Calibration

2.3. OVERVIEW OF THE CUTTING FORCE MEASUREMENT SYSTEM

It is known for orthogonal cutting that the X-component (radial-component) of force is theoretically zero. Preliminary tests show that this assumption is practically valid. The X- component of force is always less than 2% of the Z-component (axial feed) of force. Therefore, this force component need not be recorded; it was only monitored online to insure the orthogonality of the cut. Only the Y- (thrust) and Z- (feed) components were recorded. A 3-axis Kistler 9251A load cell (f_x, f_y, f_z) output was connected to two dual-mode Kistler type 5010 charge amplifiers operated in charge mode with a long time constant. The outputs from the charge amplifier were connected to Channels 1, 2 and 3 of a Tektronix TDS 420 4-channel digitizing oscilloscope, where they were digitalized and acquired with the help of a floppy disk. A low pass filter of 2.2 KHz and a scale of 200 mechanical units per volt (mu/v) for the charge amplifier were carefully selected after due consideration of numerous preliminary tests. The triggering threshold used to trigger the oscilloscope was 20 mv. The filtered signals then were acquired in a Tektronix TDS 420 digitizing oscilloscope with a sampling frequency set to 2.5 KHz and record length of 5000 data points. This combination of sampling frequency and record length allowed for an acquisition window of 2 seconds, as shown in Figures 14 and 15.

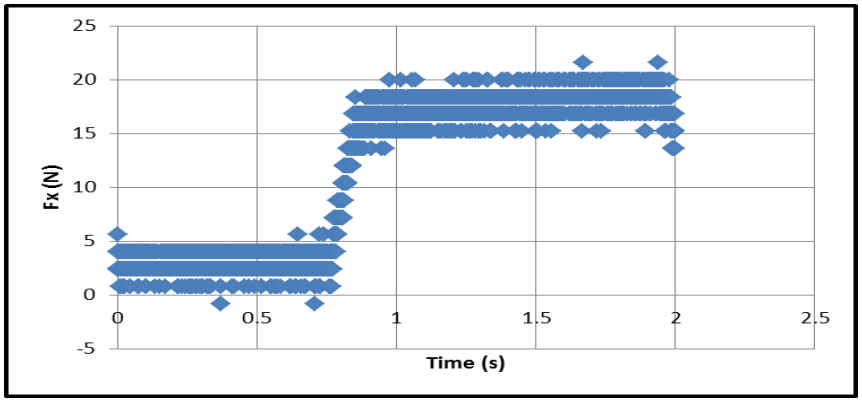

(a) Unprocessed F_x/feed signal

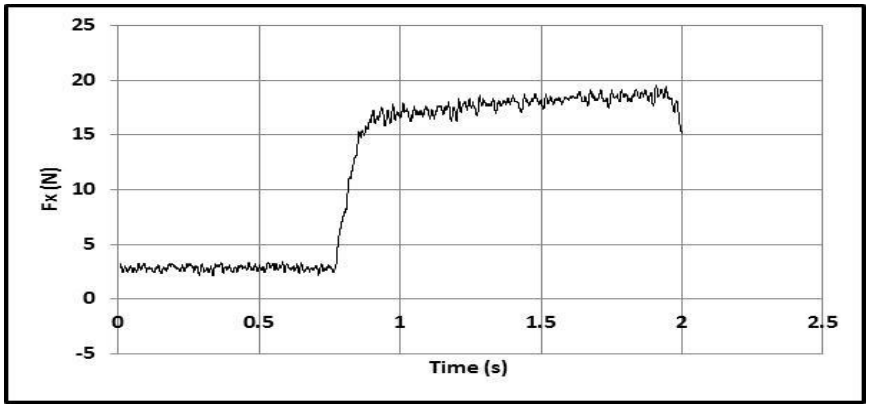

(b) Processed F_x/feed Signal

Figure 14. Unprocessed and Processed F_x/feed Signal

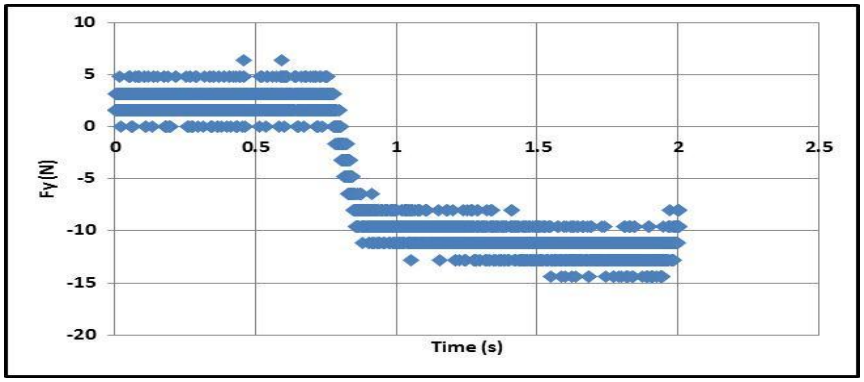

(a) Unprocessed Fy/tangential signal

Figure 15. Unprocessed and Processed Fy/tangential Signal

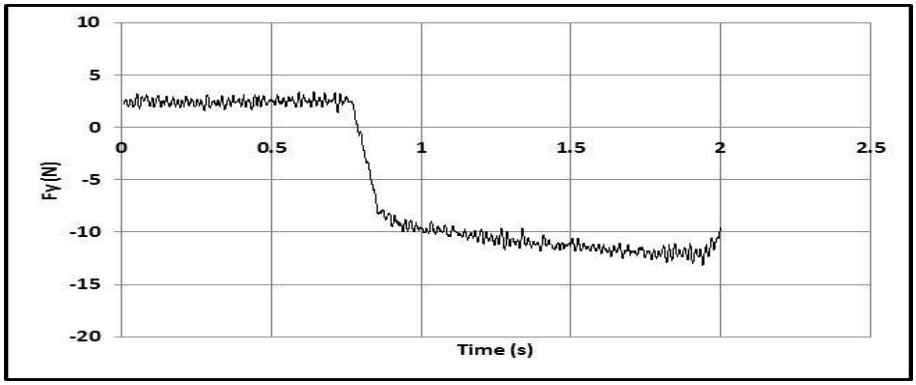

(b) Processed Fy/tangential signal

Figure 15. Unprocessed and Processed Fy/tangential Signal (cont.)

Figures 14 and 15 show that each force trace exhibits an initial overshoot, which corresponds to the entry of the cutting tool into the workpiece, and the subsequent, relatively constant force corresponds to the steady state force. The steady state force condition is maintained until the tool exits the workpiece.

2.4. SIGNAL PROCESSING

The digitized cutting force signals were acquired and saved on a floppy disk and later processed via a Dell desktop computer with the Windows Vista operating system and Microsoft Office 2010. The data were processed in MS Excel 2010 to remove extraneous noise. Figures 14 and 15 show the unprocessed and processed signals for the cutting forces in the feed (Fx) and tangential (Fy) direction, respectively. A moving average value of 20 was used for processing in order to eliminate the fluctuations in the cutting force signals due to the interaction of chips with the tool. The forces at the tool tip were calculated using the relationship (equations 14 -16) developed by Okafor and

Onyishi during the calibration process. The following equations give the relationship between the cutting forces at the tool tip and the corresponding Kistler 9251A load cell force output.

$$F_t = F_f = 71 + 12f_x - 0.3f_y - 20f_z \quad \ldots R^2 = 0.9621 \quad (17)$$

$$F_r = 77.4 - 59f_x - 36f_y - 1f_z \quad \ldots R^2 = 0.9889 \quad (18)$$

$$F_c = F_t = 56 - 14f_x - 32f_y - 4f_z \quad \ldots R^2 = 0.9461 \quad (19)$$

Even though three equations were generated during the calibration process, F_r, the radial direction of the force components, was discarded and not recorded due to the orthogonal nature of the experiment, as stated previously.

The physical properties and chemical composition of the titanium alloy are listed in the Tables 1 and 2 above, respectively. Table 7 gives the summary machining parameters used for the orthogonal cutting tests.

Table 7. Summary of Machining Parameters Used for the Orthogonal Cutting Tests

Tool holder	SGCR163 with 0^0 rake angle
Cutting tool insert	CPGT3251HP KC5010 and CPGT3251LF KC5010
	CPGT3251HP K313 and CPGT3251LF K313
Rake angles	5^0 and 15^0
Relief angles	7^0
Cutting speeds	120 and 240 m/mins
Feedrates	0.05, 0.075 and 0.1 mm/rev
Radial in-feed	1.27mm
Coolant	Flooded emulsion coolant

3. RESULTS AND DISCUSSION

The determined calibration equations 14, 15, and 16, giving the relationship between the cutting forces (thrust force, radial force, and the cutting force) at the tool tip and the corresponding Kistler 9251A load cell force outputs were used to estimate the cutting force and thrust force from load cell force measurements during the orthogonal turning tests, and the results are reported in Tables 3, 4, 5, and 6, columns 6 and 7 for all the test conditions investigated. These experimentally determined cutting forces (F_c, F_t) along with the given machining parameters (rake angles, undeformed and deformed chip thickness), Table 4, were used to calculate the shear angle, coefficient of friction, shear force, friction force and shear stress, using the derived equations 1-10. The calculated values are also reported in Tables 3, 4, 5, and 6, as well as the machining parameters. The effect of machining parameters on cutting forces, shear angle and friction are plotted in Figures 16, and 17.

3.1. EFFECTS OF FEEDRATE ON CUTTING FORCES

The plots of cutting force and thrust force as function of feedrate at low cutting speed of 120 m/min for uncoated and coated tool with 5^o rake is shown in Figure 16a. It is seen from Figure 16a and Tables 4 and 6 that both cutting force and thrust force increases with increase in feedrate for uncoated tungsten carbide (W/Co) and WC/Co PVD coated inserts. This is because the chip thickness and cutting ratio increases with increase in feedrate, thus requiring more force to deform the material, see 3^{rd} and 4^{th} column of Table 4. Uncoated tungsten carbide (WC/Co) inserts exhibit much lower cutting force than tungsten carbide (WC/Co) PVD coated with TiAlN. Also thrust force

is much lower than the cutting force. Similar increasing trends in cutting force and thrust force with increase in feedrate are obtained for both uncoated and coated tool inserts at higher cutting speed of 240 m/min and 5^o rake angle, Figure 16c, and Tables 4 and 6, but with higher force magnitudes than at lower cutting speed. Similar results were reported by Ozel et al. for orthogonal machining of Ti-6Al-4V but under dry machining condition. At higher rake angle of 15^0 the cutting forces also increase with increase in feedrate both at low cutting speed (120 m/min) and at higher cutting speed (240 m/min), but with lower maximum forces than those obtained with lower rake angle of 5^o,(Figures 16b and d). Shear force and friction force also increase with increase in feedrate. The lower cutting force resulted in a lower shear force and friction force.

3.2. EFFECTS OF CUTTING TOOL COATING ON CUTTING FORCES AND FRICTION

Figures 16 and Tables 3 – 6 indicate that cutting forces are greatly affected by cutting tool insert coating. As discussed above, lower cutting forces in all cases were obtained with uncoated tungsten carbide tool insert (WC/Co) than with WC/Co PVD coated TiAlN.

Both tools displayed similar trends with regards to increase of the cutting forces as the feedrate increases. As the feedrate increased from 0.05 to 0.1mm/rev, both the uncoated and coated cutting tool inserts exhibit large variations in the upward trending of cutting forces. This can be explained by the fact that the tool is subjected to larger cutting load. Therefore, more materials are removed at a higher feedrate than at a lower feedrate within the same machining time. From Tables 3 – 6, it is observed that at lower cutting speed, uncoated tool insert exhibits higher average friction coefficient at

low rake angle than coated insert, thus the coating serves to reduce friction; but at the higher rake angle and low cutting speed, coated tool exhibits higher average friction coefficient. On the other hand, for the case of higher cutting speed, uncoated insert gives lower average friction coefficient at low rake angle than coated inserts, but at higher rake angle, coated insert gives lower average friction coefficient than uncoated insert.

Based on the effect of insert coating of increasing cutting forces, and from the point of view of using high speed machining to decrease cutting forces, especially for monolithic machining of thin walls in titanium components used in aerospace structures, coated cutting tool inserts are not recommended for machining titanium alloys. Ezeugwu (2005) in his review of key improvements in the machining of difficult-to-cut aerospace superalloys, concluded that there is negligible difference between coated and uncoated carbide tools in terms of tool life, and therefore there is no tangible benefit in machining with coated carbide tools with associated additional cost of typically 15%. Cutting tool coatings serve as diffusion barriers, and they prevent the interaction between the chip formed during machining and cutting tool material. These coatings such as TiAlN are extremely hard, and thus very abrasion resistant. TiAlN has the added advantage of lowering coefficient of friction at higher cutting speed and higher rake angle compared to WC/Co.

3.3. EFFECTS OF RAKE ANGLE ON CUTTING FORCES AND FRICTION COEFFICIENT

From Table 3 – 6, for both the uncoated and coated tools, it is observed that an increase in the positive rake angle from 5^0 to 15^0 led to a decrease in the cutting force,

which agrees with what is reported in published literature regarding cutting tools with higher rake angles exhibiting lower cutting forces and power. This can be attributed to the drop in the shear strength in the primary shear deformation zone as the tool temperature rises, as well as to the decrease in the length of the shear plane and shear plane area. These results provide valuable information about the best rake angle to use for machining titanium alloy Ti-6Al-4V. Similarly, the thrust force, Ft, followed the same trend as Fc in all cases. Figures 16 show that the thrust forces were always lower than the main cutting force because more forces were being exacted on the feed direction. The result of this experiment also helps to explain why uncoated and coated tools of the same high positive (15^0) rake angles under the same cutting conditions (Figures 16b and 16d) did not generate equal cutting forces. The reason is because the coated tool mainly influences the tool-chip contact zone (secondary shear zone) due to its larger contact area, whereas the uncoated counterpart can plunge easily into the workpiece and produces a smaller contact area.

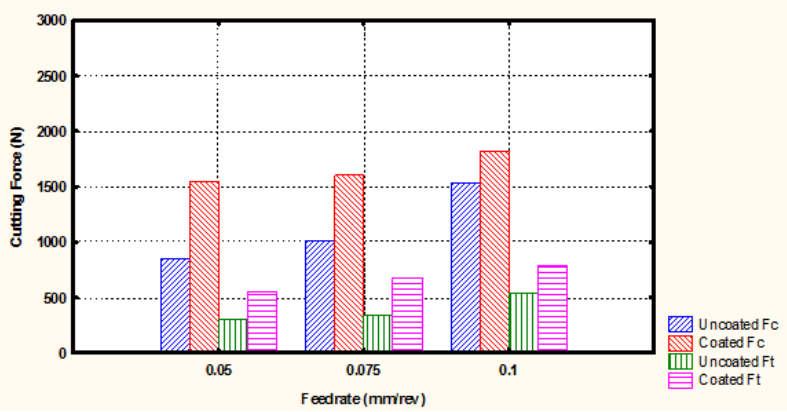

(a) Cutting tool with 5^o rake angle at cutting speed V= 120 m/min

Figure 16. Cutting Forces vs Feedrate in Orthogonal Turning

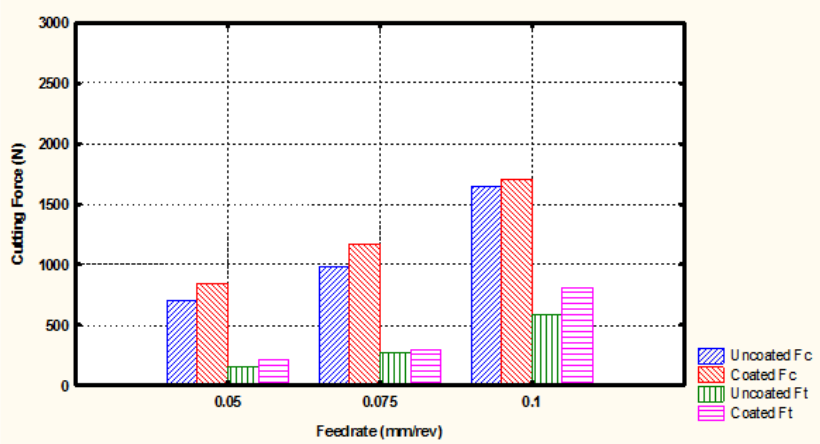

(b) Cutting tool with 15^{o} rake angle at cutting speed V= 120 m/min

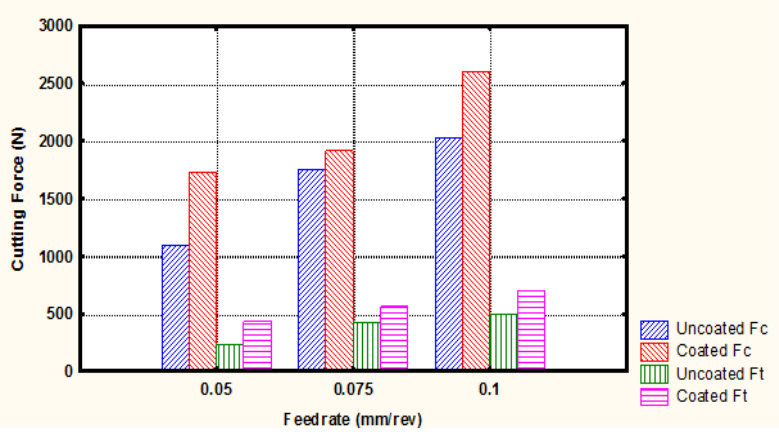

(c) Cutting tool with 5^{o} rake angle at cutting speed V= 240 m/min

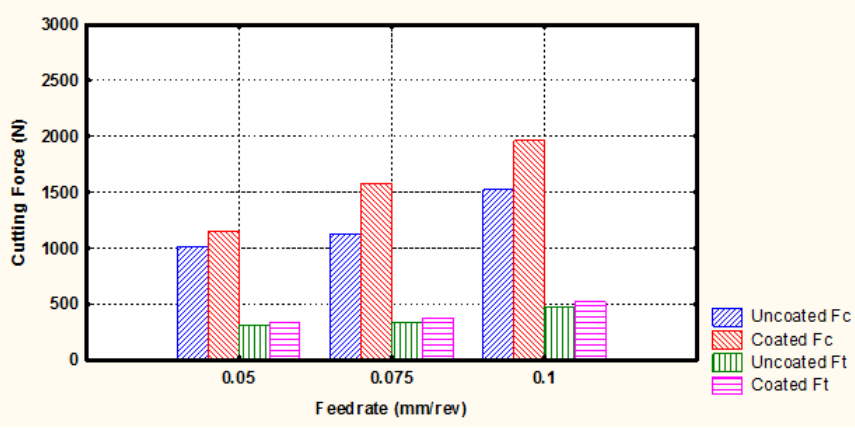

(d) Cutting tool with 15^{o} rake angle at cutting speed V= 240 m/min

Figure 16. Cutting Forces vs Feedrate in Orthogonal Turning (cont.)

3.4. EFFECT OF RAKE ANGLE ON SHEAR FORCE

Figure 17 shows that increasing the positive rake angles from 5^0 to 15^0 decreases the shear forces significantly at both low and high cutting speed, for the coated and uncoated tool insert. This occurs because positive rake angles produce larger shear angle and shorter shear plane and thus, less shear force, which helps to reduce the friction force and cutting forces, thus producing a better surface finish because it helps the chip to flow away from the workpiece material.

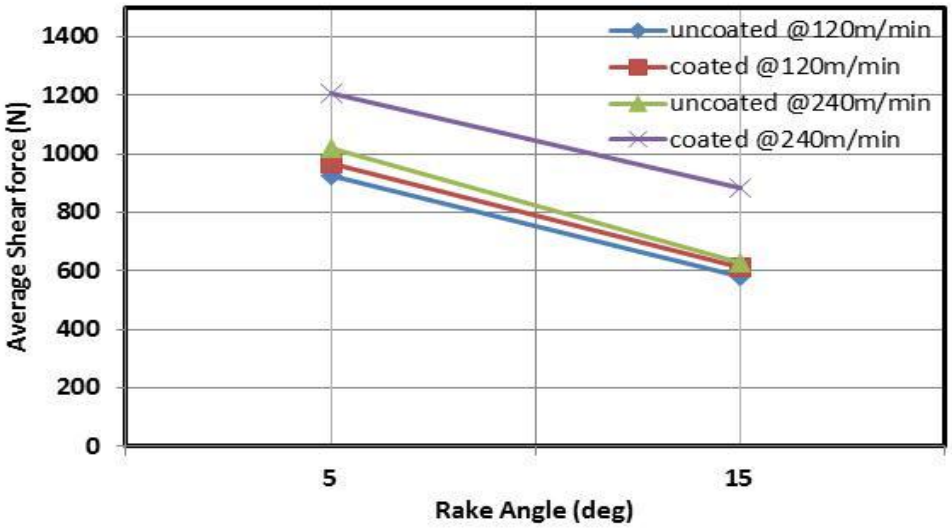

Figure 17. Average Shear Force vs Rake Angle

This result indicates that the machinability of titanium alloys could be improved by the use of cutting tools with higher positive rake angle.

3.5. EFFECT OF CUTTING SPEED ON MAIN CUTTING FORCE

The effect of cutting speed on main cutting force is plotted in Figure 18, which shows the average main cutting forces at two selected cutting speeds of 120 and 240 m/min for uncoated and coated cutting tools with 5^0 and 15^o rake angles. It is observed that the main cutting force increased with an increase in the cutting speed for both the uncoated and coated cutting tool inserts with 5^0 and 15^o rake angles.

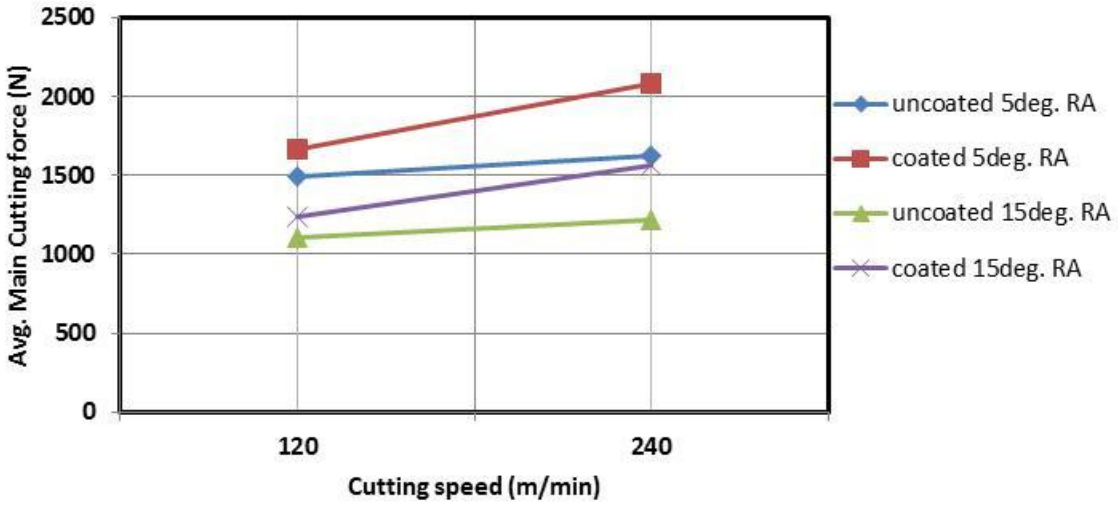

Figure 18. Average Cutting Force vs Cutting Speed

The coated cutting tool insert in general generate higher cutting forces. The uncoated tool inserts have similar rate of increase of cutting force with increase in cutting speed for the 5^0 and 15^o rake angles. Also coated tool inserts have similar rate of increase of cutting force with increase in cutting speed for the 5^0 and 15^o rake angles.

In general, the coated cutting tools generated higher cutting forces. This result of WC/Co PVD coated TiAlN tool insert generating higher cutting forces than uncoated WC/Co insert agree with the result reported by Srivastava et al. (2010) for similar material and cutting tool insert

3.6. EFFECTS OF FEEDRATES ON COEFFICIENT OF FRICTION

Figure 19 indicates that an increase in feedrates slightly increases the coefficient of friction, and increases in rake angles for both uncoated and coated cutting tools increases the coefficient of friction.

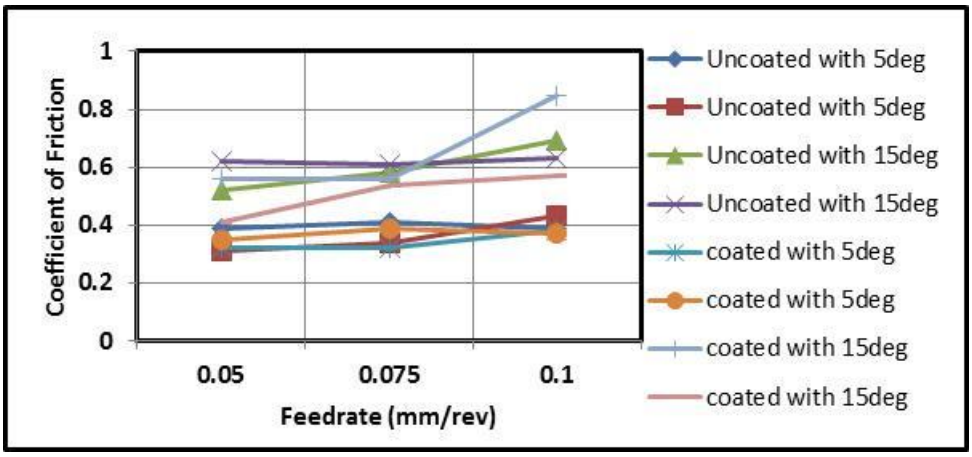

Figure 19. Coefficient of Friction vs Feedrate

3.7. EFFECTS OF FEEDRATES ON SHEAR ANGLE

Figure 20 shows that the shear angle increases significantly with an increase in the feedrate from 0.05 to 0.075 mm, but tends to decrease at the highest feedrate of 0.1

mm. Additionally, the shear angle shows remarkable increases with cutting tools with large rake angles but shows no noticeable increase with increases in cutting speed.

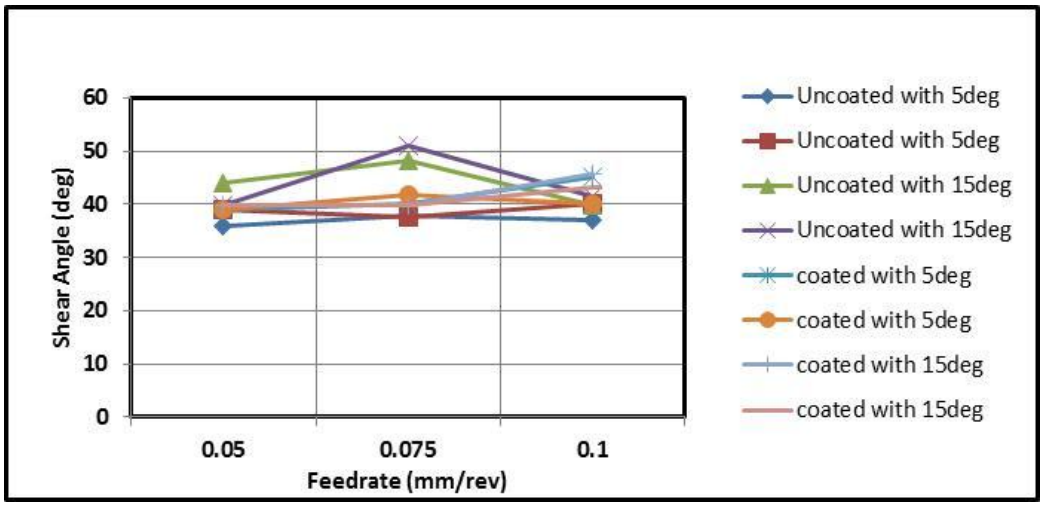

Figure 20. Shear Angle vs Feedrates

4. CONCLUSION

This paper investigated the effects of machining parameters on cutting forces, shear angle and friction during orthogonal turning of titanium alloy Ti-6Al-4V tube. From the results the following conclusions are made:

1. Cutting force and thrust force increases with increase in feedrate for uncoated tungsten carbide (W/Co) and WC/Co PVD coated inserts at both low positive rake angle of 5^{o} C and high positive rake of 15^{o} C, and at both low cutting speed of 120 m/min and high cutting speed of 240 m/min, for the feedrate range of 0.05 – 0.1 mm/rev.
2. Chip thickness and cutting ration increases with increase in feedrate for the same feedrate range.
3. Uncoated tungsten carbide (WC/Co) inserts exhibit much lower cutting force than tungsten carbide (WC/Co) PVD coated with TiAlN.
4. Thrust force is much lower than the cutting force.
5. Cutting force and thrust force increases with increase in cutting speed from 120 m/min to 240 m/min, for both the uncoated and coated cutting tool inserts. The coated cutting tool in general generates higher cutting forces.
6. Uncoated tool inserts exhibit higher average friction coefficient than coated tool inserts at low rake angle and low cutting speed, and thus the coating serves to reduce friction; but at higher rake angle and low cutting speed, coated tool inserts exhibits higher average friction coefficient.
7. Uncoated tool inserts exhibit lower average friction coefficient than coated tool inserts at lower rake angle and higher cutting speed.

8. Coated cutting tool inserts are not recommended for machining titanium alloys because they increase cutting forces.

9. An increase in the positive rake angle from 5^0 to 15^0 leads to a higher shear angle and less shear force, which decreases the cutting force, thrust force, and friction force.

10. Machinability of titanium alloys could be improved by using cutting tool inserts with higher positive rake angle.

ACKNOWLEDGEMENTS

The financial support of National Science Foundation (NSF) under grant no. CMMI 800871 is gratefully acknowledged. The financial assistance provided in the form of Graduate Teaching Assistantship by the Department of Mechanical and Aerospace Engineering at Missouri University of Science and Technology is also gratefully acknowledged.

REFERENCES

Baldoukas, A.K., Soukatzidis, F.A., Demosthenous, G. A., and Lontos, A.E., "Experimental Investigation of the Effect of Cutting Depth, Tool Rake Angle and Workpiece Material Type on the Main Cutting Force During a Turning Process," *Proceedings of the 3rd International Conference on Manufacturing Engineering (ICMEN)*, 1-3 October 2008, Chalkidiki, Greece, pp. 47-55.

Cotterell, M., and Byrne, G. "Dynamics of chip formation during orthogonal cutting of titanium alloy Ti–6Al–4V," *CIRP Annals - Manufacturing Technology*, Vol. 57, (2008), pp. 93-96. Amsterdam: Elsevier.

M. Eugene Merchant, "Mechanics of Metal Cutting Process. I. Orthogonal Cutting and Type 2 Chip," Journal of Applied Physics, Vol. 16, No. 5, (May 1945), pp 267-275

H. Ernst and M. E. Merchant, "Chip Formation, Friction and High Quality Machined Surfaces," Surface Treatment of Metals (American Society for Metals, 1941), pp. 299-378.

Fang, N., and Wu, Q., "A Comparative Study of the Cutting Forces in High Speed Machining of Ti-6Al-4V and Inconel 718 with a Round cutting Edge Tool," *Journal of Material Processing Technology*, Vol. 209 (2009), pp. 4385-4389.

Gunay, M., Aslan, E., Korkut, I., and Seker, U., "Investigation of the Effect of Rake Angles on Main Cutting Force," *International Journal of Machine Tool and Manufacture*, Vol. 44 (2004) pp. 953-959.

Iqbal, S.A., Mativenga, T.P., and Sheikh, A.M., "Cutting using the Finite Element Method Determining the Effect of Interface Friction on Tool-Chip Contact Length in Orthogonal," Manufacturing and Laser Processing Group, School of Mechanical, Aerospace and Civil Engineering, Sachville Street Building. The University of Manchester, Manchester, M60 1QD, Uk.

Khidhir, A., Basim., Mohamed,Bashir., "Selecting of Cutting Parameters from Predictions Model of Cutting force for Turning Nickel Based Hastelloy C-276 Using Response Methodology," *European Journal of Scientific Research*, Vol.33 No.3 (2009), pp. 525-535.

Lazoglu, I., and Altintas Y., "Prediction of Tool and Chip Temperature in Continuous and Interrupted Machining," *International Journal of Machines Tools and Manufacture*, Vol. 42, pp. 1011 – 1022. Amsterdam Elsevier.

Liu, C., Ai, X., and Liu, Z**. "**Experimental Study on Wear Mechanism of Cutting Tool and Cutting Temperature in High Speed Machining Super alloy," *Advanced Materials Research*, Vols. 102-104, (2010), pp. 525-528. (www.scientific.net/AMR.102-104.525).

Liu, M., Ming, W.W., Zhang, Y.S., Xu, H., and Chen, M., "Machinability Evaluation of TC11 Titanium Alloy in Finish Hard Turning Based on the Response Surface Methodology" Mechanical Science and Technology, Vol. 21, (2007), pp. 1651 – 1655.

Luo, M., Zhang, L.Q., and Chen, M., "Machinability and Tool Wear Behavior in Turning High Nickel-base Alloy-G3," *Advanced Materials Research*, Vols 69-70, (2009), pp. 485-489. (www.scientific.net/AMR.69-70. 485).

Marusich, D. Troy, "Effect of Friction and Cutting Speed on Cutting Force," *Proceedings of ASME Congress*, November 2001, pp. 11-16, New York.

Ming, W.W., Chen, M., and Rong, B., "Analysis of Finish Hard Turning of Ti-6.5Al-3.5Mo-1.5Zr-0.3Si Alloy," *Material Science Forum*, Vols. 626-627 (2009), pp. 225-230. (www.scientific.net/MSF.626-627.225).

Seker, U., Kurt, A., and Ciftci, I., "The Effect of Feedrate on the Cutting Force When Machining with Linear Motion," *Journal of Materials Processing Technology*, Vol.146 (2004) pp. 403-407.

Srivastava, K. Anil., Iverson, C. Jonathan., "An Experimental Investigation into High Speed Turning of Ti- 6Al- 4V," *Proceeding of the ASME 2010*, International Manufacturing Science and Engineering Conference. MSEC2010-34205.

Stephenson, A. David., Agapiou, S. John." Metal Cutting Theory and Practice," (1997) pp. 447- 481.

Saglam Haci, Unsacar Faruk, Yaldiz Suleyman " Effects of Rake Angle and Approach Angle on the Main Cutting Force and Tool-tip Temperature" *International Journal of Machine Tools & Manufacture*, Vol.46 (2006), pp. 132-141.

Sun, S., Brandt, M., and Dargusch, M.S., "Characteristics of Cutting Forces and Chip Formation in Machining of Titanium Alloys," *International Journal of Machine Tools & Manufacture*, Vol.49 (2009), pp. 561-568.

Sutter, G., Faure, L., Molinari, A., Ranc, N., and Pina, V., "An Experimental Technique for the Measurement of Temperature Fields for the Orthogonal Cutting in High Speed Machining," *International Journal of Machine Tools & Manufacturing*, Vol.43 (2003), pp. 671-678.

Okafor, A.C., and Ukpon, A.U., "Real-Time Status Monitoring During Turning on CNC Turret Lathe in a Production Environment, Part1: Development of a Cutting Force Measuring System for CNC Turret Lahe," in "Real-Time Intelligence Monitoring and Diagnostic System for A CNC Turret Lathe in A Production Environment," PhD Dissertation, University of Missouri – Rolla, 1998; pp. 43-77.

Wang, Z. G., Rahman, M., Wong, Y.S., Neo, K.S., Sun, J., Tan, C.H., and Onozuka, H., "Study on Orthogonal Turning of Titanium Alloys with Different Coolant Supply Strategies," *International Journal of Advanced Manufacture Technology*, Vol. 42 (2009) pp. 621-632.

Wu, W., Wang, G., Shen, C., "Analysis of Cutting Forces in Precision Turning Based on Oblique Cutting Model," *Advanced Material Research*, Vol.97-101 (2010), pp. 1961-1964.

II. INVESTIGATIONS ON THE EFFECTS OF MACHINING PARAMETERS ON CUTTING FORCES, SHEAR ANGLES, AND FRICTIONS DURING ORTHOGONAL TURNING OF TITANIUM ALLOY USING SOLID RIBBED BAR

A. Chukwujekwu Okafor, Hilary Onyishi
Laboratory for Industrial Automation and Flexible Manufacturing
Department of Mechanical and Aerospace Engineering
Missouri University of Science and Technology
327 Toomey Hall, Rolla, MO-65409-005, USA
E-mail:okafor@mst.edu

ABSTRACT

Titanium alloys, due to their unique and excellent combination of low density, high strength-to-weight ratio, ability to retain strength at high temperatures, and exceptional resistance to corrosion, are attractive materials for aerospace industries. However, titanium alloys are difficult to machine because of their high chemical reactivity and low thermal conductivity, the latter of which leads to poor heat conduction and high temperature at the tool-tip and edges. These thermo-mechanical phenomena affect the machinability of titanium alloys and lead to the generation of high cutting forces and rapid tool wear during the machining operations. The quest for enhanced material removal and tool life has necessitated research into cutting forces during high-speed cutting of titanium alloys. Most orthogonal cutting test reported in the literature used end turning of tubular workpiece. This paper presents the result of experimental investigations on the effects of machining parameters on cutting forces, shear angle and

friction in orthogonal turning of Ti-6Al-4V using solid ribbed bar. The results are compared with those from orthogonal turning of tubular workpiece. Uncoated fine-grained cemented tungsten carbide (WC/Co) and Physical Vapour Deposition (PVD) TiAlN coated grade turning tool inserts, with 5^0 and 16^0 rake angles were used under low and high cutting speeds of 120 and 240m/min at three different feedrates (0.05, 0.075 and 0.1 mm/rev). The experiments were conducted under flooded emulsion coolant to reflect what is practically obtainable in manufacturing industries.

The experimental results show that the cutting force components, F_c, are significantly higher that the thrust force components, F_t, and that all cutting force components (F_c,F_t,and F) at two selected cutting speeds of 120 and 240 m/min and at the three selected feedrates increased with increase in feedrate for both uncoated and coated cutting tools. However, for both uncoated and coated tools, an increase in the positive rake angle from 5^0 to 16^0 led to a decrease in cutting force. The 16^o tool rake angle results in an increase of the shear angle and friction coefficient, and thus lower shear force and friction force. In contrast, PVD coated tools gave the largest cutting forces. In comparison with the results obtained using tubular workpiece, the cutting forces generated by the ribbed workpiece material are higher in all cases investigated.

Keywords: Orthogonal turning of ribbed solid bar , Cutting forces, Shear angle, Friction coefficient, Machining parameters, Titanium machining.

1. INTRODUCTION

Titanium alloys, due to their unique properties such as high tensile strength-to-density ratio, high corrosion resistance, and the ability to retain their strength at high temperatures, are extensively used in aerospace (for manufacturing aircraft landing gear and structural parts), marine (for manufacturing naval ship structures and propeller shafts), biomedical, aviation, and oil industries. Titanium alloys are classified into three main groups: α- alloys, β- alloys, and α-β alloys. Alpha (α) titanium alloys have low tensile strength and produce low cutting forces. In contrast, α-β and β- alloys have higher tensile strength and generate significantly higher cutting forces. Titanium alloy Ti-6Al-4V, which is α-β alloy, is the most widely used titanium alloy for manufacturing aircraft parts. Ti-6Al-4V offers a number of important properties that have advantages over steel, including a high melting point, low density, high specific strength, high ratio of yield stress to tensile strength, and high hot strength; hence, they are used at elevated temperatures up to 600^0C. However, Ti-6Al-4V is classified as one of the most difficult-to-cut metals due to its low thermal conductivity, and as a result, the significant heat generated by the cutting action does not dissipate quickly from the tool's cutting edge. Therefore, most of the generated heat is concentrated on the tool's cutting edge and face, thus causing high tip temperatures, excessive deformation of cutting tool and friction, tool wear and brakeage. Also, titanium alloys work-harden with increasing temperatures and when combined with thin chips (caused by a high shearing angle) sliding on a relatively small area on the tool face, which increases the cutting force on the cutting edge, resulting in rapid tool wear and breakage.

Cutting forces are the most essential determinants in machining processes. These forces generated in machining have direct influence on heat generation; tool deflection, wear and failure; power requirements and the quality of the machined parts. Excessive cutting forces cause the cutting tool, workpiece, machine tool and machined part to suffer unacceptable large deformations, excessive cutting temperatures, unstable vibrations, tool breakage, and poor quality of machined parts. Therefore, adequate knowledge of cutting forces and the effects of cutting parameters on those forces is highly important in machining process. Details regarding cutting forces, shear angle and friction coefficients are required not only for designing machine tools and cutting tools, but also for the analysis of the cutting process to determining optimum machining parameters; and to provide machining data for the formulation of mechanistic, Finite Element (FE) and empirical cutting force models for machining simulation. The quest to lower cutting force at the cutting tool-chip interface when cutting hard metals like titanium alloys has posed enormous challenges for manufacturing industries.

Few studies have been conducted to determine the correlations between cutting forces and cutting parameters when cutting titanium alloys. Kosaraju et al. (2011) investigated the effect of rake angle and feedrate on cutting force in an orthogonal turning of EN8 steel. They observed that cutting force increased with increase in feedrate and decreased with increase in rake angle from 0^0 to 20^0. An experimental investigation into high-speed turning of the titanium alloy Ti-6Al-4V (with coated and uncoated carbide turning inserts) was conducted by Srivastava et al. (2010); they found that cutting forces increased with increase in cutting speed and feedrate, except at the lowest feedrate, where lower forces were observed with uncoated inserts; in addition, they reported that cutting

forces decreased with an increase in rake angle from 0^o to 5^o. Fang and Wu (2009) conducted a comparative study of cutting forces in orthogonal high speed finish machining of Ti-6Al-4V and Inconel 718 tube workpiece materials, using coated carbide tools with no cutting fluids or coolant. They reported that for both Ti-6Al-4V and Inconel 718 workpiece materials, the cutting force, thrust force, and resultant force all decrease as cutting speed increases, while the force ratio (F_c/F_t) increases. They also reported that as the feedrate increases, the cutting force, the thrust force, the resultant force, as well as the force ratio all increases however, cutting force and thrust force in machining Inconel 718 are higher than those in machining Titanium Ti-6Al-4V. Baldoukas et al. (2008) investigated the effects of depth of the cut, tool rake angle and workpiece type on the main cutting force during an orthogonal turning process. They concluded that the influence of rake angle on the main cutting force depends on the type of workpiece material; also, they reported that the main cutting force increased linearly with increase in depth of cut. Similar observations were also made by Saglam et al. (2006), as they investigated the effects of rake angle and approach angle on the main cutting force and tool-tip temperature in orthogonal turning of AlSl 1040 steel. They discovered that approach angle and rake angle have considerable effect on cutting forces and temperature at the tool-chip interface. Their findings on the effect of tool rake angle corresponds with the finding by Baldoukas et al. that increasing positive rake angle decreases the cutting forces significantly. This occurs because a positive rake angle produces a higher shear angle, which helps to reduce cutting forces and thus produces a better surface finish because it assists the chip to flow away from the workpiece. Another notable effort was made by Gunay et al. (2004), when they investigated the effect of rake

angle on main cutting force. They reported that the main cutting force increased with increase of negative rake values and decreased with increase of positive rake values. This was attributed to a reduction in the tool-chip contact area and friction force. Marusich (2001) investigated the effects of friction and cutting speed on cutting force in simulation validation process, and suggested that a decrease in the cutting force must come from a reduction in the effective friction at the tool-chip interface. Additionally, Iqbal et al. (2007), investigated the effect of interface friction on tool-chip contact length in orthogonal cutting using the finite element method. Their results showed that reduced chip compression ratios lead to a lower tool-chip contact length. Their finite element analysis revealed that friction distribution schemes significantly affect the ability to predict contact length, while chip thickness seemed insensitive to friction schemes. Seker et al. (2004) investigated the effect of feedrate on cutting forces when machining with linear motion. They concluded that the main cutting force increased with an increase in the feedrate when the depth of cut and cutting speed were held constant. Considering cutting tools, Ezugwu et al. (2005), Zoya and Krishnamurthy (2000), and Ozel et al. (2010) independently reported that coated tools exhibited the largest cutting forces at high cutting speeds than uncoated tools, but less tool wear were observed, during dry machining of Ti-6Al-4V alloy.

Although several studies have investigated the effects of machining parameters on cutting forces in orthogonal cutting of low strength alloys, there is insufficient knowledge on the effects of cutting parameters (cutting speed, feedrate, tool rake angle and workpiece geometry) on orthogonal cutting of difficult-to-cut metals such as titanium. Also most published orthogonal cutting tests were conducted using tubular workpiece,

and only very few using ribbed solid workpiece, and there is no comparative study of the two orthogonal cutting test approaches is reported in published literature. Most studies on the machinability of titanium alloys were based on dry cutting operations and low cutting speeds; thus, they do not reflect actual practices in manufacturing industries today. Therefore, the objective of the study reported in this paper, is to investigate the effects of machining parameters (feedrate, cutting speed, rake angle, uncoated and coated tool inserts) on cutting forces (cutting force, $F_{c,}$ thrust force, F_t, friction force, F, and normal to friction force, N), shear angle friction coefficient, and shear stress during high speed orthogonal turning of titanium Ti-6Al-4V alloy workpiece with ribs under flooded coolant conditions, typical of the practice in manufacturing industry. The second objective of the research is to obtain orthogonal cutting data base, which will be transformed to oblique milling geometry, and used to determine specific cutting and edge force coefficients, for mechanistic modeling and simulation of cutting forces in high speed bull nose helical end-milling of titanium alloys. A third objective is to compare the results obtained by the two approaches of orthogonal cutting tests – using tubular and ribbed solid workpiece - in terms of accuracy and ease of use. A comparative study of the two approaches is essential to ascertain the accuracy of data and ease of use in cutting force modeling and simulation. Uncoated fine-grained cemented tungsten carbide (WC/Co) and Physical Vapour Deposition (PVD) TiAlN coated grade turning tool inserts, with 5^0 and 16^0 rake angles were used under low and high cutting speeds of 120 and 240m/min at three different feedrates (0.05, 0.075 and 0.1 mm/rev).

In recent years, many predictive models have been developed successfully for practical machining operations. These approaches depend upon a detailed understanding

of orthogonal and oblique cutting processes traditionally used in fundamental studies of cutting actions. Orthogonal cutting is the process by which a straight-edged tool moves with a constant speed perpendicularly to the cutting edge. It is a two-dimensional (2D) case of machining that can be approximated in the planing, shaping, and end turning of a thin-walled tube Stephenson et al. (2006) or a specially prepared ribbed (grooved) workpiece. Experimentally, it has been found that the shear angle and, hence, the cutting ratio, depend upon the workpiece, tool material and cutting conditions. Several attempts have been made to establish a theoretical law that predicts the shear angle. Ernst and Merchant (developed the first reasonable theory) Stephenson et al. (2006). They assumed that the shear angle would adopt a value that would minimize the work of cutting.

1.1. MECHANICS OF ORTHOGONAL CUTTING

The shear plane model of orthogonal cutting (Figure 1) was first proposed by Ernst and Merchant (1941, 1945) (Stephenson et al., 2006).

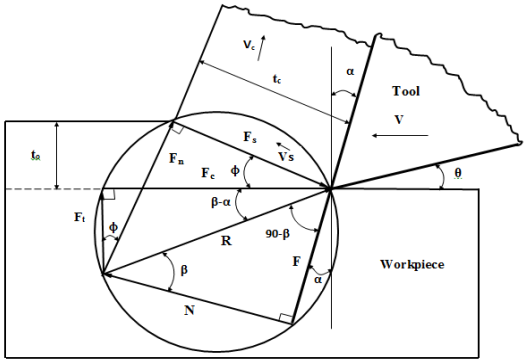

Figure 1. Circular Force Diagram (Ernest & Merchant 1941, 1945) for Orthogonal Cutting

They assumed that the chip is formed by shear along a single plane inclined at an angle, ϕ, (the shear angle) with respect to the machined surface. This assumption is consistent with deformation patterns observed in many chip samples from quick-stop tests. The shear angle can be calculated from the cutting ratio, r, according to the geometric relationships shown in Figure 1.

When the chip thickness ratio is known from Eq. 1, the shear angle [ϕ], can be estimated from Eq. 2. The shear force and shear stress, τ_s, can be calculated from Eq. 3 and Eq 4. From the experimentally obtained cutting and trust forces, the normal force and friction force can be deduced as shown in Eq. 5 and Eq. 6. The coefficient of friction can be estimated from Eq. 7.

Cutting ratio: $r = \frac{t_o}{t_c} = \frac{\sin\phi}{\cos(\phi-\alpha)}$ (1)

Shear angle: $\phi = \tan^{-1}\frac{r\cos\alpha}{1-r\sin\alpha}$ (2)

Shear force: $F_s = F_c\cos\phi - F_t\sin\phi$ (3)

Normal to shear force: $F_n = F_c\sin\phi + F_t\cos\phi$ (4)

Shear stress: $\tau_s = \frac{F_c\cos\phi\sin\phi - F_t\sin^2\phi}{Wt_0}$ (5)

Cutting force: $F_c = N\cos\alpha + F\sin\alpha$ (6)

Thrust force: $F_t = F\cos\alpha - N\sin\alpha$ (7)

Normal force $N = F_c\cos\alpha - F_t\sin\alpha$ (8)

Friction force: $F = F_c\sin\alpha + F_t\cos\alpha$ (9)

Coefficient of friction: $\mu = \frac{F}{N} = \frac{F_c\sin\alpha + F_t\cos\alpha}{F_c\cos\alpha - F_t\sin\alpha} = \frac{F_t + F_c\tan\alpha}{F_c - F_t\tan\alpha}$ (10)

2. EXPERIMENTAL SET- UP AND PROCEDURE

A schematic diagram of the experimental set-up and data acquisition system for the orthogonal cutting of ribbed solid workpiece is shown in Figure 2. All machining operations were carried out on an Okuma LB15 CNC turret lathe. The workpiece material used in this experiment was α-β titanium alloy Ti-6Al-4V; its physical property and chemical composition are listed in Tables 1 and 2, respectively. A Ti-6Al-4V solid bar with an outer diameter of 50.8 mm, and length of 88.9 mm was pre-machined to simulate orthogonal turning by creating four ribs on the outer diameter of the solid bar. The depth and width of the ribs are 10.16 (diameter value) and 3.175 mm, respectively, as shown in Figure 2.

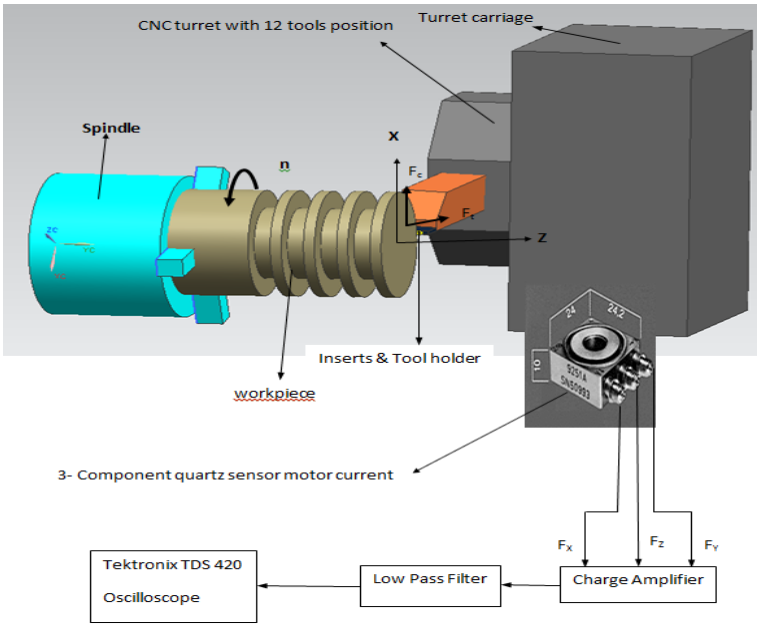

Figure 2. Schematic Diagram of the Experimental Set-up and Data Acquisition System for Orthogonal Turning

Table 1. Physical Properties of Titanium Alloy Ti-6Al-4V

Density $g.cm^{-3}$	Melting Point ^0C	Young's modulus (GPa)	Poisson ratio	Shear modulus (Gpa)	Electrical Resistivity $n.\Omega.m^{-1}$	Thermal Conductivity $(w.m^{-1}.k^{-1})$	Corrosion resistance
4.506	1668	116	0.32	44	420	21.9	<1

Table 2. Chemical Composition of Titanium Alloy Ti-6Al-4

Titanium Ti-6Al-4V	Ti	Mo	V	Al	C0	Cr	Fe	Si	C
Elements (%)	88	6.3	3.0	2.0	0	0	0	0	0

The ribbed solid workpiece was rotated at the selected cutting speed about its central axis, and the straight-edge cutting tool insert was fed directly into the workpiece perpendicular to the axial direction, thus continuously reducing the diameter of the rib by removing a chip from its outer diameter. Thus the condition of cutting by a single edge is satisfied, where the rib width becomes the chip width, w, and the uncut chip thickness, t_o, is equal to the feed per revolution of the ribbed solid workpiece, f_r. A4 turn/groove, flat top, WC/Co uncoated tungsten carbide (A4G0605M06U04B K313) and (A4G0600M06P04GUP KU10) inserts with 5^0 and 16^0 rakes angles, and A4 turn/groove, flat top, PVD TiAlN coated carbide (A4G0605M06U04BKC5025) and (A4G0600M06P04GUP KCU25) inserts with 5^0 and16^0 rake angles respectively, were

used in this experiment. Each of the uncoated and coated carbide tools has two cutting edges with relief angle of 7^0.

For each experiment, total radial diameter depth of cut d = 1.27mm (0.05 in.) was made with a new cutting edge, at each selected feedrate, to eliminate tool wear. Each condition was replicated once with the same cutting edge to reduce experimental error under all cutting conditions. Two cutting speeds (120 and 240 m/min) and three feedrates (0.05, 0.075, and 0.1mm/rev) were investigated. At a cutting speed of 120 m/min, uncoated carbide tools with 5^0 and 16^0 rake angles was used to cut the workpiece for the three selected feedrates; each cut was replicated once. To maintain consistency, the initial position (zero) was reset for every cut. At a high cutting speed of 240m/min, the same processes were performed for the same uncoated tools with 5^0 and 16^0 rake angles, respectively. The same procedures were carried out for coated carbide tools with 5^0 and 16^0 rake angles, respectively. In all the cuttings, a large amount of emulsion coolant was flooded at the cutting zone at low pressure to serve as a coolant and lubricant, and to reflect actual practices in manufacturing industries, unlike most experiments reported in the literature, which were conducted under dry conditions. During these cutting tests, chips were collected and later their thicknesses were measured at three different cross-sectional points along its length. The average thickness per sample per test condition was obtained, recorded for all the cutting conditions and replications, and used for further calculations. Chip thickness was measured using a Neiko 01407A Stainless steel 6–inch digital caliper with extra-large LCD screen. Tables 3, 4, 5 and 6 show all the experimental plans and the measured and calculated parameters.

The CNC program containing the G and M codes for machining one test run is given below:

G00 X2.008 Z-0.188 S120 T050505 M41 M03

G01 X1.828 F0.05

G00 X2

G00 X7 Z8 M05

Table 3. Machining Parameters, Measured and Calculated Cutting Forces and Friction Coefficients at V=120m/min Using Uncoated Tool Inserts

Test No.	Rake Angle (^{0})	Feed rate (mm/rev) $t_o = f$ [in/rev]	Chip thickness t_c (mm) [in]	Cutting ratio $r = t_o/t_c$	$F_r=F_t$ (N)	$F_T = F_c$ (N)	ϕ (^{0})	Coeff. of friction μ	F_s (N)	Shear stress τ_s
1	5	0.05 [0.002]	0.0035	0.59	445	1141	32.10	0.49	730.10	1.55E6
2	5	0.075 [0.003]	0.0038	0.81	628	1555	41.86	0.51	739.05	1.31E6
3	5	0.1 [0.004]	0.0058	0.70	656	1562	37.16	0.53	848.05	1.03E6
4	16	0.05 [0.002]	0.0025	0.80	273	783	48.19	0.71	318.51	954349
5	16	0.075 [0.003]	0.004	0.75	344	932	45.12	0.73	413.89	784000
6	16	0.1 [0.004]	0.0058	0.70	469	1365	42.05	0.70	699.47	937546

Table 4. Machining Parameters, Measured and Calculated Cutting Forces and Friction Coefficients at 240m/min Using Uncoated Tool Inserts

Test No.	Rake Angle (^{0})	Feed rate (mm/rev) $t_o = f$ [in/rev]	Chip thickness t_c (mm) [in]	Cutting ratio $r = t_o/t_c$	$F_r=F_t$ (N)	$F_T = F_c$ (N)	ϕ (^{0})	Coeff. of friction μ	F_s (N)	Shear stress τ_s
1	5	0.05 [0.002]	0.003	0.67	569	1554	35.81	0.47	927.31	2.17E6
2	5	0.075 [0.003]	0.0045	0.67	639	1578	35.81	0.51	905.82	1.41E6
3	5	0.1 [0.004]	0.0063	0.65	773	1684	34.90	0.57	938.82	1.07E6
4	16	0.05 [0.002]	0.003	0.69	303	850	41.44	0.72	436.67	1.16E6
5	16	0.075 [0.003]	0.0035	0.86	345	1016	51.88	0.69	355.77	743143
6	16	0.1 [0.004]	0.0058	0.70	535	1534	42.05	0.71	780.76	1.05E6

Table 5. Machining Parameters, Measured and Calculated Cutting Forces and Friction Coefficients at 120m/min Using Coated Tool Insert

Test No.	Rake Angle (^{0})	Feed rate (mm/rev) to = f [in/rev]	Chip thickness t_c (mm) [in]	Cutting ratio $r = t_o/t_c$	$F_r=F_t$ (N)	$F_T = F_c$ (N)	φ (0)	Coeff. of friction μ	F_s (N)	Shear stress τ_s
1	5	0.05 [0.002]	0.0028	0.74	685	1461	38.91	0.53	706.61	1.77E6
2	5	0.075 [0.003]	0.0048	0.64	746	1755	34.44	0.53	1025.49	1.55E6
3	5	0.1 [0.004]	0.0058	0.70	781	1842	37.16	0.53	996.23	1.20E6
4	16	0.05 [0.002]	0.0025	0.80	457	1160	48.19	0.77	432.70	1.30E6
5	16	0.075 [0.003]	0.0045	0.67	465	1200	40.21	0.76	616.22	1.06E6
6	16	0.1 [0.004]	0.0058	0.70	547	1532	42.05	0.72	771.23	1.03E6

Table 6. Machining Parameters, Measured and Calculated Cutting Forces and Friction Coefficients at 240m/min Using Coated Tool Insert

Test No.	Rake Angle (^{0})	Feed rate (mm/rev) to = f [in/rev]	Chip thickness t_c (mm) [in]	Cutting ratio $r = t_o/t_c$	$F_r=F_t$ (N)	$F_T = F_c$ (N)	φ (0)	Coefficient of friction μ	F_s (N)	Shear stress τ_s
1	5	0.05 [0.002]	0.003	0.67	627	1600	35.81	0.50	930.68	2.18E6
2	5	0.075 [0.003]	0.0048	0.64	752	1608	34.44	0.58	900.86	1.36E6
3	5	0.1 [0.004]	0.0058	0.70	859	1861	37.16	0.57	964.25	1.24E6
4	16	0.05 [0.002]	0.0028	0.74	553	1552	44.50	0.72	719.36	2.00E6
5	16	0.075 [0.003]	0.0048	0.64	681	1605	38.37	0.81	835.63	1.39E6
6	16	0.1 [0.004]	0.0058	0.70	794	1816	42.05	0.83	816.69	1.10E6

Round solid titanium bars 50.8 mm (2 inches) in diameter and 88.9 mm (3.5 inches) in length were bought and pre-machined into workpieces with 4 grooves and 4 ribs. Each ribbed workpiece was clamped in the CNC lathe chuck as shown in Figure 3 to simulate orthogonal turning with a solid bar workpiece , with the cutting tool positioned for orthogonal turning experiments.

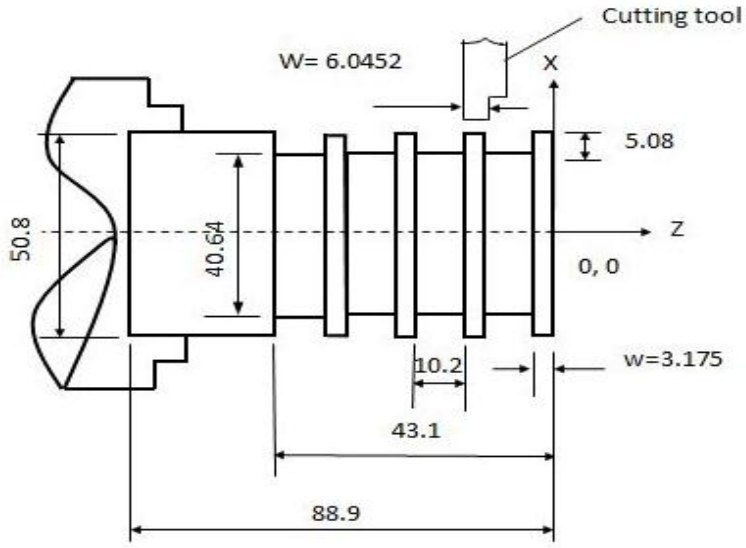

Figure 3. Titanium Alloy Workpiece with Ribs Clamped in the Lathe Chuck to Simulate Orthogonal Turning

According to the popular chip classification developed by ISO 3685 and issued in 1977, chip types usually have the following forms: straight ribbon, tubular, corkscrew (washer), and conical helical. Based on this definition, chips obtained in this study varied depending on the cutting conditions. Figure 4a shows a conical helical chip obtained under a low cutting speed of 752 rpm (120 m/mins) and a feedrate of 0.075mm/rev, Figure 4b shows a spiral chip obtained under a high cutting speed of 1504 rpm (240

m/min) and a feedrate of 0.05mm/rev, and Figure 4c shows the corkscrew (washer) chip obtained under a low cutting speed of 752 rpm (120 m/min) and a feedrate of 0.1 mm/rev.

(a)  (b)  (c) 

Figure 4. Chip Morphologies
(a) Conical Helical Chips: v = 120m/mins, Feedrate = 0.075mm/rev, (b) Spiral Chips: v = 240m/mins, Feedrate = 0.05mm/rev, (c) Corkscrew (Washer) Chips: v = 120m/mins, feedrate = 0.1mm/rev

2.1. CALIBRATION OF THE FORCE MEASUREMENT SYSTEM

Before calibrating the force measurement system to establish the relationship between cutting tool-tip forces (feed, radial, and tangential) with the measured X, Y, and Z force load cell outputs, a 3-axis Kistler load cell (model number 9251A) was installed on the machined slot using a Kistler preloading wedge (model number 9463) by Okafor and Ukpong [1998]. Preloading the load cell at mounting with the specified 25 KN load limit was necessary to allow shear transmission through friction. Once installed, the load cell becomes a permanent fixture of the machine tool structure and requires no maintenance. Calibrating the measuring system is not only necessary for establishing the tool's point-load cell output force relationship; it is also a vital step for checking the behavior of the transducer to the applied forces. Figure 5 offers a picture of the

experimental set-up of the calibrations, while Figures 6a, 6b and 6c show the schematic diagrams of the calibration set-up for the feed, radial and tangential axis, respectively. Calibration was carried out using a steel clamp plate specially fabricated in-house. Each axis has a different fixture for loading and unloading. A Kistler 9212 single-axis load cell was mounted on top of a pro-lift hydraulic jack, which in turn was mounted on the respective steel clamp plate fixture and used to apply loading and unloading forces at the tool tip in the respective coordinate directions for tool (5) used for the orthogonal cutting experiment.

Figure 5. Set-up for the Calibration of the Load Cell

(a)

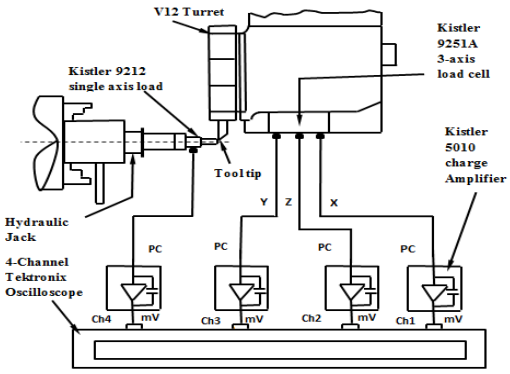

Figure 6. Calibration Set-up: (a) Feed Axis

(b)

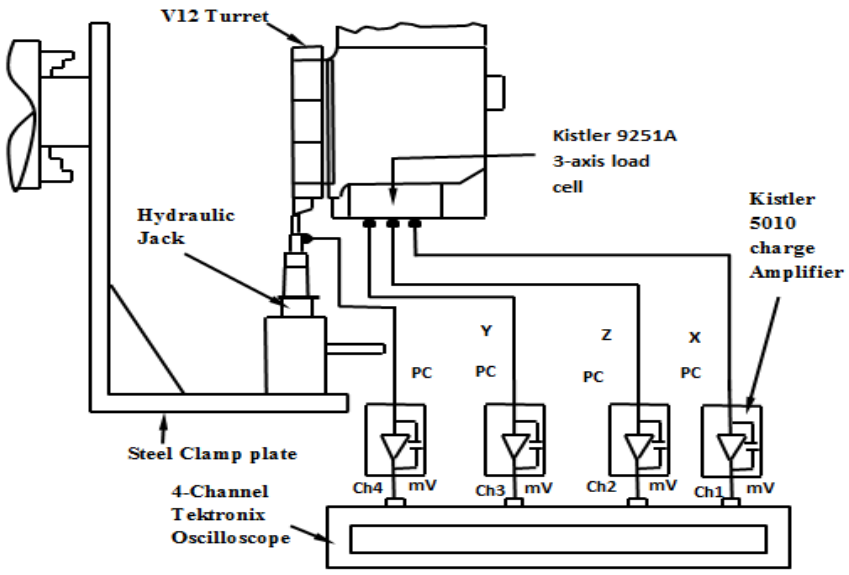

(c)

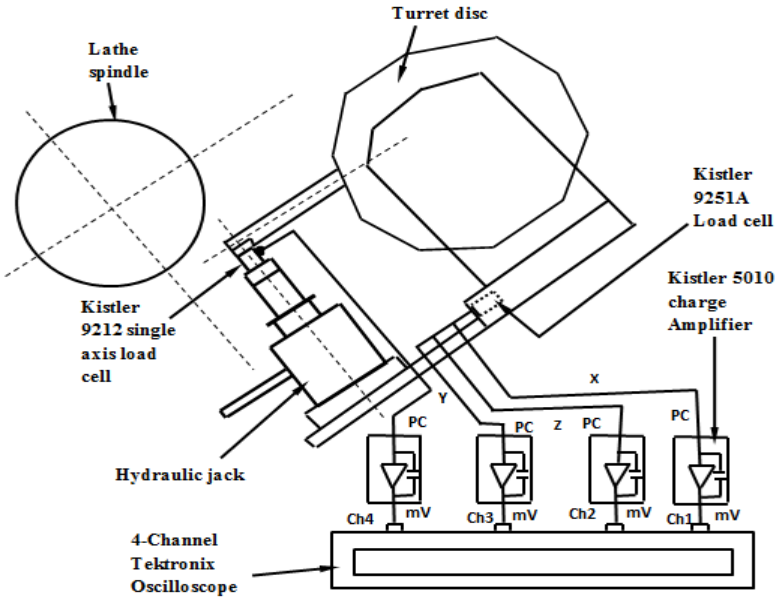

Figure 6. Calibration Set-up: (b) Radial Axis, (c) Tangential Axis (cont.)

Calibration was performed for different turret positions because the position of the tool in the X, Y, and Z coordinates obviously affects the point of force application on the structure. For the loading and unloading cycles, the single axis transducer, Kistler

9212 output, and 3-axis Kistler 9251A load cell output were passed through a Kistler 5010 dual-mode amplifier and were acquired using a 4-channel Tektronix TDS 420A oscilloscope. The sensitivity of the single-axis Kistler 9212 transducer was set to 11.24 pC/N (50pC/N); the sensitivities of the 3-axis Kistler 9251A load cell were set to 8 pC/N for the X and Y axis components and to 4 pC/N for the Z axis component of the Kistler 5010 dual-mode amplifier. The X, Y and Z output components of the charge amplifier were connected to Channels 1, 2, and 3 of the Tektronix oscilloscope, respectively, while the transducer output was connected to Channel 4 of the Tektronix oscilloscope, as was shown in Figure 5. The vertical scales of Channels 1 and 2 were set to 200mV/division each in the Tektronix TDS 420A oscilloscope at the scale of 1000 mechanical units (MU) per volt in the charge amplifier, Channel 3 was set to 500mV/division at 2000 mechanical units (MU/Volt), and Channel 4, which is connected to the transducer, was set to 1Volt/division in the Tektronix TDS 420A oscilloscope at the scale of 4000 mechanical units (MU/Volt) in the charge amplifier. A sampling rate of 50Hz, 1000 data points and a trigger level of 20mV were used during the calibration process. Each axis was calibrated by applying an unspecified unilateral load on the handle of the pro-lift hydraulic jack (model number B-002 NC) until it reached maximum loading. The unloading was observed when the continuous unilateral load on the pro-lift hydraulic jack caused no further significant increment. At this point, the force wave signals were acquired using the 4-channel Tektronix oscilloscope. The same procedure was repeated for all the axes of Tool 5. The calibration load limit used does not prevent higher values of force from being used on the lathe, but does allow better accuracy to be obtained in the normal working range for tool status monitoring.

Figures 7, 8, and 9 show the applied load versus time and the transducer force response for the feed, radial and tangential tool-tip coordinates, respectively, for Tool 5. The data were processed using a moving average period of 20 for each signal captured.

Particularly interesting was the unusual behavior of the load cell during the tangential and radial axes loading and unloading of the turret-tool tip. For higher load limits, the turret housing behaved as if it were to be lifted off the bolted base, so the transducer attempted to mimic the profile. Linearity was kept in check by applying lower load limits for both axes. Figures 10, 11, and 12. show the load cell force response and applied force relationships for the 3-coordinate directions using Tool 5. The data were processed using a polynomial of 5 degrees. The loading and unloading follows similar trends in nearly all cases, thus indicating a desirable linear transducer response.

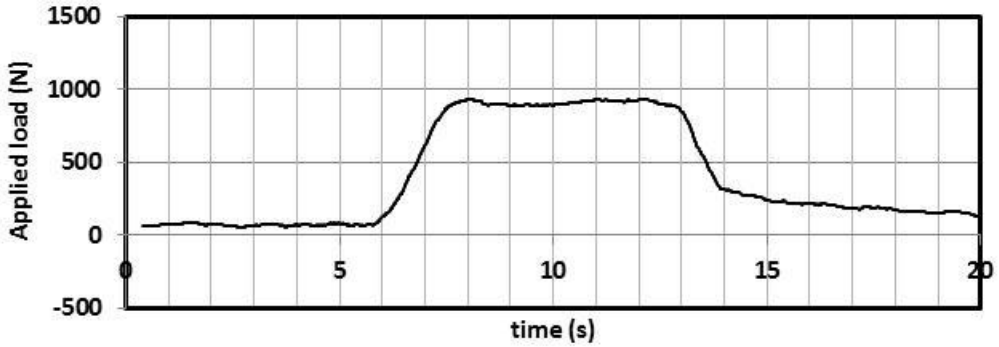

(a) Load cell input

Figure 7. Feed Axis Calibration for Tool 5

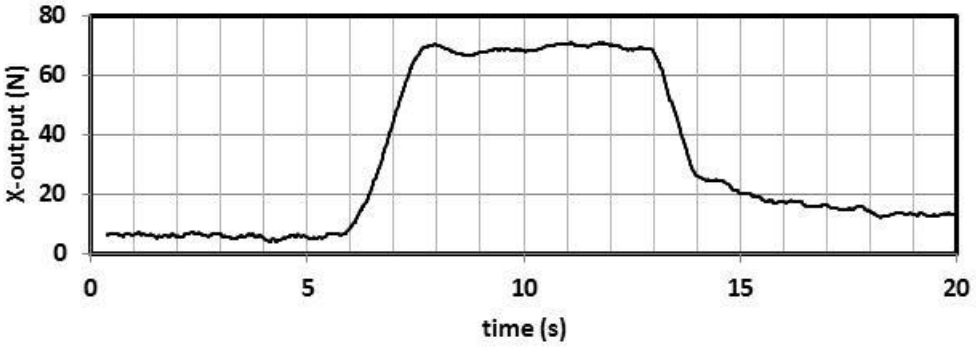

(b) X-output

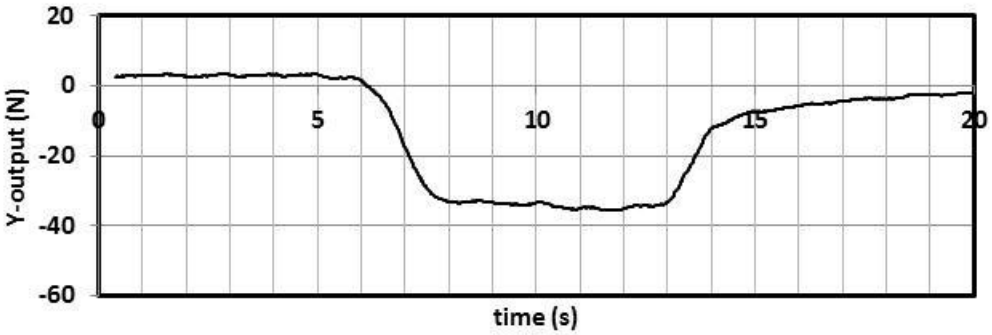

(c) Y-output

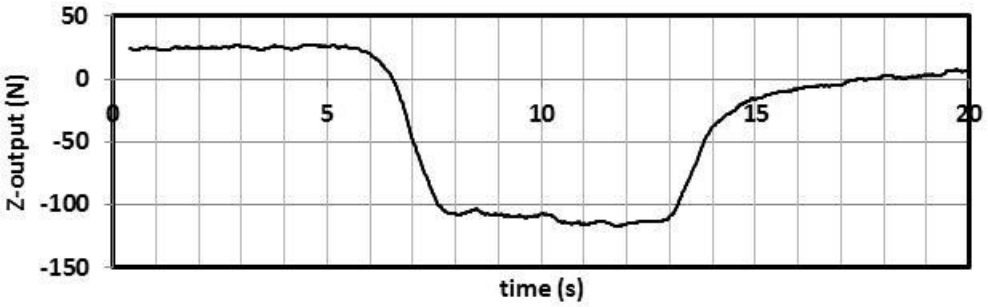

(d) Z-output

Figure 7. Feed Axis Calibration for Tool 5 (cont.)

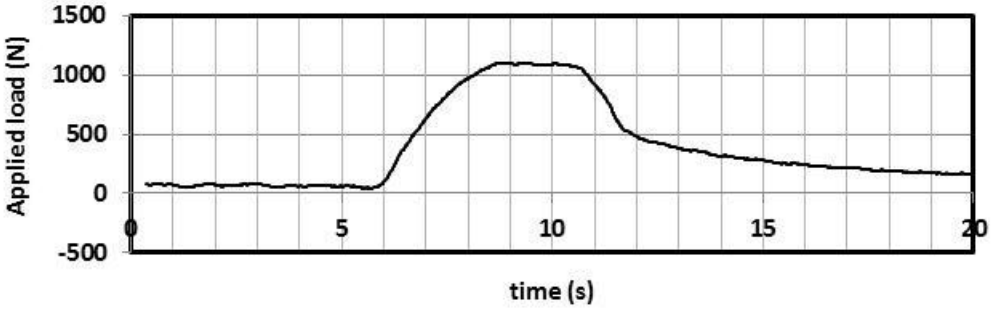

(a)

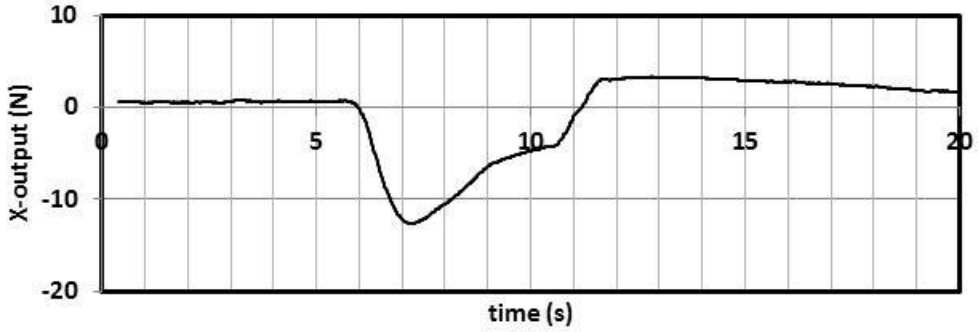

(b)

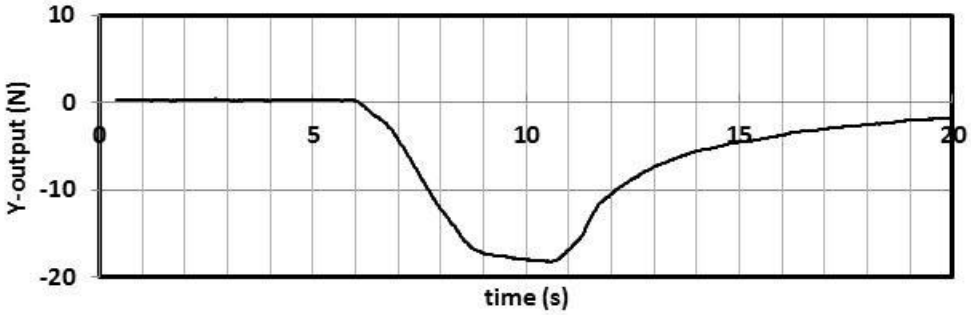

(c)

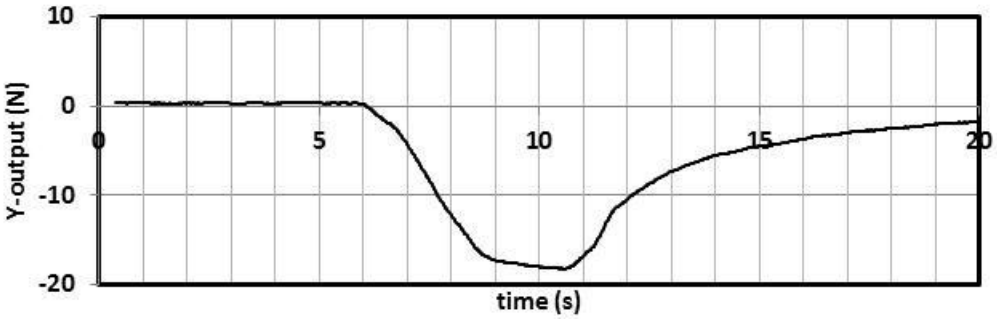

(d)

Figure 8. Radial Axis Calibration for Tool 5: (a) Load Cell Input, (b) X-output, (c) Y-output, (d) Z-output

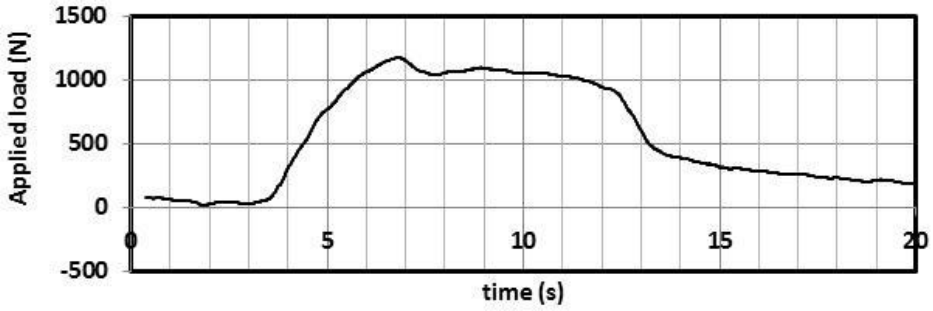

(a)

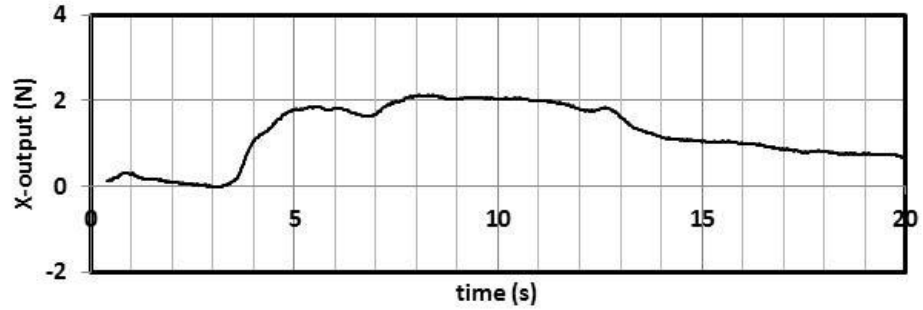

(b)

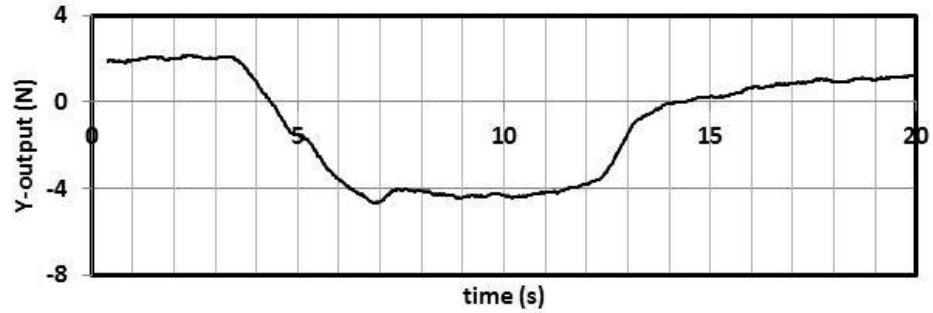

(c)

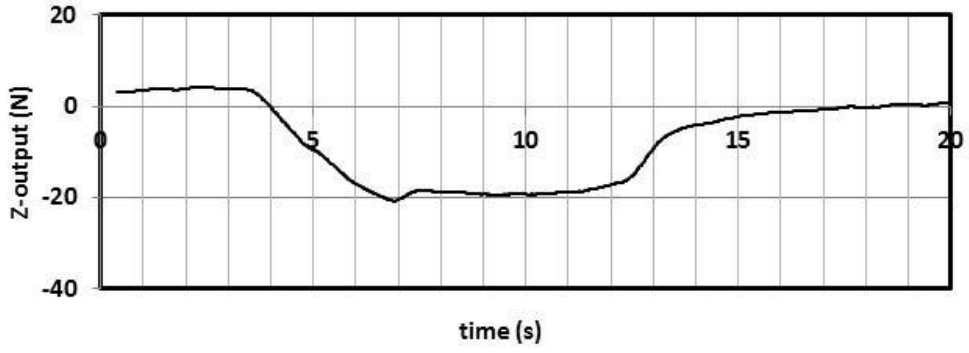

(d)

Figure 9. Tangential Axis Calibration for Tool 5: (a) Load Cell Input, (b) X-output, (c) Y-output, (d) Z-output

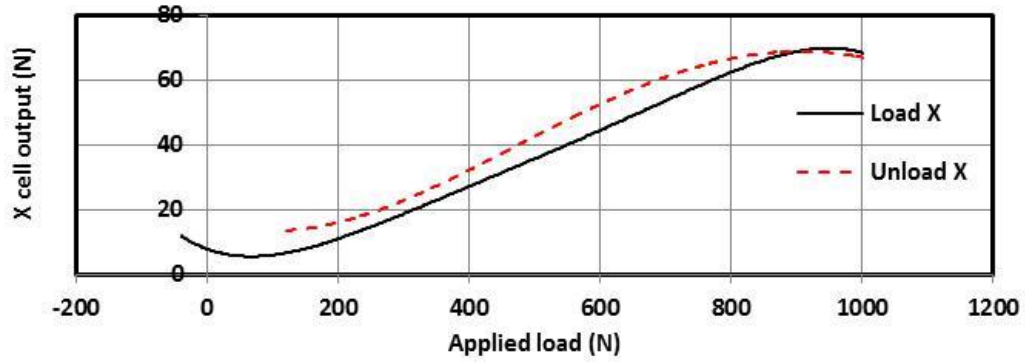

(a)

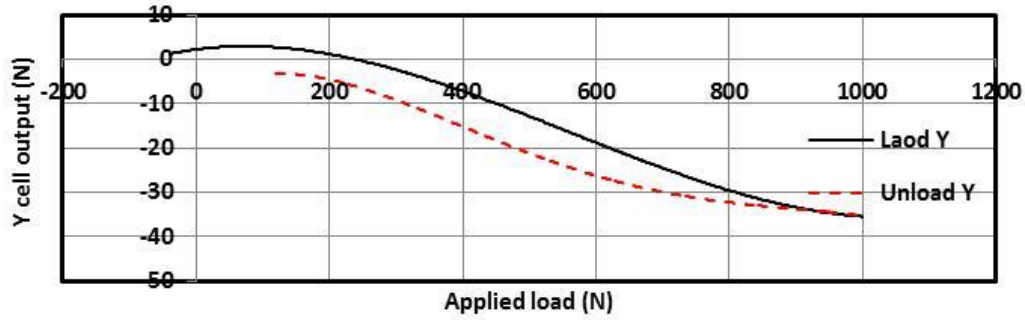

(b)

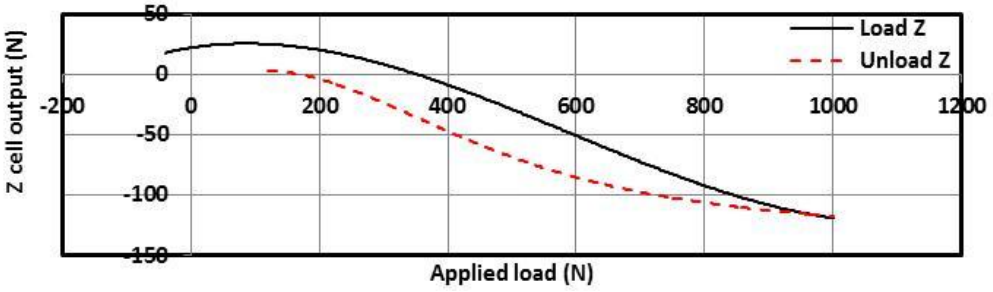

(c)

Figure 10. Load Cell Response to Applied Load (Feed Axis, Tool 5): (a) X-axis Cell Output, (b) Y-axis Cell Output, (c) Z-axis Cell Output

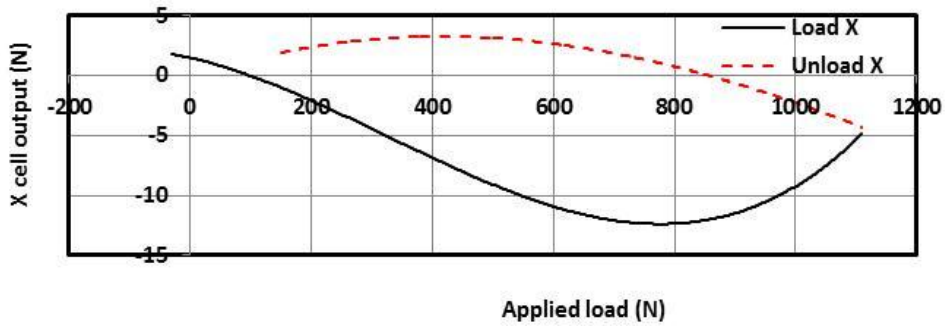

(a)

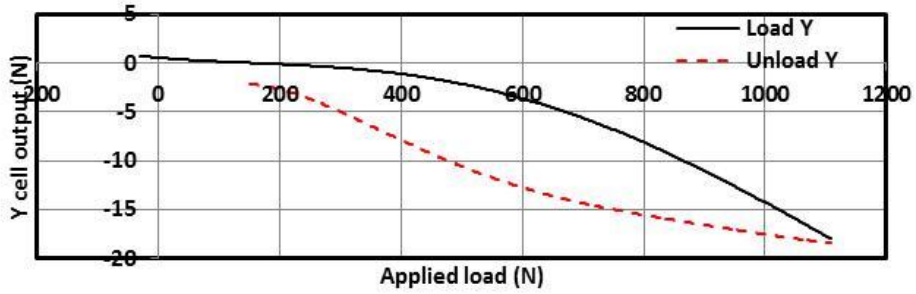

(b)

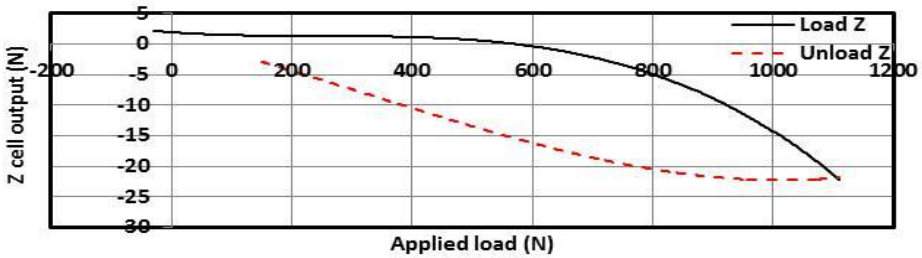

(c)

Figure 11. Load Cell Response to Applied Load (Radial Axis, Tool 5): (a) X-axis Cell Output, (b) Y-axis Cell Output, (c) Z-axis Cell Output

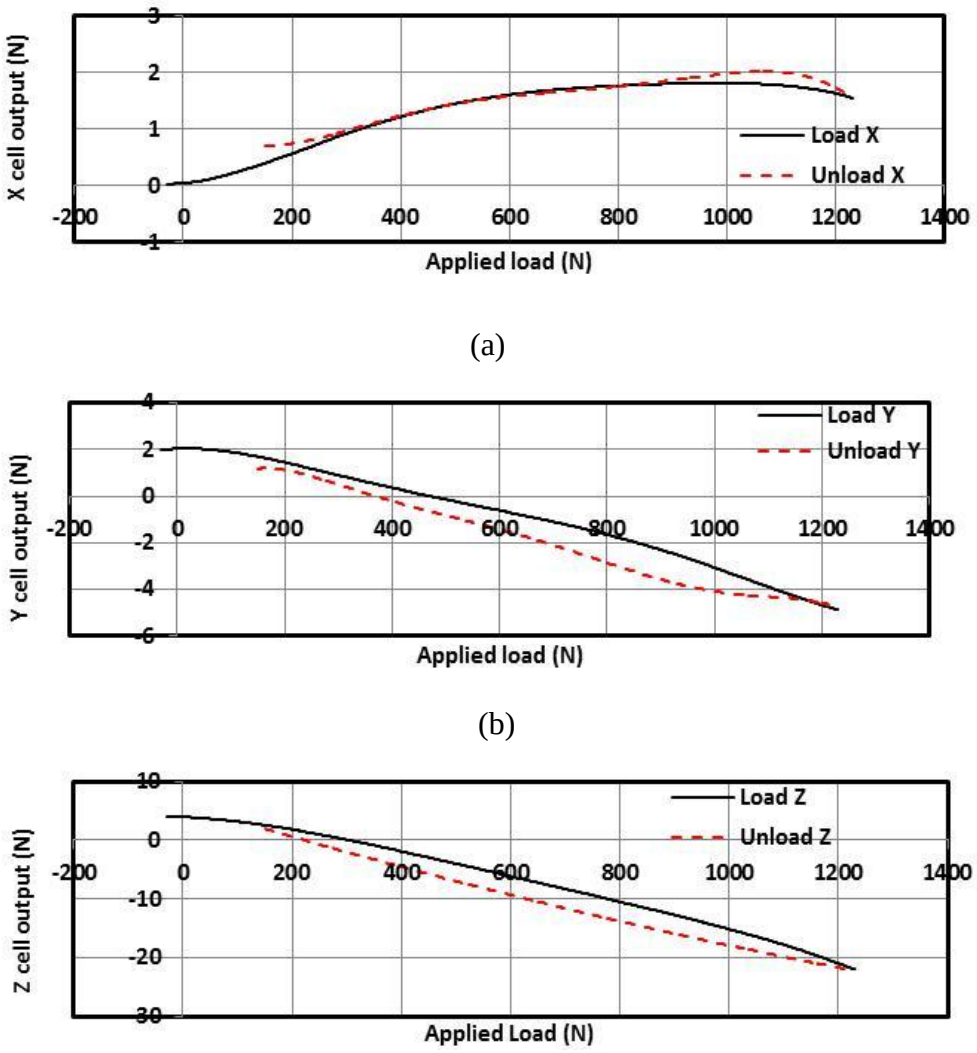

Figure 12. Load Cell Response to Applied Load (Tangential Axis, Tool 5): (a) X-axis Cell Output, (b) Y-axis Cell Output, (c) Z-axis Cell Output

2.2. MULTIPLE REGRESSION TO ESTABLISH THE CALIBRATION MATRIX

The following linear relationships are assumed to exist between the cutting forces at the tool tip (feed, radial and tangential) and the corresponding transducer (X, Y, and Z) measured force outputs.

$$F_f = A_f f_x + B_f f_y + C_f f_z \quad (11)$$

$$F_r = A_r f_x + B_{rfy} + C_{rfz} \quad (12)$$

$$F_t = A_t f_x + B_t f_y + C_t f_z \quad (13)$$

Where F_f, F_r, and F_t are the feed, radial and tangential cutting forces at the tool tip, respectively. For the orthogonal cutting of the ribbed titanium workpiece, the feed force F_f = the thrust force (F_t), and the tangential force F_t = the cutting $F_{c;}$ f_x, f_y, and f_z are the measured load cell output forces in the X, Y and Z load cell coordinates, respectively, and A_f, B_f, and C_t are the parameters to be estimated.

A simple least square model fitting technique was applied to each respective loading/unloading data record using STATISTICA^{TM} software from StarSoft^{R}. The calibration equations for Tool 1 become:

$$F_f = 11.30 f_x - 4.71 f_y + 0.35 f_z \quad \ldots. R^2 = 0.9894 \quad (14)$$

$$F_t = F_r = -7.2 f_x - 108.33 f_y + 39.85 f_z \quad \ldots. R^2 = 0.9766 \quad (15)$$

$$F_c = F_t = 134.84 f_x + 120.03 f_y - 68.58 f_z \quad \ldots. R^2 = 0.9951 \quad (16)$$

The normal probability plot and residual plot for the regression are given in Figures 13 a and b, which again confirms the adequacy of the regression models.

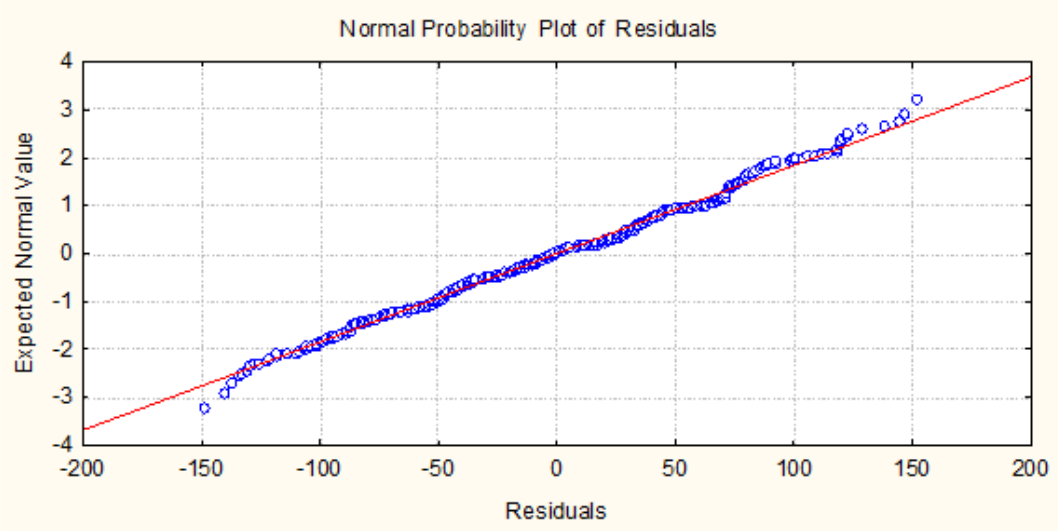

(a)

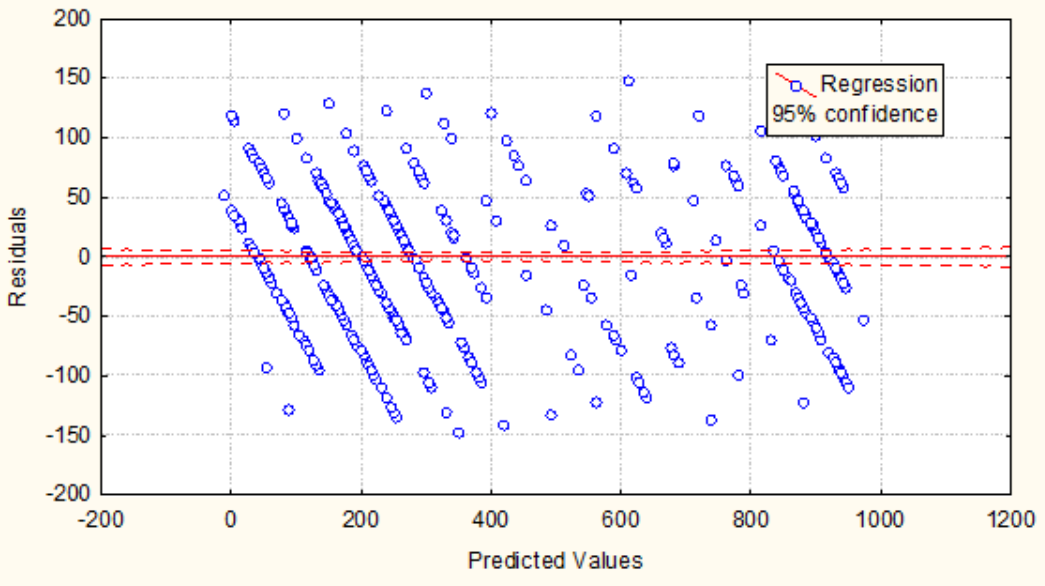

(b)

Figure 13. Tool 5 Feed Axis Calibration: (a) Normal Probability Plot, (b) Residual Plot

2.3. OVERVIEW OF THE CUTTING FORCE MEASUREMENT SYSTEM

It is known for orthogonal cutting of ribbed workpiece that the Z-component (axial) of force is theoretically zero. Preliminary tests show that this assumption is practically valid. The Z- component of force is always less than 2% of the X-component (radial feed force). Therefore, this component of force need not be recorded and was only monitored online to insure the orthogonality of the cut. Only the X- thrust (radial feed force) and Y- tangential (cutting force) components were recorded. A 3-axis Kistler 9251A load cell (f_x, f_y, f_z) output was connected to two dual-mode Kistler type 5010 charge amplifiers operated in charge mode with a long time constant. The outputs from the charge amplifier were connected to Channels 1, 2 and 3 of a Tektronix TDS 420 4-channel digitizing oscilloscope, where they were digitalized and acquired with the help of a floppy disk. A low pass filter of 2.2 KHz and a scale of 200 mechanical units per volt (mu/v) for the charge amplifier were carefully selected after due consideration of numerous preliminary tests. The triggering threshold used to trigger the oscilloscope was 20 mv. The filtered signals then were acquired in a Tektronix TDS 420 digitizing oscilloscope with a sampling frequency set to 2.5 KHz and record length of 5000 data points. This combination of sampling frequency and record length allows for an acquisition window of 2 seconds, as shown in Figures 14 and 15.

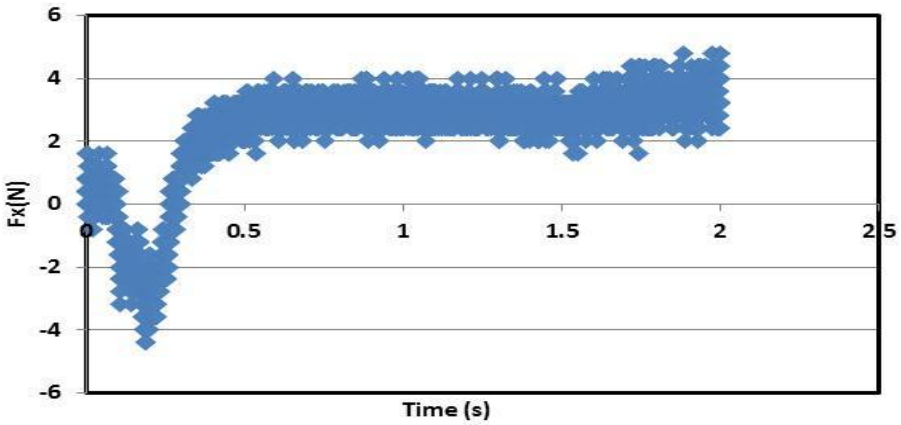

(a)

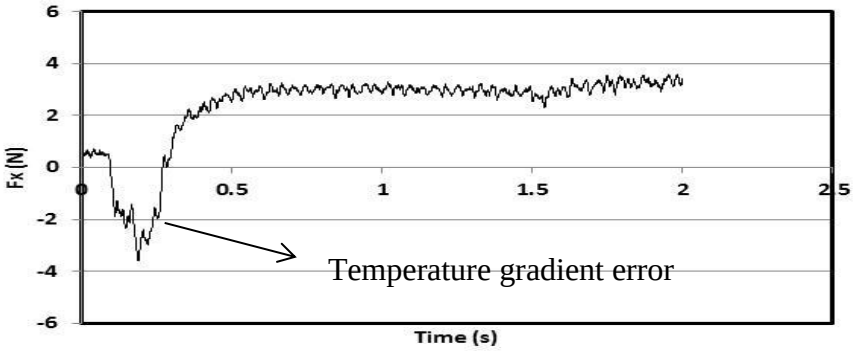

(b)

Figure 14. Unprocessed and Processed F_x Signal

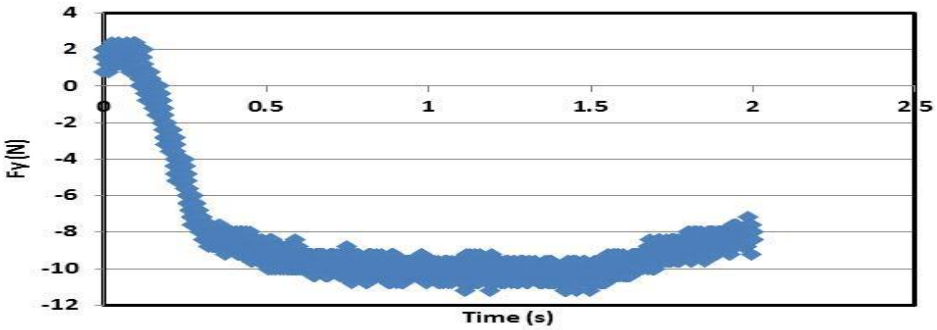

(a) Unprocessed F_y signal

Figure 15. Unprocessed and Processed F_y Signal

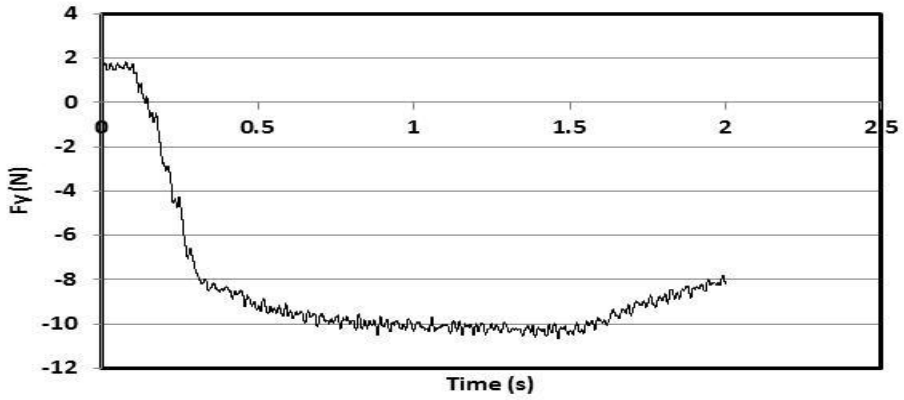

(b) Processed F_y signal

Figure 15. Unprocessed and Processed Fy Signal (cont.)

2.4. SIGNAL PROCESSING

The digitized cutting force signals were acquired and saved on a floppy disk and later processed via a Dell desktop computer with the Windows Vista operating system and Microsoft Office 2010. The data were processed in MS Excel 2010 to remove extraneous noise. Figures 14 and 15 show the unprocessed and processed signals for the cutting forces in the feed (Fx) and tangential (Fy) direction, respectively. A moving average value of 20 was used for processing in order to eliminate the fluctuations in the cutting force signals due to the interaction of chips with the tool. The forces at the tool tip were calculated using the relationship (equations 14 -16) developed by Okafor and Onyishi during the calibration process. The following equations give the relationship between the cutting forces at the tool tip and the corresponding Kistler 9251A load cell force output.

$$F_f = 11.30\ f_x - 4.71\ f_y + 0.35\ f_z \quad \ldots R^2 = 0.9894 \quad (17)$$

$F_t = F_r = -7.2\ f_x - 108.33 f_y + 39.85 f_z$ ….$R^2 = 0.9766$ (18)

$F_c = F_t = 134.84\ f_x + 120.03 f_y - 68.58\ f_z$ ….$R^2 = 0.9951$ (19)

Even though three equations were generated during the calibration process, the axial feed direction of the force components, F_f , was discarded and not recorded due to the orthogonal nature of the experiment, as stated previously.

A temporary change in the output signal is denoted as temperature gradient error, when the temperature of the environment or surrounding medium changes with a certain rate. In this case, the sensor is not in thermal equilibrium with the environment. The temperature gradient error is primarily determined by the installation conditions and application, and cannot be generally specified. However, the temperature gradient error can be significant, particularly in the case of sensitive measurements and small measured values. It is therefore extremely important to keep the sensor temperature constant during the actual measuring time.

The physical properties and chemical composition of the titanium alloy are listed in Tables 1 and 2 above, respectively. Table 7 gives the summary of machining parameters used for the orthogonal cutting tests.

Table 7. Summary of Machining Parameters

Tool Holder	A4SMR160620 with 0^0 rake angle
Cutting tools	A4G0605M06U04B KC5025 and A4G0600M06P04GUP KCU25 A4G0605M06U04B K313 and A4G0600M06P04GUP KU10
Rake Angles	5^0 and 16^0
Relief Angles	7^0
Cutting Speeds	120 and 240 m/mins
Feedrates	0.05, 0.075 and 0.1 mm/rev
Radial In-feed	2.032mm
Coolant	Flooded emulsion coolant

3. RESULTS AND DISCUSSION

The determined calibration equations 14, 15, and 16, giving the relationship between the cutting forces axial (feed force), radial (thrust force), and the tangential (cutting) force) at the tool tip and the corresponding Kistler 9251A load cell force outputs were used to estimate the cutting force and thrust force from load cell force measurements during the orthogonal turning tests, and the results are reported in Tables 3, 4, 5, and 6, columns 6 and 7 for all the test conditions investigated. These experimentally determined cutting forces (F_c, F_t) along with the given machining parameters (rake angles, undeformed and deformed chip thickness), Table 3, were used to calculate the shear angle, coefficient of friction, shear force, friction force, and shear stress, using the derived equations 1 -10. The calculated values are also reported in Tables 3, 4, 5, and 6, as well as the machining parameters. The effect of machining parameters on cutting forces, shear angle and friction are plotted in Figures 16, and 17.

3.1. EFFECTS OF FEEDRATE ON CUTTING FORCES

The plot cutting force and thrust force as function of feedrate at low cutting speed of 120 m/min for uncoated and coated tool with 5^o rake is shown in Figure 16a. It is seen from Figure 16a and Tables 4 and 6 that both cutting force and thrust force increases with increase in feedrate for uncoated tungsten carbide (W/Co) and WC/Co PVD coated inserts. This is because the chip thickness and cutting ratio increases with increase in feedrate, thus requiring more force to deform the material, see 3^{rd} and 4^{th} column of Table 4. Uncoated tungsten carbide (WC/Co) inserts exhibit much lower cutting force than tungsten carbide (WC/Co) PVD coated with TiAlN. Also thrust force

is much lower than the cutting force. Similar increasing trends in cutting force and thrust force with increase in feedrate are obtained for both uncoated and coated tool inserts at higher cutting speed of 240 m/min and 5^o rake angle, Figure 16c, and Tables 4 and 6, but with higher force magnitudes than at lower cutting speed. Similar results were reported by Ozel et al. for orthogonal machining of Ti-6Al-4V but under dry machining condition. At higher rake angle of 16^0 the cutting forces also increase with increase in feedrate both at low cutting speed (120 m/min) and at higher cutting speed (240 m/min), but with lower maximum forces than those obtained with lower rake angle of 5^o,(Figures 16b and d). Shear force and friction force also increase with increase in feedrate. The lower cutting force resulted in a lower shear force and friction.

3.2. EFFECTS OF CUTTING TOOL COATING ON CUTTING FORCES AND FRICTION

Figures 16 and Tables 3 – 6 indicate that cutting forces are greatly affected by cutting tool insert coating. As discussed above, lower cutting forces in all cases were obtained with uncoated tungsten carbide tool insert (WC/Co) than with WC/Co PVD coated TiAlN.

Both tools displayed similar trends with regards to increase of the cutting forces as the feedrate increases. As the feedrate increased from 0.05 to 0.1mm/rev, both the uncoated and coated cutting tools exhibit large variations in the upward trending of cutting forces. This can be explained by the fact that the tool is subjected to larger cutting load. Therefore, more materials are removed at a higher feedrate than at a lower feedrate within the same machining time. From Tables 3 – 6, it is observed that at lower cutting speed, uncoated tool insert exhibits higher average friction coefficient at low rake angle

than coated insert, thus the coating serves to reduce friction; but at the higher rake angle and low cutting speed, coated tool exhibits higher average friction coefficient. On the other hand, for the case of higher cutting speed, uncoated insert gives lower average friction coefficient at low rake angle than coated inserts, but at higher rake angle, coated insert gives lower average friction coefficient than uncoated insert.

Based on the effect of insert coating of increasing cutting forces, and from the point of view of using high speed machining to decrease cutting forces, especially for monolithic machining of thin walls in titanium components used in aerospace structures, coated cutting tool inserts are not recommended for machining titanium alloys. Ezeugwu (2005) in his review of key improvements in the machining of difficult-to-cut aerospace superalloys, concluded that there is negligible difference between coated and uncoated carbide tools in terms of tool life, and therefore there is no tangible benefit in machining with coated carbide tools with associated additional cost of typically 15%. Cutting tool coatings serve as diffusion barriers, and they prevent the interaction between the chip formed during machining and cutting tool material. These coatings such as TiAlN are extremely hard, and thus very abrasion resistant. TiAlN has the added advantage of lowering coefficient of friction at higher cutting speed and higher rake angle compared to WC/Co.

3.3. EFFECTS OF RAKE ANGLE ON CUTTING FORCES AND FRICTION COEFFICIENT

From Table 3 – 6, for both the uncoated and coated tools, it is observed that an increase in the positive rake angle from 5^0 to 16^0 led to a decrease in the cutting force, which agrees with what is reported in published literature regarding cutting tools with

higher rake angles exhibiting lower cutting forces and power. This can be attributed to the drop in the shear strength in the primary shear deformation zone as the tool temperature rises, as well as to the decrease in the length of the shear plane and shear plane area. These results provide valuable information about the best rake angle to use for machining titanium alloy Ti-6Al-4V. Similarly, the thrust force, Ft, followed the same trend as Fc in all cases. Figures 16 show that the thrust forces were always lower than the main cutting force because more forces were being exacted on the feed direction. The result of this experiment also helps to explain why uncoated and coated tools of the same high positive (16^0) rake angles under the same cutting conditions (Figures 16b and 16d) did not generate equal cutting forces. The reason is because the coated tool mainly influences the tool-chip contact zone (secondary shear zone) due to its larger contact area, whereas the uncoated counterpart can plunge easily into the workpiece and produces a smaller contact area.

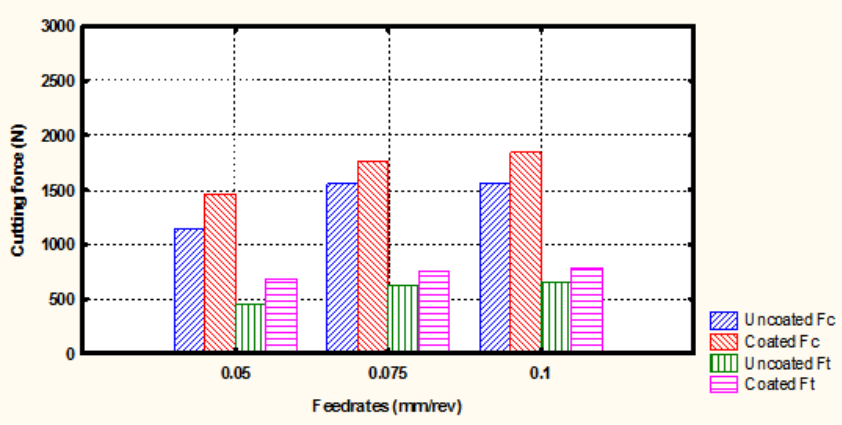

(a) Cutting tool with 5^o rake angle at cutting speed V= 120 m/min

Figure 16. Cutting Forces vs Feedrate in Orthogonal Turning of Ribbed Workpiece

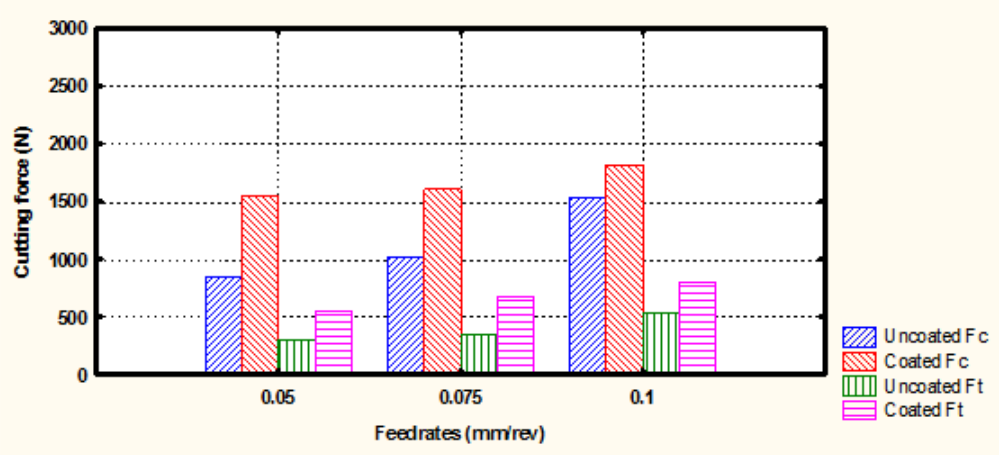

(b) Cutting tool with 16^{o} rake angle at cutting speed V= 120 m/min

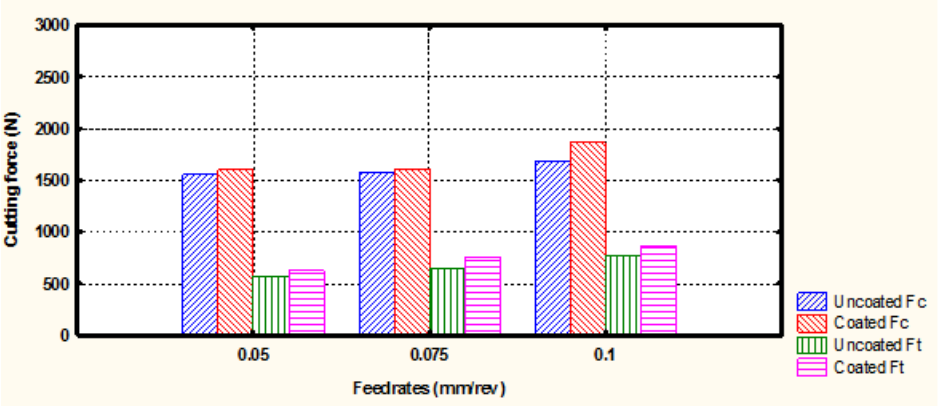

(c) Cutting tool with 5^{o} rake angle at cutting speed V= 240 m/min

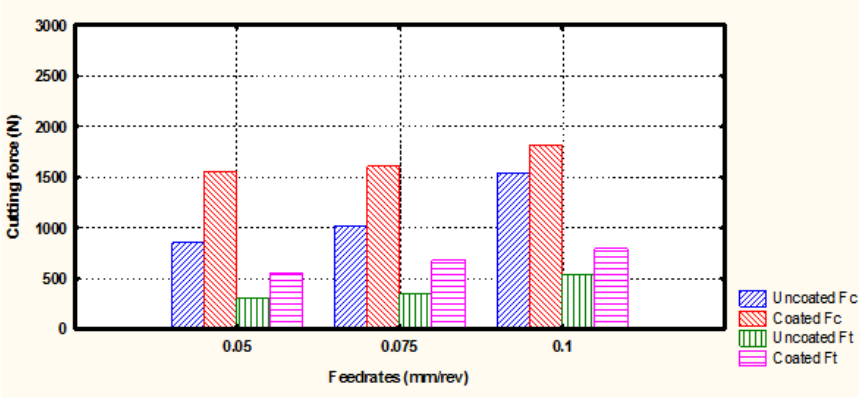

(d) Cutting tool with 16^{o} rake angle at cutting speed V= 240 m/min

Figure 16. Cutting Forces vs Feedrate in Orthogonal Turning of Ribbed Workpiece (cont.)

3.4. EFFECT OF RAKE ANGLE ON SHEAR FORCE

Figure 17 shows that increasing the positive rake angles from 5^0 to 16^0 the shear force decreases significantly at both low and high cutting speed, for the coated and uncoated tool insert.

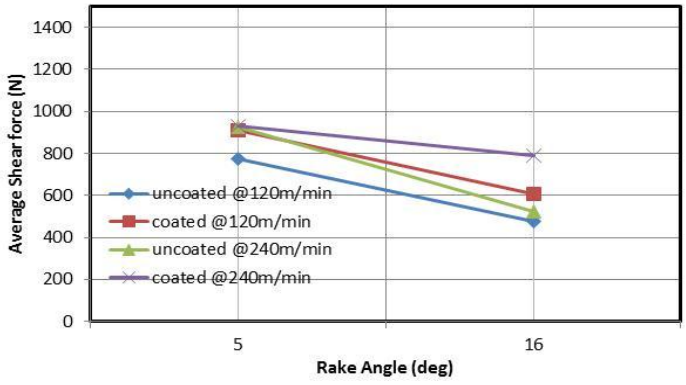

Figure 17. Average Shear Force vs Rake Angles

This occurs because positive rake angles produce lager shear angle and shorter shear plane and thus, less shear force, which helps to reduce the friction force and cutting forces, thus producing a better surface finish because it helps the chip to flow away from the workpiece material. This result indicates that the machinability of titanium alloys could be improved by the use of cutting tools with higher positive rake angle.

3.5. EFFECT OF CUTTING SPEED ON MAIN CUTTING FORCE

The effect of cutting speed on main cutting force is plotted in Figure 18, which shows the average main cutting forces at two selected cutting speeds of 120 and 240

m/min for uncoated and coated cutting tools with 5^0 and 16^o rake angles. It is observed that cutting the main cutting force increased with an increase in the cutting speed for both the uncoated and coated cutting tool inserts with 5^0 and 16^o rake angles.

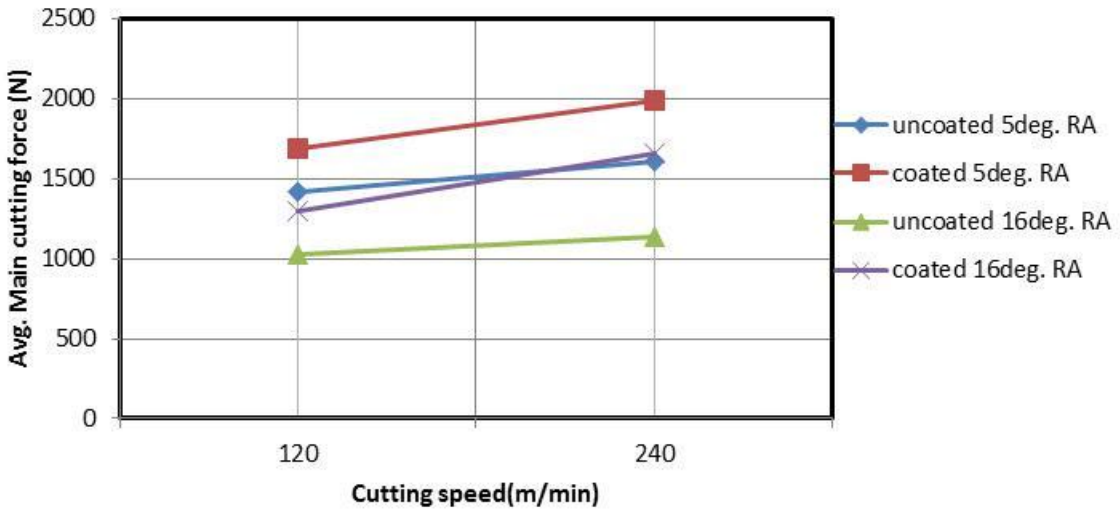

Figure 18. Average Cutting Force vs Cutting Speed

The coated cutting tool insert in general generate higher cutting forces. The uncoated tool inserts have similar rate of increase of cutting force with increase in cutting speed for the 5^0 and 16^o rake angles. Also coated tool inserts have similar rate of increase of cutting force with increase in cutting speed for the 5^0 and 16^o rake angles.

In general, the coated cutting tools generated higher cutting forces. This result of WC/Co PVD coated TiAlN tool insert generating higher cutting forces than uncoated WC/Co insert agree with the result reported by Srivastava et al. (2010) for similar material and cutting tool insert.

3.6. EFFECT OF FEEDRATES ON COEFFICIENT OF FRICTION

Figure 19 shows the coefficient of friction vs feedrate and rake angle, indicating that an increase in feedrates slightly increases the coefficient of friction, and increases in rake angles of both the uncoated and coated cutting tools increases the coefficient of friction.

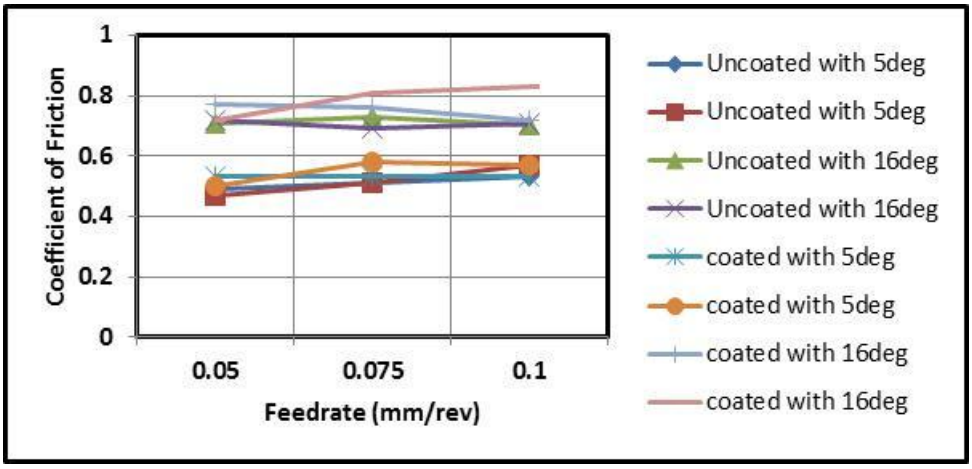

Figure 19. Coefficient of Friction vs Feedrate

.

3.7. EFFECT OF FEEDRATES ON SHEAR ANGLE

Figure 20 shows that shear angle increases significantly with increases in the feedrate/ depth of cut but tends to decrease at highest feedrates. Additionally, the shear angle shows remarkable increases with cutting tools with large rake angles but shows no noticeable increase with increases in cutting speed.

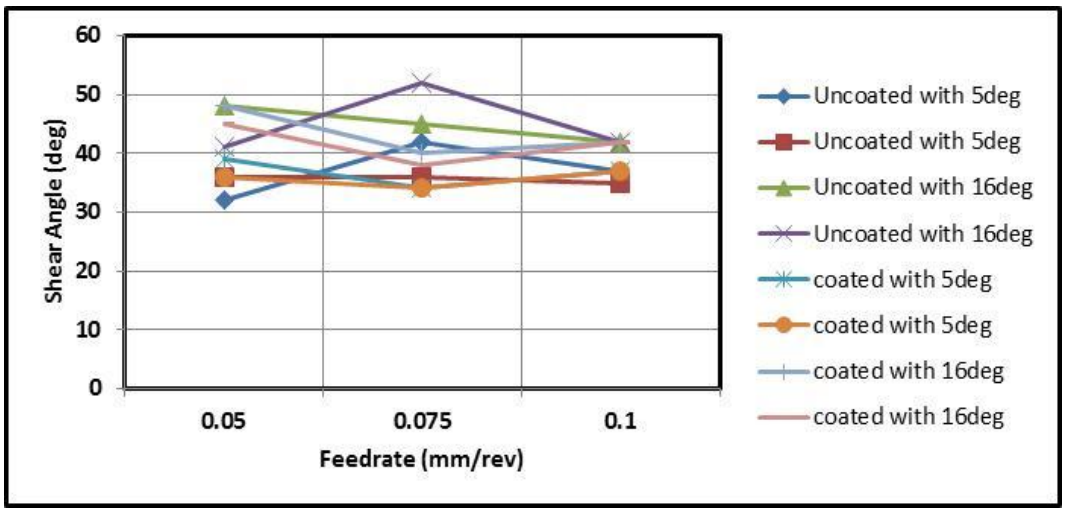

Figure 20. Factors Influencing Shear Angle

One may deduce from Table 8 that the cutting forces generated with the ribbed workpiece material are higher than the forces generated with the tubular workpiece in all cases investigated. Therefore, reflecting on the objective investigation of this research works, using tube simulated titanium alloy workpiece could be recommended given to the fact that it is more efficient and generated less cutting and thrust forces during the machining test.

Table 8. Comparative Table of Thrust Force and Cutting Force for Titanium Tube and Ribbed Alloys

Ti-6Al-4V Tubular workpiece				**Ti-6Al-4V Ribbed workpiece**			**Diff. (%)**	
Feed rates (in/rev)	**Rake Angles (^{0})**	**Thrust Force (N)**	**Cutting Force (N)**	**Rake Angles (^{0})**	**Thrust Force (N)**	**Cutting Force (N)**		
0.05	**5**	**318**	**1078**	**5**	**445**	**1141**	**+39.9**	**+5.8**
0.75	**5**	**477**	**1515**	**5**	**625**	**1555**	**+31.0**	**+2.6**
0.1	**5**	**552**	**1897**	**5**	**656**	**1562**	**+18.8**	**-17.7**
0.05	**15**	**152**	**700**	**16**	**273**	**783**	**+79.6**	**+11.9**
0.75	**15**	**267**	**979**	**16**	**344**	**932**	**+28.8**	**-4.8**
0.1	**15**	**586**	**1643**	**16**	**469**	**1365**	**-20.0**	**-16.9**

4. CONCLUSION

This paper investigated the effects of machining parameters on cutting forces, shear angle and friction during orthogonal turning of titanium alloy Ti-6Al-4V solid bar with ribs. From the results, the following conclusions are made:

1. Cutting force and thrust force increases with increase in feedrate for uncoated tungsten carbide (W/Co) and WC/Co PVD coated inserts at both low positive rake angle of 5^{o} C and high positive rake of 16^{o} C, and at both low cutting speed of 120 m/min and high cutting speed of 240 m/min, for the feedrate range of 0.05 – 0.1 mm/rev.
2. Chip thickness and cutting ration increases with increase in feedrate for the same feedrate range.
3. Uncoated tungsten carbide (WC/Co) inserts exhibit much lower cutting force than tungsten carbide (WC/Co) PVD coated with TiAlN.
4. Thrust force is much lower than the cutting force.
5. Cutting force and thrust force increases with increase in cutting speed from 120 m/min to 240 m/min, for both the uncoated and coated cutting tool inserts. The coated cutting tool in general generates higher cutting forces.
6. Uncoated tool inserts exhibit higher average friction coefficient than coated tool inserts at low rake angle and low cutting speed, and thus the coating serves to reduce friction; but at higher rake angle and low cutting speed, coated tool inserts exhibits higher average friction coefficient.
7. Uncoated tool inserts exhibit lower average friction coefficient than coated tool inserts at lower rake angle and higher cutting speed.

8. Coated cutting tool inserts are not recommended for machining titanium alloys because they increase cutting forces.

9. An increase in the positive rake angle from 5^0 to 16^0 leads to a higher shear angle and less shear force, which decreases the cutting force, thrust force, and friction force. Machinability of titanium alloys could be improved by using cutting tool inserts with higher positive rake angle.

ACKNOWLEDGEMENTS

The financial support of National Science Foundation (NSF) under grant no. CMMI 800871 is gratefully acknowledged. The financial assistance provided in the form of Graduate Teaching Assistantship by the Department of Mechanical and Aerospace Engineering at Missouri University of Science and Technology is also gratefully acknowledged.

REFERENCES

Kosaraju Satyanarayana, Anne VenuGopal, Ghanta VenkateswaraRao "Effect of Rake Angle and Feedrate on Cutting Forces in an Orthogonal Turning Process" International Conference on Trend in Mechanical and Industrial Engineering (ICTMIE'2011) Bangkok December 2011.

Baldoukas, A.K., Soukatzidis, F.A., Demosthenous, G. A., and Lontos, A.E., "Experimental Investigation of the Effect of Cutting Depth, Tool Rake Angle and Workpiece Material Type on the Main Cutting Force During a Turning Process," *Proceedings of the 3rd International Conference on Manufacturing Engineering (ICMEN),* 1-3 October 2008, Chalkidiki, Greece, pp. 47-55.

Cotterell, M., and Byrne, G. "Dynamics of chip formation during orthogonal cutting of titanium alloy Ti–6Al–4V," *CIRP Annals - Manufacturing Technology,* Vol. 57, (2008), pp. 93-96. Amsterdam: Elsevier.

H. Ernst and M. E. Merchant, "Chip Formation, Friction and High Quality Machined Surfaces," Surface Treatment of Metals (American Society for Metals, 1941), pp. 299-378.

Fang, N., and Wu, Q., "A Comparative Study of the Cutting Forces in High Speed Machining of Ti-6Al-4V and Inconel 718 with a Round cutting Edge Tool," *Journal of Material Processing Technology,* Vol. 209 (2009), pp. 4385-4389.

Gunay, M., Aslan, E., Korkut, I., and Seker, U., "Investigation of the Effect of Rake Angles on Main Cutting Force," *International Journal of Machine Tool and Manufacture,* Vol. 44 (2004) pp. 953-959.

Iqbal, S.A., Mativenga, T.P., and Sheikh, A.M., "Cutting using the Finite Element Method Determining the Effect of Interface Friction on Tool-Chip Contact Length in Orthogonal.

Khidhir, A., Basim., Mohamed,Bashir., "Selecting of Cutting Parameters from Predictions Model of Cutting force for Turning Nickel Based Hastelloy C-276 Using Response Methodology," *European Journal of Scientific Research*, Vol.33 No.3 (2009), pp. 525-535.

Lazoglu, I., and Altintas Y., "Prediction of Tool and Chip Temperature in Continuous and Interrupted Machining," *International Journal of Machines Tools and Manufacture*, Vol. 42, pp. 1011 – 1022. Amsterdam Elsevier.

Liu, C., Ai, X., and Liu, Z**. "**Experimental Study on Wear Mechanism of Cutting Tool and Cutting Temperature in High Speed Machining Super alloy," *Advanced Materials Research*, Vols. 102-104, (2010), pp. 525-528. (www.scientific.net/AMR.102-104.525).

Liu, M., Ming W.W., Zhang Y.S., Xu H., and Chen M., "Machinability Evaluation of TC11 Titanium Alloy in Finish Hard Turning Based on the Response Surface Methodology," Mechanical Science and Technology, Vol. 21, (2007), pp. 1651 – 1655.

Luo, M., Zhang, L.Q., and Chen, M., "Machinability and Tool Wear Behavior in Turning High Nickel-base Alloy-G3," *Advanced Materials Research*, Vols 69-70, (2009), pp. 485-489. (www.scientific.net/AMR.69-70. 485)

Marusich, D. Troy., "Effect of Friction and Cutting Speed on Cutting Force," *Proceedings of ASME Congress*, November 2001, pp. 11-16, New York.

Ming, W.W., Chen, M., and Rong, B., "Analysis of Finish Hard Turning of Ti-6.5Al-3.5Mo-1.5Zr-0.3Si Alloy," *Material Science Forum*, Vols. 626-627 (2009), pp. 225-230. (www.scientific.net/MSF.626-627.225).

Saglam Haci, Unsacar Faruk, Yaldiz Suleyman "Effects of Rake Angle and Approach Angle on the Main Cutting Force and Tool-tip Temperature," *International Journal of Machine Tools & Manufacture*, Vol.46 (2006), pp. 132-141.

Seker, U., Kurt, A., and Ciftci, I., "The Effect of Feedrate on the Cutting Force When Machining with Linear Motion," *Journal of Materials Processing Technology*, Vol.146 (2004) pp. 403-407.

Srivastava, K. Anil., Iverson, C. Jonathan., "An Experimental Investigation into High Speed Turning of Ti- 6Al- 4V," *Proceeding of the ASME 2010*, International Manufacturing Science and Engineering Conference. MSEC2010-34205.

Stephenson, A. David., Agapiou, S. John." Metal Cutting Theory and Practice," (1997) pp. 447- 481.

Sun, S., Brandt, M., and Dargusch, M.S., "Characteristics of Cutting Forces and Chip Formation in Machining of Titanium Alloys," *International Journal of Machine Tools & Manufacture*, Vol.49 (2009), pp. 561-568.

Sutter, G., Faure, L., Molinari, A., Ranc, N., and Pina, V., "An Experimental Technique for the Measurement of Temperature Fields for the Orthogonal Cutting in High Speed Machining," *International Journal of Machine Tools & Manufacturing*, Vol.43 (2003), pp. 671-678.

Okafor, A.C., and Ukpon, A.U., "Real-Time Intelligence Monitoring and Diagnostic System for A CNC Turret Lathe in A Production Environment," PhD Dissertation, University of Missouri – Rolla, 1998. Modify as in paper 1.

Wang, Z. G., Rahman, M., Wong, Y.S., Neo, K.S., Sun, J., Tan, C.H., and Onozuka, H., "Study on Orthogonal Turning of Titanium Alloys with Different Coolant Supply Strategies," *International Journal of Advanced Manufacture Technology*, Vol.42 (2009) pp. 621-632.

Wu, W., Wang, G., Shen, C., "Analysis of Cutting Forces in Precision Turning Based on Oblique Cutting Model," *Advanced Material Research*, Vol.97-101 (2010), pp. 1961-1964

SECTION

2. CONCLUSION

This two-paper thesis investigated the effects of machining parameters on cutting forces, shear angle and friction during orthogonal turning of titanium alloy Ti-6Al-4V tube and solid ribbed bar. From the results the following similar conclusions are made:

1. Cutting force and thrust force increases with increase in feedrate for uncoated tungsten carbide (W/Co) and WC/Co PVD coated inserts at both low positive rake angle of 5^{o} C and high positive rake of 15^{o} C, and at both low cutting speed of 120 m/min and high cutting speed of 240 m/min, for the feedrate range of 0.05 – 0.1 mm/rev. Also
2. Cutting force and thrust force increases with increase in feedrate for uncoated tungsten carbide (W/Co) and WC/Co PVD coated inserts at both low positive rake angle of 5^{o} C and high positive rake of 16^{o} C, and at both low cutting speed of 120 m/min and high cutting speed of 240 m/min, for the feedrate range of 0.05 – 0.1 mm/rev.
3. Chip thickness and cutting ration increases with increase in feedrate for the same feedrate range.
4. Uncoated tungsten carbide (WC/Co) inserts exhibit much lower cutting force than tungsten carbide (WC/Co) PVD coated with TiAlN.
5. Thrust force is much lower than the cutting force.

6. Cutting force and thrust force increases with increase in cutting speed from 120 m/min to 240 m/min, for both the uncoated and coated cutting tool inserts. The coated cutting tool in general generates higher cutting forces.
7. Uncoated tool inserts exhibit higher average friction coefficient than coated tool inserts at low rake angle and low cutting speed, and thus the coating serves to reduce friction; but at higher rake angle and low cutting speed, coated tool inserts exhibits higher average friction coefficient.
8. Uncoated tool inserts exhibit lower average friction coefficient than coated tool inserts at lower rake angle and higher cutting speed.
9. Coated cutting tool inserts are not recommended for machining titanium alloys because they increase cutting forces.
10. An increase in the positive rake angle from 5^0 to 15^0 leads to a higher shear angle and less shear force, which decreases the cutting force, thrust force, and friction force.
11. An increase in the positive rake angle from 5^0 to 16^0 leads to a higher shear angle and less shear force, which decreases the cutting force, thrust force, and friction force.
12. For both cases, machinability of titanium alloys could be improved by using cutting tool inserts with higher positive rake angle.

VITA

Hilary Anayochukwu Onyishi was born in Enugu State, Nigeria. He received his primary and secondary education in Nigeria and earned his Bachelor of Engineering degree in Mechanical/Production Engineering in 2006 from Nnamdi Azikiwe University in Awka, Nigeria. Hilary has held many political positions, including Secretary of the Association of African Students at Missouri S&T, President of the Association of Mechanical Engineering Students, and President of the Association of Enugu State Students at Nnamdi Azikiwe University Awka, Nigeria. He worked as an Assistant Project Engineer at ExxonMobil Nigeria before proceeding to the United States to begin his graduate program. Hilary received his MS in Mechanical Engineering from the Missouri University of Science and Technology, Rolla in May 2013. He served as a Graduate Research Assistant and Graduate Teaching Assistant at the same university. He is a member of the National Society of Black Engineers (NSBE) and the Society for Petroleum Engineers (SPE).